Methods and Strategies to Identify the Mode of Action of Phytoactive Compounds

Dissertation

Zur Erlangung des Grades

„Doktor der Naturwissenschaften“

Am Fachbereich Biologie

Der Johannes-Gutenberg-Universität Mainz

von

Stefan Tresch

geb. am 04.11.1978 in Bad Dürkheim

Mainz, 2012

Dekan:

1. Berichterstatter:

2. Berichterstatter:

[Die Namen von Dekan und Gutachtern sind gelöscht.]

Tag der mündlichen Prüfung: 05.11.2012

The most exciting phrase to hear in science,
the one that heralds new discoveries,
is not „Eureka!“ (“I found it!”).
But rather, “Hmmm … That’s funny …”
ISAAC ASIMOV

Contents

Abbreviations

2,4-D	2,4-Dichlorophenoxyacetic acid
ABPP	Activity-based-protein-profiling
ACCase	Acetyl CoA carboxylase (E. C. 6.4.1.2)
ALS	Acetolactate synthase (E. C. 4.1.3.18)
CA1	Ethyl (2Z)-3-amino-2-cyano-4-ethylhex-2-enoate
CA2	Isopropyl (2Z)-3-amino-2-cyano-4-ethylhex-2-enoate
CPTA	2-(4-Chlorophenylthio)-triethylamine hydrochloride
DNA	Deoxyribonucleic acid
EMS	Ethylmethanesulfonate
EPSPS	5-Enoylpyruvylshikimic acid 3-phosphate synthase (E. C. 2.5.1.19)
GS	Glutamine synthase (E. C. 2.7.7.42)
GSA	Glutamate 1-semialdehyde aminotransferase (E. C. 5.4.3.8)
GUS	β-Glucuronidase
HPPD	4-Hydroxyphenylpyruvate dioxygenase (E. C. 1.13.11.27)
KCS	3-Ketoacyl-CoA synthase
MoA	Mode of action
NAD	Nicotinamide adenine dinucleotide
PPO	Protoporphyrinogen oxidase (E. C. 1.3.3.4)
PSI	Photosystem I
PSII	Photosystem II
SAR	Structure-activity relationship
SE	Standard error
HTS	High-throughput screen
VLCFAS	Very-long-chain fatty acid synthase
Y3H	Yeast three-hybrid

1. Abstract

Small molecules affecting biological processes in plants are widely used in agricultural practice as herbicides or plant growth regulators and in basic plant sciences as probes to study the physiology of plants. Most of the compounds were identified in large screens by the agrochemical industry, as phytoactive natural products and more recently, novel phytoactive compounds originated from academic research by chemical screens performed to induce specific phenotypes of interest. The aim of the present PhD thesis is to evaluate different approaches used for the identification of the primary mode of action (MoA) of a phytoactive compound. Based on the methodologies used for MoA identification, three approaches are discerned: a phenotyping approach, an approach based on a genetic screen and a biochemical screening approach.

Four scientific publications resulting from my work are presented as examples of how a phenotyping approach can successfully be applied to describe the plant MoA of different compounds in detail.

I. A subgroup of cyanoacrylates has been discovered as plant growth inhibitors. A set of bioassays indicated a specific effect on cell division. Cytological investigations of the cell division process in plant cell cultures, studies of microtubule assembly with green fluorescent protein marker lines *in vivo* and cross resistant studies with *Eleusine indica* plants harbouring a mutation in α-tubulin, led to the description of α-tubulin as a target site of cyanoacrylates (Tresch *et al.*, 2005).

II. The MoA of the herbicide flamprop-m-methyl was not known so far. The studies described in Tresch *et al.* (2008) indicate a primary effect on cell division. Detailed studies unravelled a specific effect on mitotic microtubule figures, causing a block in cell division. In contrast to other inhibitors of microtubule rearrangement such as dinitroanilines, flamprop-m-methyl did not influence microtubule assembly in vitro. An influence of flamprop-m-methyl on a target within the cytoskeleton signalling network could be proposed (Tresch *et al.*, 2008).

III. The herbicide endothall is a protein phosphatase inhibitor structurally related to the natural product cantharidin. Bioassay studies indicated a dominant effect on dark-growing cells that was unrelated to effects observed in the light. Cytological characterisation of the microtubule cytoskeleton in corn tissue and heterotrophic tobacco cells showed a specific effect of endothall on mitotic spindle formation and ultrastructure of the nucleus in combination with a decrease of the proliferation index. The observed effects are similar to those of other protein phosphatase inhibitors such as cantharidin and the structurally different okadaic acid. Additionally, the observed effects show similarities to knock-out lines of the TON1 pathway, a protein phosphatase-regulated signalling pathway. The data

presented in Tresch *et al.* (2011) associate endothall's known *in vitro* inhibition of protein phosphatases with *in vivo*-effects and suggest an interaction between endothall and the TON1 pathway.

IV. Mefluidide as a plant growth regulator induces growth retardation and a specific phenotype indicating an inhibition of fatty acid biosynthesis. A test of the cuticle functionality suggested a defect in the biosynthesis of very-long-chain fatty acids (VLCFA) or waxes. Metabolic profiling studies showed similarities with different groups of VLCFA synthesis inhibitors. Detailed analyses of VLCFA composition in tissues of duckweed (*Lemna paucicostata*) indicated a specific inhibition of the known herbicide target 3-ketoacyl-CoA synthase (KCS). Inhibitor studies using a yeast expression system established for plant KCS proteins verified the potency of mefluidide as an inhibitor of plant KCS enzymes. It could be shown that the strength of inhibition varied for different KCS homologues. The *Arabidopsis* Cer6 protein, which induces a plant growth phenotype similar to mefluidide when knocked out, was one of the most sensitive KCS enzymes (Tresch *et al.*, 2012).

The findings of my own work were combined with other publications reporting a successful identification of the MoA and primary target proteins of different compounds or compound classes. The literature was compiled in order to extract the relevant information for a successful MoA description.

An evaluation of the compiled data indicates that the target sites of compounds addressing primary or secondary metabolism were identified most successfully with a phenotyping approach. Target sites for compounds that influence cell structures, like cell wall biosynthesis or the cytoskeleton, or compounds that interact with the hormone system, were only in some cases identified by phenotypic approaches. Most of these target sites were found by using a genetic approach. Examples showing the power and bottlenecks of the different approaches are discussed in detail. Additionally, new techniques that could contribute to future MoA identification projects are reviewed. In particular, next-generation sequencing techniques may be used for the fast-forward mapping of mutants identified in genetic screens.

Finally, a revised three-tier approach for the MoA identification of phytoactive compounds is proposed. The approach consists of a 1st level aiming to address compound stability, uniformity of effects in different species, general cytotoxicity and the effect on common processes like transcription and translation. Based on these findings advanced studies can be defined to start the 2nd level of MoA characterisation, either with further phenotypic characterisation, starting a genetic screen or establishing a biochemical screen. At the 3rd level, enzyme assays or protein affinity studies should show the activity of the compound on the hypothesized target and should associate the *in vitro* effects with the *in vivo* profile of the compound.

2. Introduction

A large variety of compounds that influence plant growth or modulate the physiology of plants are known. Most of them are used as crop protection products (Phillips McDougall, 2011), as probes to study physiological processes in plants (Dayan *et al.*, 2010), or in combination with genes as selectable marker systems to generate transgenic plants (Rosellini, 2011). These compounds can be classified in two classes, (i) natural products or structurally related compounds derived thereof and (ii) synthetic compounds. Most of the phytotoxic natural products were isolated from bacteria, fungi or insects (Dayan *at el.* 2012), but also natural products of plant origin were used as baits for herbicides (Vyvyan, 2002). The discovery of the synthetic compounds was mainly based on extensive screens of the crop protection industry to identify compounds that can be used as pesticides. More than 250 compounds are actually registered as herbicides or plant growth regulators (Phillips McDougall, 2011). Additionally, several plant active compounds or lead compound classes are described in literature, but they were never registered as market products. Moreover, since the late 1990s several chemical screens have been performed in the academic community to identify specific inhibitors of pathways of interest (Min *et al.*, 1999; Grozinger *et al.*, 2001; Armstrong *et al.*, 2004). In contrast to the simple screens in the crop protection industry, which detect mainly phytotoxic activity, the chemical screens in the academic community were often designed to identify compounds that influence a specific process of interest or biosynthetic pathway. One of the first chemical screens described in academia aimed to identify compounds affecting specifically brassinosteroid biosynthesis (Min *et al.*, 1999). In addition, a screen described by He *et al.* (2011) was performed to search for specific suppressors of the constitutive ethylene response phenotypes of *Arabidopsis thaliana* mutant *ethylene overproducer 1-2* (*eto1-2*).

In academia, chemical screens were introduced to support gene function studies. After extensive use of knock-out or activation tagging populations (Weigel *et al.*, 2000) and knock-down techniques, such as antisense RNA, RNAi or miRNA, to study gene functions (Waterhouse and Helliwell, 2003), the limitations of such techniques became obvious. A single knock-out or knock-down may not lead to any phenotype if the gene function is covered by several redundant proteins (Cutler and McCourt, 2005). Additionally, for essential gene functions, which are encoded by one single gene, a knock-out often leads to embryonic lethal phenotypes. These bottlenecks are avoided by chemical screens and are addressed in several reviews (Blackwell and Zhao, 2003; Walsh, 2007; Toth and van der Hoorn, 2009; Hicks and Raikhel, 2012). The main advantage of a chemical screen is the possibility to inhibit homologous proteins with redundant functions, which do not lead to a visible phenotype when knocked out. Additionally, it is possible to modulate the potency of inhibition

by changing the compound concentration or by using pulse treatment to temporarily block the pathway of interest. This can also be achieved by the technique of inducible miRNA (Wielopolska *et al.*, 2005). A chemical probe, however, directly blocks protein activity and is not dependent on the transcription machinery; the direct effect of the probe is only limited by cell permeability.

As mentioned previously, the goal of a chemical screen performed in academia is to identify compounds that induce a specific phenotype and influence a pathway of interest. This is also the case for the discovery of new herbicides to support the quest for new market products. The identification and precise definition of the molecular target site of an active compound, not only the identification of the compound itself, is the scientifically challenging part. This is illustrated by studies of the group of auxin herbicides. The herbicidal effects of 2,4-dichlorophenoxyacetic acid (2,4-D) was observed in the 1940's, but it took more than 60 years to describe the class of TIR and AFB receptors as the molecular target site of natural auxin hormones and auxin herbicides (Dharmasiri *et al.*, 2005; Kepinski and Leyser, 2005; Walsh *et al.*, 2006).

2.1. Importance of identifying the mode of action of plant active compounds

To make use of the *in vivo* screening compounds discovered in academia as well as in the crop protection industry, it is of general interest to understand the principles of the compound uptake, metabolism within the plant, and inhibitory activity on the primary target and potential secondary target sites. The goal of MoA studies is to understand the compound action *in planta* in its entirety. Finally, the MoA studies aim to identify the molecular target sites of the compounds, which is then termed as the mechanism of action.

To accelerate the herbicide research process in industry, it is of great interest to identify the target proteins of new lead compounds. With the knowledge of the target protein, it is possible to optimize the structure of the lead compound towards a more potent inhibitor in enzyme assays (Lein *et al.*, 2004; Duff *et al.*, 2007), and if a 3D protein structure of the target can be generated, *in silico* modelling techniques can further support lead structure optimization (Congreve *et al.*, 2005; Occhipinti *et al.*, 2010, Witschel *et al.*, 2011). At an early stage of the research process, it is of great help to either assign a new lead compound class to a well-known MoA class or to classify it as a compound inhibiting a new molecular target. The identification of new 'druggable' target proteins and suitable inhibitors is important to develop new herbicide market products with improved agronomic or regulatory performance and low risk for resistance issues (Duke, 2012). In addition to excellent herbicide activity, it is one of the main goals in the development of a new herbicide to avoid causing any negative

effect on the environment and non-target organisms and, therefore, meet the regulatory requirements (Rüegg *et al.* 2007). Low toxicity is often directly linked to the compound mode of action (Shaner, 2003). Additionally, knowledge of the target sites of new herbicidal active compounds is the basis to develop herbicide tolerant crops by biotechnological methods or traditional breeding (Mulwa and Mwanza, 2006).

During life cycle management and market introduction of new products, knowledge of the molecular target site is of great benefit to establish resistance management strategies for agricultural practice (Scott *et al.*, 2009). Due to the fact that more than 74% of the herbicide market is covered by only six MoA classes (Phillips McDougal, 2011; Figure 1) and due to the evolution of resistant weed populations (Beckie and Tardif, 2012), new compound classes with new modes of action are urgently needed.

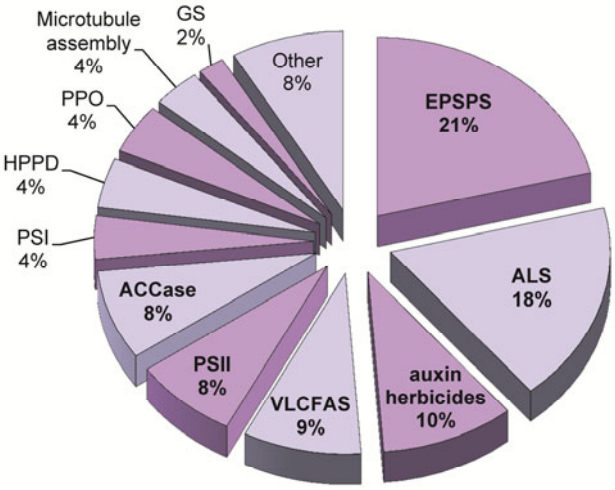

Figure 1: Herbicide market by MoA – 2010

Percent market share of herbicides targeting the respective mode of action. The %-values of the MoA classes were calculated based on market volume of single compounds as listed in Phillips McDougall (2011). EPSPS: 5-enoylpyruvylshikimic acid 3-phosphate synthase; ALS: acetolactate synthase; VLCFAS: very-long-chain-fatty acid synthase; PSII: photosystem II; ACCase: acetyl CoA carboxylase; PSI: photosystem I; HPPD: hydroxyphenylpyruvate dioxygenase; PPO: protoporphyrinogen oxidase; GS: glutamine synthetase

A strategy to identify the MoA and the molecular target site of a chemical probe is not only important for the crop protection industry, but also of interest in basic plant science. In most cases, chemical screens lead to the identification of an active compound that induces the phenotype of interest, but information on target sites and MoAs is not published concomitantly (e.g., Zhao *et al*., 2007; Park *et al.* 2009). The precise description of the compound-induced phenotype in combination with the knowledge of the molecular target of a compound can be used to support functional gene annotation. In order to characterise a new compound as a good chemical probe for the use in basic plant science, according to the five principles of a high quality chemical probe defined by Frye (2010), several compound

properties should be clarified. It is a common phenomenon that some compounds act on different target sites (Min *et al.*, 1999; Grossmann *et al.*, 2001) or have to be activated by metabolizing enzymes in plant cells. The latter was the case for sirtinol, identified as an inhibitor of the sirtuin family of NAD-dependent deacetylases (Grozinger *et al.*, 2001); *in planta* however, sirtinol acts as synthetic auxin after metabolic activation (Dai *et al.*, 2005). Therefore, a stringent strategy is needed to investigate the target site of new compounds derived from any plant screen for efficient characterisation of their MoA.

2.2. How to identify the mode of action of plant active compounds

In parallel with the identification of the first synthetic herbicides after World War II, experimental studies described the MoA of the new plant active compounds. The first investigations of the MoA used physiological studies, and further progress in MoA identification was clearly driven by technological progress (exemplary described for auxin herbicides by Grossmann, 2009). A similar case was described for the progress in MoA identification of drugs (Williams, 2007). Using physiological studies and biochemical methods, it was possible to identify the MoA of several important herbicides like Glyphosate (Steinbrücken and Amrhein, 1980) or inhibitors of acetolactate-synthase (ALS; Shaner *et al.*, 1984; LaRossa and Schloss, 1984) and photosystem II (PSII, Wessel and van der Veen, 1951; Pfister *et al.*, 1981). Since the 1980s, introduction of molecular biological techniques allowed the identification of nucleic acid mutations in target resistant mutants (Yamamoto *et al.*, 1998) and production of recombinant proteins for enzyme assays (Berg *et al.*, 1999). The third phase, the genomic stage, started with the publication of the *Arabidopsis thaliana* genome in 2000, which allowed more rapid mapping of resistant mutants (Scheible *et al.*, 2001) and has been the basis for an efficient setup of chemical genetic screens for target identification (Walsh, 2007). Similar to drug discovery (Williams, 2007), the innovations of the different stages do not replace any of the former technologies, but rather complement the methodological portfolio to address MoAs.

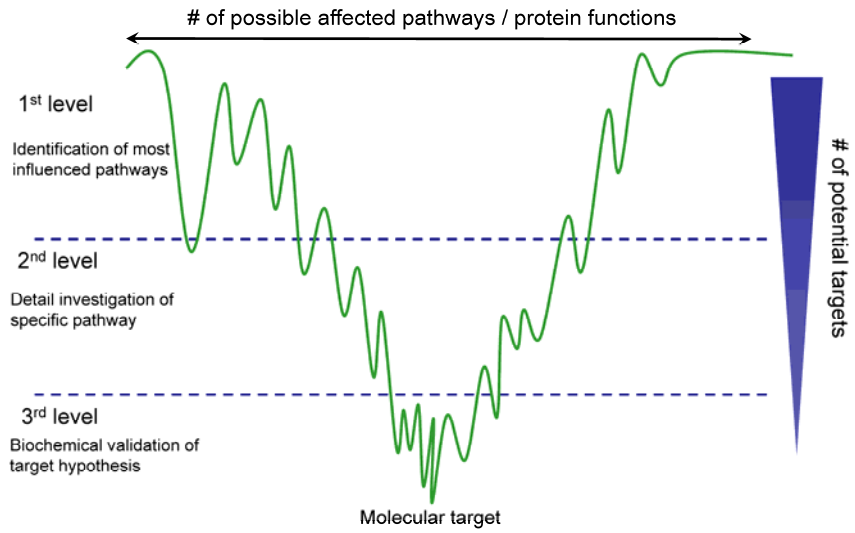

Figure 2: Level scheme from phenotype to molecular target

The available techniques and methods are the basic tools for MoA identification. The strategy to identify the primary target protein of a compound out of several thousands of possible targets has to take into account the biological background to efficiently use the applicable techniques and methods. The variables and different levels of complexity to identify the MoA of a compound could be seen as the number of possible affected pathways on one axis and the number of potential targets on the second axis (Figure 2). This scheme could be translated into a MoA strategy that describes which methods should be applied during the different levels of target identification. It is the goal of the 1st level to get an idea of the affected pathways or type of target (see 2.2.2). The 1st level is characterised by the use of holistic tests and detailed interpretations of the compound's *in vivo* effects. With this initial characterisation it is possible to choose the appropriate methodologies for the 2nd and 3rd levels. This scheme is adapted and discussed in detail in section 4.4, according to literature examples that successfully described a target site of phytoactive compounds.

2.2.1. Types of screens and respective MoA identification strategies

Screens to identify phytoactive compounds can be separated into forward and reverse screens (Figure 3). In a forward screen, typically a library of structurally diverse compounds is applied on whole plants to identify compounds that induce a phenotype of interest. The range of such a screen could be from a simple readout of general phytotoxicity, observation of specific growth phenotypes, or a more sophisticated screen on the reversal of a specific mutant phenotype (e.g., ethylene mutants; He *et al.*, 2011). The result of a forward screen is a compound that induces the phenotype of interest, but the specific target protein is unknown. Also, pure natural products extracted from microbes or plants that produce allelochemicals, may be classified as hits from a forward screen with an unknown target. These natural products were identified because of their activity on plant systems, but a target

protein is initially not known. The MoA identification strategy for synthetic compounds or natural products is the same. Reverse screens start with the definition of the protein target that should be addressed by a chemical compound. Identification of compounds that act on the defined target is done with the use of an *in vitro* assay for enzyme inhibitors or compounds with high affinity to receptor proteins. This type of screen became available with the introduction of biotechnological high-throughput screening (HTS) techniques directed towards specific protein inhibitors. The compounds from reverse screens have a described target by definition, but it is often unclear if the *in vitro* target is also the main target *in vivo*, like in cellular models or whole plants. To confirm the *in vivo* target, phenotyping tools or genetic screens have to be applied to reach the definitions of a chemical probe in basic science, as defined by Frye (2010).

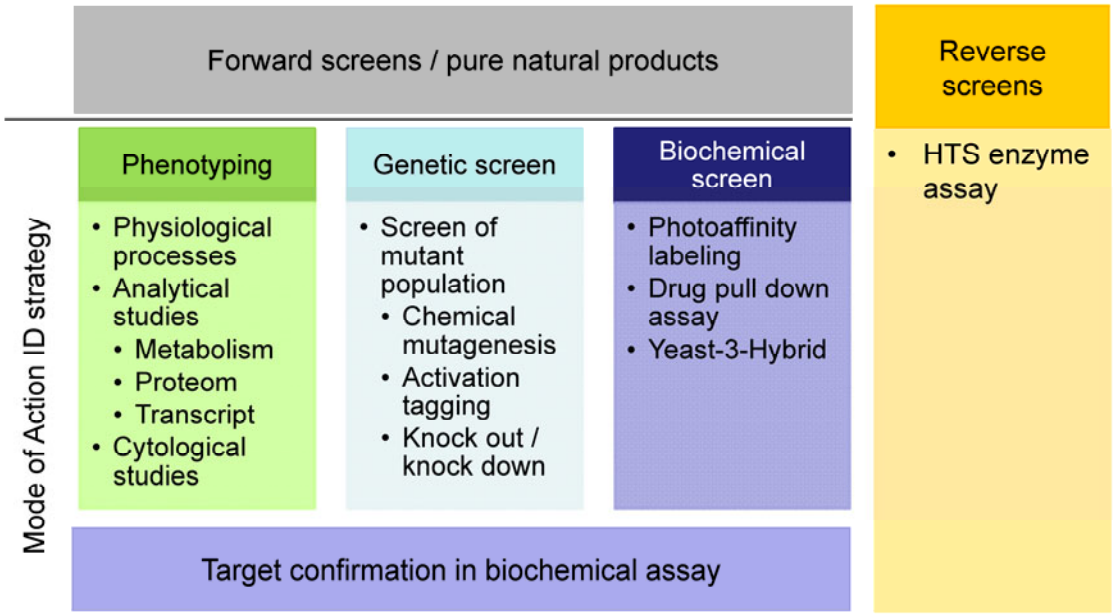

Figure 3: Types of screens and principal methodologies for MoA identification

Forward and reverse chemical screens lead to the identification of phytoactive compounds. The specific target sites of compounds from a forward screen within an organism have to be addressed with dedicated methodologies. In principle, three different approaches can be differentiated: phenotyping, genetic screens or biochemical screens. The *in vivo* MoA of compounds identified in a reverse screen, from which the target site is defined, has to be proven by phenotyping or genetic screening.

There are three different methodologies to identify the molecular target of a new active compound (Figure 3) based on the approaches developed during the physiological and biochemical, the molecular biological and the genomic phases previously mentioned in section 2.2. Within the phenotyping approach, several physiological, analytical and basic biochemical methods were applied to understand and interpret the compound-induced phenotype to generate a target hypothesis. With the publication of the first plant genome in 2000 (The *Arabidopsis* Genome Initiative, 2000), the genetic mapping of compound resistant mutants became much easier. Additionally, the availability of large ethylmethanesulfonate

(EMS)-induced mutation, activation tagging and knock-out seed populations, enables genetic screens towards mutants lacking the compound-induced phenotype. Also, biochemical methods such as photoaffinity labelling, drug pull-down assays and yeast-3-hybrid (Y3H) screens might have the ability to identify a compound's target protein (Cottier *et al.*, 2011).

2.2.2. Druggable protein targets and their classification

In order to choose an efficient MoA identification strategy, it is important to consider the potential number and different types of protein targets that can be affected by chemical compounds. On average, plant genomes encode for more than 25,000 protein-coding genes (http://phytozome.org) which could all be possible compound target sites. In an *in vivo* screen, however, several factors limit the number of compound target sites. To reach their target site in a forward screen, compounds have to cross several barriers such as the cell wall and cell or organelle membranes. Therefore, the physicochemical properties of a compound determine if it can reach the target site. Based on the 'Lipinski's rule of 5', Tice (2001) defined simple physicochemical parameters for agrochemicals with a high likelihood to reach a possible target within a whole-organism. In a whole organism screen, these physicochemical properties could be incompatible with the properties needed for binding to the possible target site. Additionally, not every protein is 'druggable', which means, has the ability to bind a small molecule with an affinity to modulate its activity. Several studies have investigated the possible number of targets for drug development with regard to the 'Lipinski's rule of 5' and the druggability of proteins (Hopkins and Groom, 2002; Perola *et al.*, 2012). These studies indicate that only a small proportion of approximately 10% of the proteins of an organism can be modulated in their activity by a small molecule. Based on the uptake barriers of a plant and applying the same rules for protein druggability *in planta* as in pharma research, a similar percentage of druggable proteins can be expected in plant cells.

According to their general function, the targets of small molecules have been classified into three main groups. Most of the known small molecule target proteins in plant research are of enzymes in metabolic pathways and belong to the first group. These proteins often have defined binding domains for small molecules and interact with cell metabolites that were synthesized within the cell or imported from the environment. The second group of targets is characterised by their function to build or control the cytological architecture of the cell or tissue. Many different molecules, often natural products, do have an effect on the microtubule cytoskeleton or synthesis of the plant cell wall. The third group was underrepresented in plant research, but became more prominent because of many chemical screens aimed at identifying compounds influencing plant development. Compounds that interact with hormone receptors (e.g., synthetic auxins) or signalling cascades have been known for more than 60 years, but limitations in techniques to identify their target proteins

hindered the identification of compounds that interact with signalling cascades. Because of the broad availability of genomic tools for plant model systems, but also for non-model plants, an increase in described target sites for compounds that interact with plant-specific signalling pathways is expected.

The strategy to identify the MoA has to be adjusted depending on the different types of targets mentioned above, with respect to the plant uptake barriers, translocation properties and metabolic behaviour of the investigated compound.

2.3. Objectives of the thesis

Many small molecules affecting the activity of target proteins in plants have been described, although for some of these compounds the exact target and the MoA are not yet known. Moreover, numerous reports on the successful identification of the plant MoA of a new phytoactive compound applying different methodologies have been published, but a clear strategy was often not obvious. As one part of the present thesis, I have published several articles describing the MoA of new compound classes that belong to different target groups. In the second part of my thesis I reviewed the current literature on successful examples of the identification of the MoA of phytoactive compounds including my own publications in this field. Based on the literature review and my own experience, I will present a strategy to efficiently identify the MoA of plant-specific compounds with a particular focus on possible bottlenecks, challenges and future trends.

3. Publications

3.1. Herbicidal cyanoacrylates with antimicrotubule mechanism of action

New cyanoacrylates were recently discovered as potential herbicides in a forward screen for inhibition of plant growth (Tresch *et al.*, 2005). The experiments described in Tresch *et al.* (2005) were designed in order to identify the herbicidal MoA of a new structural type of cyanoacrylates, which is characterised by a typical ethylpropyl moiety. The study clearly separates the ethylpropyl-cyanoacrylates from the formerly described cyanoacrylates with a primary effect on inhibition of photosystem II (Huppatz *et al.* 1981). Using a phenotyping approach to investigate the MoA of ethyl (2Z)-3-amino-2-cyano-4-ethylhex-2-enoate (CA1) and its isopropyl ester (CA2), it was possible to correlate the phenotypic symptoms observed after compound treatment with the effects observed at the cytological level. Because of the in-depth knowledge of the MoAs of other compound classes with similar MoAs as the cyanoacrylates, cross-resistant investigations with dinitroaniline resistant *Eleusine indica* led to a description of the molecular mechanism of action. It was possible to propose a binding of the ethylpropyl-cyanoacrylates at α-tubulin in a similar manner as the dinitroaniline binding mode.

Pest Management Science

Pest Manag Sci **61**:1052–1059 (2005)
DOI: 10.1002/ps.1093

Herbicidal cyanoacrylates with antimicrotubule mechanism of action

Stefan Tresch,[1] Peter Plath[2†] and Klaus Grossmann[1*]

[1]*BASF Agricultural Center Limburgerhof, D-67117 Limburgerhof, Germany*
[2]*BASF Aktiengesellschaft, D-67056 Ludwigshafen, Germany*

Abstract: The herbicidal mode of action of the new synthetic cyanoacrylates ethyl (2*Z*)-3-amino-2-cyano-4-ethylhex-2-enoate (CA1) and its isopropyl ester derivative CA2 was investigated. For initial characterization, a series of bioassays was used indicating a mode of action similar to that of mitotic disrupter herbicides such as the dinitroaniline pendimethalin. Cytochemical fluorescence studies including monoclonal antibodies against polymerized and depolymerized tubulin and a cellulose-binding domain of a bacterial cellulase conjugated to a fluorescent dye were applied to elucidate effects on cell division processes including mitosis and microtubule and cell wall formation in maize roots. When seedlings were root treated with 10 μM of CA1 or CA2, cell division activity in meristematic root tip cells decreased within 4 h. The chromosomes proceeded to a condensed state of prometaphase, but were unable to progress further in the mitotic cycle. The compounds caused a complete loss of microtubular structures, including preprophase, spindle, phragmoplast and cortical microtubules. Concomitantly, in the cytoplasm, an increase in labelling of free tubulin was observed. This suggests that the herbicides disrupt polymerization and microtubule stability, whereas tubulin synthesis or degradation appeared not to be affected. In addition, cellulose labelling in cell walls of root tip cells was not influenced. The effects of CA1 and CA2 were comparable with those caused by pendimethalin. In transgenic *Arabidopsis* plants expressing a green fluorescent protein-microtubule-associated protein4 fusion protein, labelled arrays of cortical microtubules in living epidermal cells of hypocotyls collapsed within 160 min after exposure to 10 μM CA1 or pendimethalin. Moreover, a dinitroaniline-resistant biotype of goosegrass (*Eleusine indica* (L) Gaertn) with a point mutation in α-tubulin showed cross-resistance against CA1 and CA2. The results strongly indicate that the cyanoacrylates are a new chemical class of herbicide which possess the same antimicrotubule mechanism of action as dinitroanilines, probably including interaction with the same binding site in α-tubulin.

Keywords: antimicrotubular herbicides; cyanoacrylates; cytochemical fluorescence; tubulin interaction

1 INTRODUCTION

The herbicidal properties of cyanoacrylates were first reported by Huppatz *et al*[1] and Phillips and Huppatz.[2] These early compounds and derivatives synthesized later were reported to act by inhibiting photosystem II electron transport.[2,3] In the course of lead optimization, cyanoacrylates containing a 1-ethylpropyl side chain were synthesized by Huppatz and chemists from American Cyanamid Company and BASF Aktiengesellschaft.[4,5] Ethyl (2*Z*)-3-amino-2-cyano-4-ethylhex-2-enoate, CA1, and the corresponding isopropyl ester CA2 (Fig 1) are representatives of this new chemical group of herbicides.[4,5] These compounds preferentially control annual grass weeds in pre-emergence applications. The herbicidal activity of these cyanoacrylates appeared not to be based on photosynthetic electron transport inhibition. Preliminary experiments indicated that the compounds affect mitosis (Iwona T Birk, Marianne K Pedersen; personal communication).

Therefore, the aim of the present work was to investigate the herbicidal mode of action of the cyanoacrylates CA1 and CA2 in more detail. For initial characterization, a set of selected bioassays including plant and algae cell suspensions, *Lemna*, isolated mustard shoots, germinating cress seeds, the Hill reaction of isolated thylakoids and carbon gas-exchange measurements was used to obtain a physiological fingerprint of the compounds.[6,7] The response pattern was compared with profiles of herbicides with known modes of action to classify the biological activity. Since similarities to mitotic (microtubule) disrupter herbicides such as dinitroanilines were found, the effects of CA1 and CA2 on cell division processes were studied in maize roots by means of immunocytochemical fluorescence

* Correspondence to: Klaus Grossmann, BASF Agricultural Center, D-67117 Limburgerhof, Germany
E-mail: klaus.grossmann@basf-ag.de
†In Memoriam Dr Peter Plath, an outstanding chemist and colleague, who died September 2004
(*Received 11 January 2005; revised version received 29 April 2005; accepted 24 May 2005*)
Published online 20 July 2005

 Pest Manag Sci 1526–498X/2005/$30.00

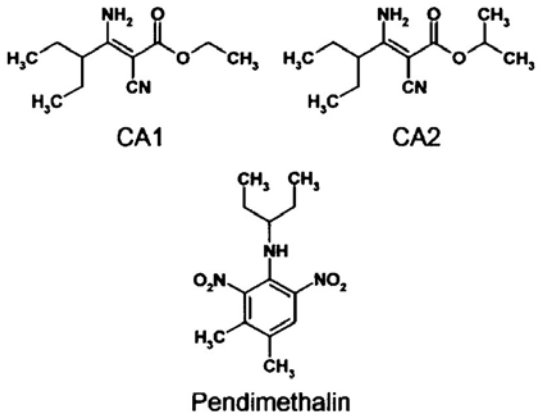

Figure 1. Structures of the cyanoacrylates CA1 and CA2 and the dinitroaniline pendimethalin.

techniques. In addition, transgenic *Arabidopsis* plants expressing a green fluorescent protein-microtubule-associated protein4 fusion protein (GFP::MAP4)[8,9] were used to visualize herbicide effects on microtubule arrangements in living epidermal cells. Moreover, a dinitroaniline-resistant biotype of *Eleusine indica* (L) Gaertn with a point mutation in α-tubulin was tested for cross-resistance against CA1 and CA2.

2 MATERIALS AND METHODS

2.1 Chemicals

The cyanoacrylates CA1 (ethyl (2*Z*)-3-amino-2-cyano-4-ethylhex-2-enoate;[4] Fig 1) and CA2 (isopropyl (2*Z*)-3-amino-2-cyano-4-ethylhex-2-enoate;[5] Fig 1) and pendimethalin (*N*-(1-ethylpropyl)-2,6-dinitro-3,4-xylidene) were obtained from BASF Aktiengesellschaft, Ludwigshafen, Germany.

2.2 Bioassays

In the heterotrophic cell suspension bioassay, freely suspended callus cells from *Galium mollugo* L (DSM Collection of Plant Cell cultures, Braunschweig, Germany) were cultivated in a modified Murashige–Skoog medium as described previously.[10] The cells were subcultured at 7-day intervals. Acetone solutions of the compounds were pipetted into plastic tubes and the solvent was allowed to evaporate before adding 2 ml of exponentially growing cell suspension. The tubes (three replicates) were shaken at 400 rpm and 25 °C in the dark on a rotary shaker. After incubation for 8 days, the conductivity of the medium was measured as the parameter for cell division growth.[10]

For the algae bioassay, cells of *Scenedesmus acutus* Pringsh (culture collection Göttingen, 276-3a, Göttingen, Germany) were propagated photoautotrophically.[10] The bioassay was carried out in plastic microtitre dishes containing 24 wells.[6,10] Before loading the wells with 0.5 ml of cell suspension each, 0.5 ml of medium and compound in acetone solution were added, allowing sufficient time for the organic solvent to volatilize. The 15 additional compartments between the wells were filled with sodium carbonate/bicarbonate buffer. The dishes were sealed with plastic lids and incubated on a shaker under continuous light at 23 °C. After 24 h, growth was measured photometrically.

For the *Lemna* bioassay, stock cultures of *Lemna paucicostata* (L) Hegelm (collection Prof R Kandeler, University of Vienna, Austria) were propagated mixotrophically in an inorganic medium containing sucrose.[10] The bioassay was conducted under aseptic conditions in plastic Petri dishes (5 cm diameter) containing 15 ml of medium without sucrose according to Grossmann *et al*.[10] The test compounds were added to the dishes in acetone solution and the organic solvent allowed to volatize before loading them with four fronds each. The culture dishes were then closed with plastic lids and incubated under continuous light (Philips TL white neon tubes, 40 μmol m^{-2} s^{-1} photon irradiance, 400–750 nm) in a growth chamber at 25 °C. Eight days after treatment, the increase of the area covered by the fronds in each dish was determined as the growth parameter, using an image analysing system (LemnaTec Scanalyzer; LemnaTec, Würselen, Germany). The area of fronds before incubation was subtracted from this value.

For the isolated shoot bioassay, seedlings of mustard (*Sinapis alba* L) were grown under standardized greenhouse conditions. The shoots were removed, weighed and placed upright in plastic vials (25 mm in diameter, 38 mm in height; Greiner, Nürtingen, Germany) containing 12 ml of double-distilled water, and the test compound was added in acetone solution.[6] To avoid evaporation, the vials were closed with plastic covers with slits into which the shoots were fitted (three shoots per vial). The vials were cultivated in growth chambers with 16:8 h light:dark photoperiod at 21 °C and 75% relative humidity (light: Osram krypton 100 W lamps and Osram universal white neon tubes, 200 μmol m^{-2} s^{-1} photon irradiance, 400–750 nm). After 3 days, the changes in fresh weight were measured by weighing the shoots and subtracting the value from the weight at the beginning.

For determination of effects on Hill reaction, thylakoids were isolated from shoots of young plants of *Triticum aestivum* L and assay was performed as described by Grossmann *et al*.[11] Isolated thylakoids were suspended in reaction medium (0.75 ml) containing sucrose (0.1 M), tricine-NaOH (pH 8.0; 50 mM), magnesium chloride (5 mM) and chlorophyll (41 μg ml^{-1}). The influence of the compounds on photosynthetic electron transport in photosystem II was performed according to the method of Avron and Shavit.[12] The assay mixture included thylakoid suspension (0.23 ml), test compound dissolved in acetone + water (80 + 20 by volume; 0.05 ml) and ferricyanide (0.02 ml). During the subsequent illumination, ferrocyanide was formed in the Hill reaction. Then, in darkness, the ferrocyanide was allowed to

react with ferric salt to form the ferrous salt which produced a complex with phenanthroline. The complex was measured photometrically at 510 nm.

For the germination bioassay, seeds of cress (*Lepidum sativum* L) and dinitroaniline-resistant and susceptible biotypes of goosegrass (*Eleusine indica* (L) Gaertn) were placed in glass Petri dishes (5 cm diameter) filled with a vermiculite substrate. In the experiments with cress, stock solutions of the test compounds in acetone were added together with 12 ml of water.[6] Control seeds were moistened only with water and acetone. The dishes were incubated in a growth chamber at 25 °C in the dark for 48 h. Inhibition of germination and seedling development was evaluated visually (0 = no influence, 100 = total inhibition). In the bioassay with *Eleusine*, stock solutions of the test compounds in dimethyl sulfoxide (DMSO) were added, together with 15 ml of half-strength Linsmaier–Skoog[13] nutrient solution. Control seeds were moistened only with nutrient solution and DMSO. The dishes were incubated in a growth chamber for 11 days (16:8 h light:dark at 20 °C/18 °C and 75% relative humidity, 230 µmol m^{-2} s^{-1} photon irradiance, 400–750 nm). Inhibition of seed germination was evaluated and the fresh weight of emerged seedlings was measured.

The results were expressed as percentage inhibition. Mean values of three replicates are given as the percentage inhibition relative to the control. Individual standard errors were less than 10%. All experiments were repeated at least twice and proved to be reproducible. The results of a representative experiment are shown.

2.3 Gas-exchange measurements

For determination of carbon dioxide uptake as a parameter for carbon dioxide assimilation, plants of *Galium aparine* L, which were raised under controlled conditions to the second whorl stage,[11] were cultivated hydroponically in illuminated glass chambers (four plants per chamber, three replications) that received a constant stream of air.[14] After foliar treatment, the amount of carbon dioxide assimilated per unit time was determined continuously from the difference between the carbon dioxide contents of the inflowing and outflowing air streams.

2.4 Histochemical determinations

Uniformly germinated seedlings of *Zea mays* L cv Dea with a root length of 3 cm were transferred into 50-ml glass vessels (one seedling per vessel, three replications) in half-strength Linsmaier–Skoog[13] nutrient solution (16:8 h light:dark at 25 °C/20 °C and 75% relative humidity, 250 µmol m^{-2} s^{-1}, photon irradiance, 400–700 nm; fluorescent lamps, radium HRLV). After 4 h of adaptation, the compounds were added to the medium in DMSO solution (1 ml $litre^{-1}$ final concentration of DMSO). Controls received a corresponding quantity of DMSO alone, with no adverse effect on seedling growth. After 4 or 24 h treatment, primary root tips of 5 mm length with meristematic and elongation zones were harvested, fixed in 37 g $litre^{-1}$ paraformaldehyde in phosphate-buffered saline (PBS, pH 7.4), and embedded in paraffin as described elsewhere.[15] Longitudinal sections of 7 µm thickness were obtained with a rotary microtome (Leica RM 2165; Bensheim, Germany) and placed on Polysine™ slides (Menzel, Braunschweig, Germany).

Specific staining for cellulose was based on a method described previously.[16] Root sections were deparaffinized and washed in phosphate–citrate buffer (pH 5.6).[15] The sections were subjected to an enzymatic digestion of pectins and hemicelluloses by incubation in phosphate–citrate buffer containing pectinase (from *Aspergillus niger* Tiegh, 2.2 U ml^{-1}) and hemicellulase (from *A niger*, 0.24 U ml^{-1}; Sigma, Taufkirchen, Germany), respectively, for 20 min at room temperature. After washing in phosphate–citrate buffer and Tris-buffered saline (TBST, pH 7.2, containing 50 mM Tris, 150 mM sodium chloride and 0.5 ml $litre^{-1}$ Tween 20), the samples were incubated in 200 µl of TBST containing 50 µg ml^{-1} bacterial cellulose-binding domain conjugated to biotin (Sigma) for 1 h at room temperature. The domain was conjugated using a biotin-protein labelling kit as described (Molecular Probes Europe BV, Leiden, Netherlands). For fluorescent staining of cellulose, the samples were treated with Alexa Fluor 488-conjugated streptavidin (Molecular Probes) against biotin-conjugated cellulose-binding domain for 30 min and washed in TBST. All slides were mounted in ProLong Antifade (Molecular Probes) for microscopic observation.

Microtubules or tubulin were labelled with monoclonal antibodies against polymerized β-tubulin (Sternberger Monoclonals, Lutherville, Maryland, USA) or a cocktail of two monoclonal antibodies against α-tubulin (polymerized/depolymerized, Clone DM1A) and β-tubulin (polymerized/depolymerized, Clone DM1B), respectively (Neomarkers, Fremont, California, USA). The primary antibodies were marked with fluorescent Alexa 488-conjugated secondary antibody (Molecular Probes) using a modification of the method described previously.[11,15] First, root tips were fixed in 40 g $litre^{-1}$ paraformaldehyde in microtubule stabilizing buffer (MSTB, pH 6.9) containing 60 mM PIPES [piperazine-*N*,*N*′-bis(2-ethanesulfonic acid)], 25 mM HEPES (*N*-2-hydroxyethylpiperazine-*N*′-2-ethanesulfonic acid), 10 mM EGTA (ethylenedioxybis(ethylenenitrilo)tetraacetic acid), 0.2 g $litre^{-1}$ $MgSO_4 \cdot 6H_2O$ for 14 h. Root tips were then subjected to a sequential series of sucrose infiltration containing 120, 140, 160 g $litre^{-1}$ sucrose in MSTB buffer for 1 h each step. Afterwards, they were frozen in liquid nitrogen. Longitudinal sections of 15 µm thickness were obtained with a cryostat (Frigocut-2800 E; Reichert-Jung, Leica, Bensheim, Germany) and placed on Polysine™ slides. The slides were incubated

with DAKO antibody diluent (DAKO Cytomation, Hamburg, Germany) for 20 min. Incubation with tubulin antibodies and the secondary antibodies was carried out for 30 min. The primary and secondary antibodies were diluted with DAKO antibody diluent to 1:200 and 1:100, respectively. The labelled slides were mounted with ProLong Antifade (Molecular Probes) for microscopic observation.

Nuclear DNA was stained with Hoechst 33 342 ($0.75\,\mu g\,ml^{-1}$) for 5 min. Microscopic observation was carried out using an Olympus BX61 epifluorescence microscope (Hamburg, Germany) and a confocal laser scanning microscope (Leica DMRXA TCS SP2) equipped with UV, krypton-argon, and green-neon laser.

2.5 *In vivo* analysis of MAP4::GFP labelled *Arabidopsis*

Transgenic *Arabidopsis* plants (Ecotype Landsberg erecta) carrying a MAP4::GFP gene driven by the cauliflower mosaic virus 35S promoter[8,9] were used in the experiments. The seed material was kindly provided by Dr Jaideep Mathur, University of Cologne, Germany. For time-lapse studies, seedlings were raised from surface-sterilized seeds in NUNC lab Tek chamber slides (NUNC, Wiesbaden, Germany) on $8\,g\,litre^{-1}$ agar in half-strength MSGV medium (Murashige Skoog nutrient solution with Gamborgs vitamins, pH 5.6; Sigma) containing $0.5\,g\,litre^{-1}$ MES (2-(*N*-morpholino)ethanesulfonic acid) and $10\,g\,litre^{-1}$ sucrose.[17] After 3 days (16:8 h light:dark at 24 °C/20 °C and 80% relative humidity, $100\,\mu mol\,m^{-2}\,s^{-1}$ photon irradiance), effects of compounds on epidermal cells of hypocotyls were observed using a Leica DMRXA TCS SP2 confocal system equipped with a krypton-argon laser (488 nm laser line was applied for GFP excitation) and 40× water immersion objective. Stock solutions of the test compounds in DMSO were added to half-strength MSGV medium which was used as immersion solution. The first stack of sections was started immediately after compound application. Subsequent stacks were taken every 20 min during a period of 3 h. The image stacks were analysed using the Leica TCS software and analysis® software package (Soft Imaging Systems, Münster, Germany).

3 RESULTS AND DISCUSSION

3.1 Physiological profiling using bioassays

In initial experiments, a set of bioassays has been used to characterize and classify the mode of action of the cyanoacrylates CA1 and CA2 in the search for their biochemical target. These systems included heterotrophic cleaver (*Galium mollugo*) and photoautotrophic green alga (*Scenedesmus acutus*) cell suspensions, duckweed (*Lemna paucicostata*), isolated mustard (*Sinapis alba*) shoots, germinating cress (*Lepidum sativum*) seeds, the Hill reaction of isolated wheat thylakoids and carbon gas-exchange measurements in cleaver (*Galium aparine*) plants. The response pattern involves effects on germination and the vegetative growth of cells and organized tissues with different types of metabolism, photosynthetic electron transport and carbon assimilation. It represents a fingerprint of a compound which has proved to be typical of its physiological mode of action.[6,7] The results can be interpreted directly, or a library of response patterns of compounds with known mode of action can be screened for similarities to provide some clues which can be used as an aid to direct further investigations.

The results clearly demonstrate that the inhibitory effects of the cyanoacrylates CA1 and CA2 on growth is not triggered through an inhibition of photosystem II electron transport (Fig 2). Even at the high concentration of 100 µM, the compounds had only slight effect on the Hill reaction, carbon assimilation and green alga growth. In contrast, CA1 and particularly CA2 inhibited frond production and growth of *Lemna* (Fig 2), which was accompanied

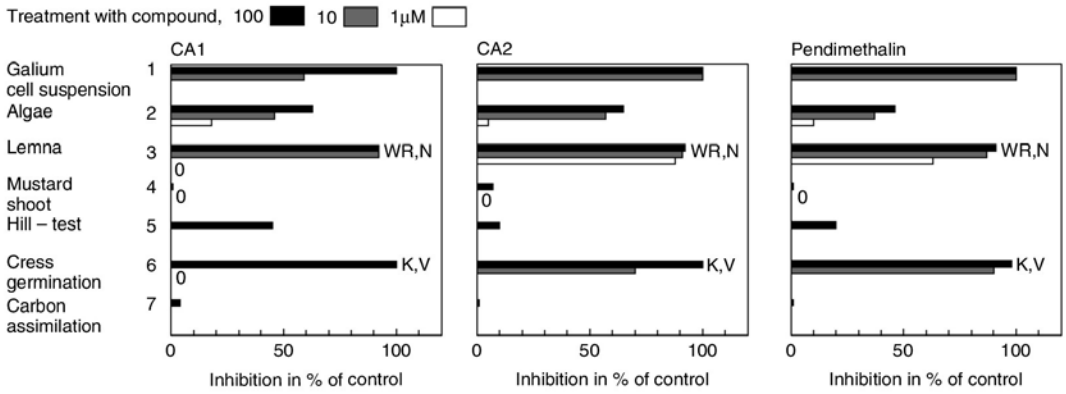

Figure 2. Effects of the cyanoacrylates CA1 and CA2 and pendimethalin in bioassays including *Galium* and algal cell suspensions, duckweed, isolated mustard shoots, the Hill reaction of isolated wheat thylakoids, germinating cress seeds and carbon assimilation in *Galium* plants. SE of the mean in all cases is less than 10%. Symptoms observed: WR, intensified green leaf pigmentation; N, necrosis; K, reduced seed germination; V, root swelling.

by an intensified chlorophyll pigmentation, followed by necrosis of the meristematic leaf area. Both compounds also showed pre-emergence activity on germinating seeds of cress in darkness (Fig 2). With increasing concentration, seed germination was reduced and hypocotyl and root growth of seedlings were stunted and both organs were swollen. In *Lemna* and cress, the symptoms resembled those caused by mitotic disrupter herbicides. Accordingly, in heterotrophic cell suspension cultures of *Galium*, cell division growth ceased at 10 µM (Fig 2). This system offers an appropriate model system for cell division growth in meristematic tissue, since growth is governed in meristems and in cell suspension cultures mainly by cell division activity and both cell species generally possess chloroplasts only as proplastids.[10] The results suggested that CA1 and CA2 act as cell division inhibitors. Accordingly, in isolated mustard shoots, which show only low growth activity during incubation, no response to compound treatment was observed (Fig 2). Overall, when compared with the effects of mitotic disrupter herbicides such as the dinitroaniline pendimethalin, CA1 and CA2 induced nearly the same type of physiological profile in the bioassays, indicating a similar mode of action (Fig 2).

3.2 Cytochemical observations

Mitotic (microtubule) disrupter herbicides such as pendimethalin affect cell division and expansion processes in plant growth by inhibiting microtubule formation. This includes preprophase, spindle and phragmoplast microtubules in mitosis and cortical microtubules in controlling growth direction and cell wall formation.[18,19] Microtubule disruption generates a decrease in cell elongation and isodiametric cell growth.[18,19] The root tips and other structures that are normally elongated swell into a characteristic club shape.[20,21]

The effects of CA1 and CA2 on cell division processes were studied in maize roots and compared with those of pendimethalin. Seedlings were treated hydroponically with 10 µM of compounds for 4 and 24 h. After 24 h, CA1 and CA2 caused club-shaped swelling of meristematic root tips and reduced root elongation similar to pendimethalin. Measured 3 mm from the top of adventitious tips ($n = 4$ to 8), root diameters increased from 90.4 (±2.2) µm in controls to 155.8 (±3.8) µm, 147.8 (±2.3) µm and 162.7 (±4.7) µm after treatment with CA1, CA2 or pendimethalin, respectively. The tips of primary and adventitious roots were sampled and serial longitudinal sections were processed for fluorescence microscopic examination. In order to investigate compound effects on mitosis and microtubules, nuclear DNA was stained with Hoechst 33 342 and microtubule arrays were visualized by means of fluorescence-labelled monoclonal antibodies against tubulin subunits. Microtubules are composed of polymers of the protein tubulin which is a heterodimer of two polypeptide subunits, α- and β-tubulin (reviewed by Anthony and Hussey[20]).

After treating seedlings with 10 µM CA1 or CA2, cell division activity in the apical root meristem decreased completely within 4 h (Plate 1A). The chromosomes proceeded to a condensed state of prometaphase, but were unable to progress further in the mitotic cycle (Plate 1A). Cells at metaphase, anaphase and telophase were not found. After 24 h, nuclear membranes reformed around the chromosomes which resulted in strongly lobed nuclei and, occasionally, in micronuclei distant from the main nucleus (not shown). Qualitatively and quantitatively identical effects were observed in pendimethalin-treated maize root cells (Plate 1A).

As observed using monoclonal antibody against polymerized β-tubulin, treatment with 10 µM of the compounds for 4 h affected all microtubule arrays in meristematic maize root cells (Plate 1B). CA1 and CA2 caused a complete loss of preprophase band and arrays of spindle and phragmoplast. Due to the loss of spindle and kinetochore microtubules, chromosomes cannot move to the poles of the cell during mitosis.[21] This results in mitotic root tip cells which are completely arrested in late prometaphase. Cortical microtubules were also absent and the cells expanded isodiametrically (Plate 1B), which leads to the phenomenon of root clubbing within 24 h. The overall loss of microtubules induced by CA1 and CA2 was comparable to that elicited by pendimethalin (Plate 1B).

A cocktail of two monoclonal antibodies against polymerized and depolymerized α- and β-tubulin subunits was used to evaluate additional effects of the herbicides on the level of free tubulin in treated maize root cells (Plate 1C). For the dinitroaniline antimicrotubule herbicide oryzalin, inhibitory effects on protein synthesis and tubulin degradation in cultured rice cells have recently been reported.[22] After 4 h of treatment with 10 µM CA1, CA2 or pendimethalin, a complete loss of microtubular structures was observed in meristematic root tip cells (Plate 1C). Concomitantly, in the cytoplasm, an increase in labelling of free tubulin was observed, compared to control cells (Plate 1C). This indicates that the herbicides disrupted polymerization and microtubule stability. In contrast, tubulin synthesis or degradation which modulates the tubulin level in cells was not affected. In accordance, when maize root tips were treated with 10 µM of the protein synthesis inhibitor cycloheximide, a decline in both microtubular structures and free tubulin labelling were observed (not shown).

A phenomenon of root clubbing is also induced by compounds which primarily inhibit cellulose biosynthesis in cell wall formation.[16,23] In this case, however, treated root tissue additionally shows a glassy appearance which is not caused by microtubule disrupter herbicides including CA1, CA2 and pendimethalin. To elucidate in more detail if CA1 and CA2 act

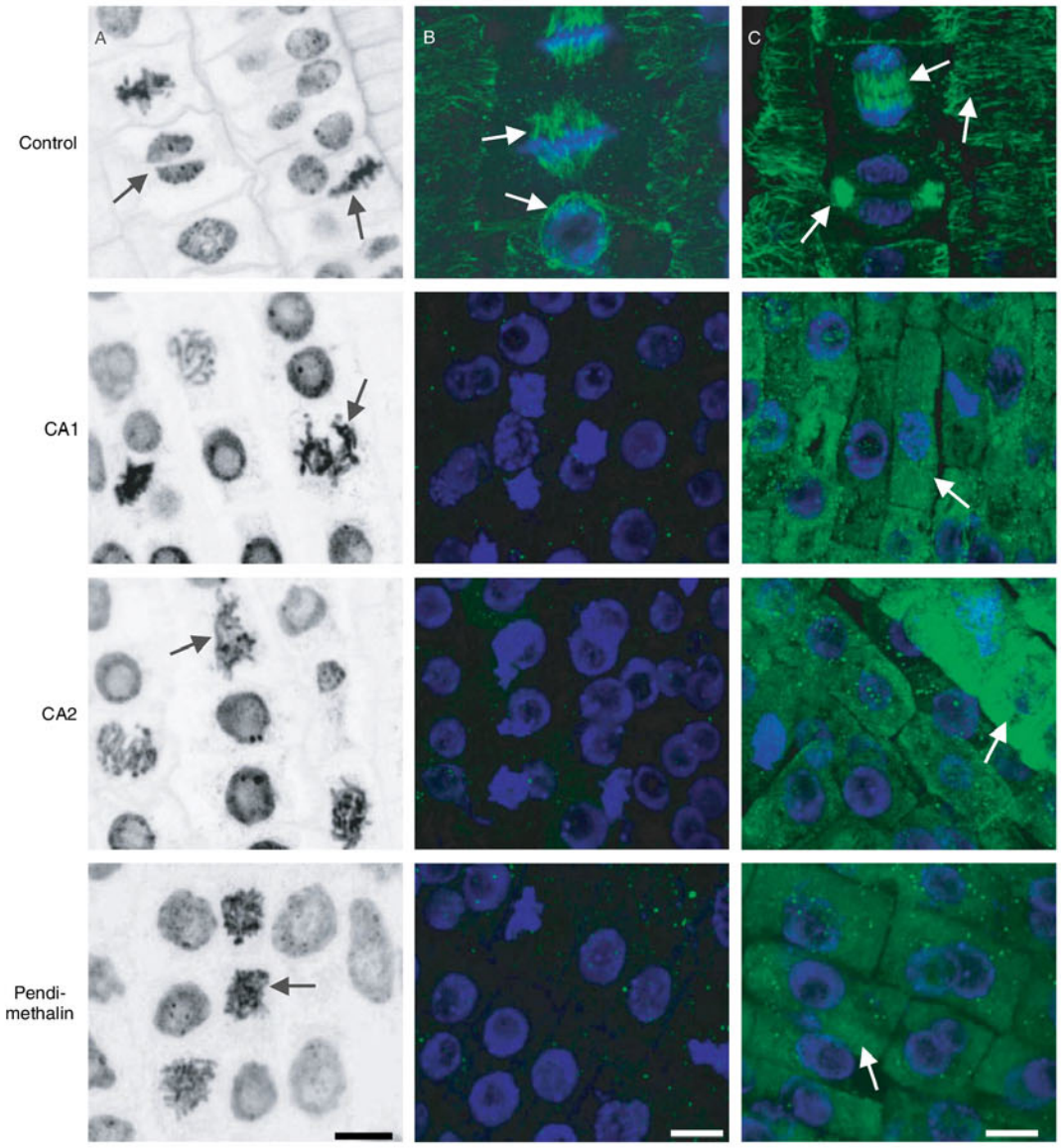

Plate 1. Effects of CA1, CA2 and pendimethalin on mitosis, the microtubule cytoskeleton and free tubulin in meristematic maize root cells. Seedlings were treated hydroponically with 10 μM of either herbicide for 4 h. Tips of primary and adventitious roots were sampled and serial longitudinal sections were processed for fluorescence microscopic examination. (A) Hoechst 33342 staining of mitotic structures. Control root tip cells undergoing mitosis; metaphase and telophase stages are denoted by arrows. CA1-, CA2- or pendimethalin-treated cells in arrested prometaphase (denoted by arrows). (B) Immunofluorescent staining of microtubules using monoclonal antibody against polymerized β-tubulin. Control cells show cortical, spindle and phragmoplast microtubules (denoted by arrows). CA1-, CA2-, or pendimethalin-treated cells show a complete loss in cortical, preprophase band, spindle and phragmoplast microtubules. (C) Immunofluorescent staining of microtubules and free tubulin using a cocktail of two monoclonal antibodies against polymerised and depolymerized α- and β-tubulin subunits. Control cells show cortical, spindle and phragmoplast microtubules (denoted by arrows). In the cytoplasm, free tubulin labelling is low. CA1-, CA2-, or pendimethalin-treated cells show a complete loss in preprophase band, spindle, phragmoplast and cortical microtubules. In contrast, in the cytoplasm, an increase in fluorescence resulting from labelling of free tubulin is observed, compared with control cells (denoted by arrows). Bar = 10 μm.

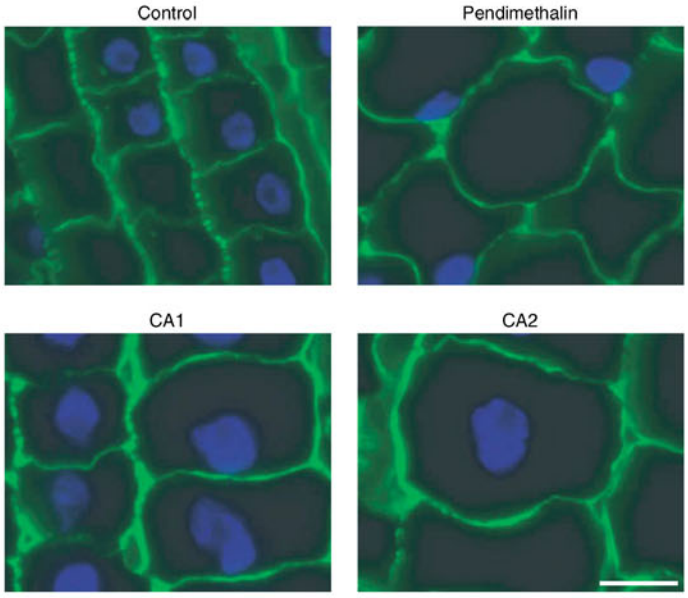

Plate 2. Effects of CA1, CA2 and pendimethalin on deposition of cellulose in cell walls of meristematic maize root cells. Seedlings were treated hydroponically with 10 μM compound for 24 h. Blue fluorescent staining of nuclear DNA was with Hoechst 33 342. Green fluorescent staining of cellulose was obtained using an isolated cellulose-binding domain of a cellulase conjugated to Alexa Fluor 488. Control cells and herbicide-treated, isodiametrically expanding cells showing similar cellulose labelling in parental walls. Bar = 20 μm.

as cellulose inhibitors, effects on cellulose deposition in meristematic root tip cells of maize were investigated (Plate 2). For cellulose localization in sections, an isolated cellulose-binding domain from a bacterial cellulase conjugated to a fluorescent dye was used. To improve labelling, cellulose localization was carried out after enzymatic digestion of hemicelluloses and pectins. As shown in the micrographs of root sections (Plate 2), treatment with 10 μM CA1, CA2 or pendimethalin for 24 h did not influence cellulose labelling in cell walls, compared with controls. This includes isodiametrically expanding root cells, which represent an appropriate means of demonstrating rapid effects on cellulose synthesis because *de novo* cellulose synthesis is needed for this growth.[16,23] The result indicates that cellulose synthesis is not affected by the compounds.

3.3 Experiments with microtubule GFP-labelled and mutant plants

For *in vivo* analysis of compound effects on the microtubular system, microtubule-targeted GFP-labelled *Arabidopsis* plants were used. These plants express constitutively a microtubule reporter gene which was constructed by fusing the microtubule binding domain of the mammalian microtubule-associated protein4 (MAP4) gene with the GFP gene.[8,9] This allows visualization of microtubule rearrangements in living epidermal cells of hypocotyls using confocal microscopy and time-course analysis of labelled cortical arrays. When *Arabidopsis* seedlings were treated with 10 μM CA1 or pendimethalin, labelled cortical microtubules in epidermal cells collapsed within 160 min (Fig 3). The collapse was initially detectable 40 and 60 min after application of pendimethalin or CA1, respectively (Fig 3). This indicates rapid microtubule depolymerization caused by the compounds. Together with the cytochemical observations, these results suggest that the cyanoacrylates are microtubule disrupter herbicides which affect processes of microtubule polymerization and depolymerization by a mechanism similar to that of dinitroanilines.

The molecular action of dinitroaniline-type herbicides has been investigated by means of a highly dinitroaniline-resistant biotype of green foxtail (*Setaria viridis* (L) Beauv)[24] and goosegrass (*Eleusine indica*).[25] In various cropping systems, *E indica* is an important weed which is effectively controlled by pre-emergence application of dinitroaniline herbicides. However, following many years of herbicide use, resistant biotypes of *Eleusine* have been identified. The molecular basis of the resistance has been found to be a point mutation in α-tubulin.[26,27] Hence, for further characterization of the antimicrotubule mechanism of CA1 and

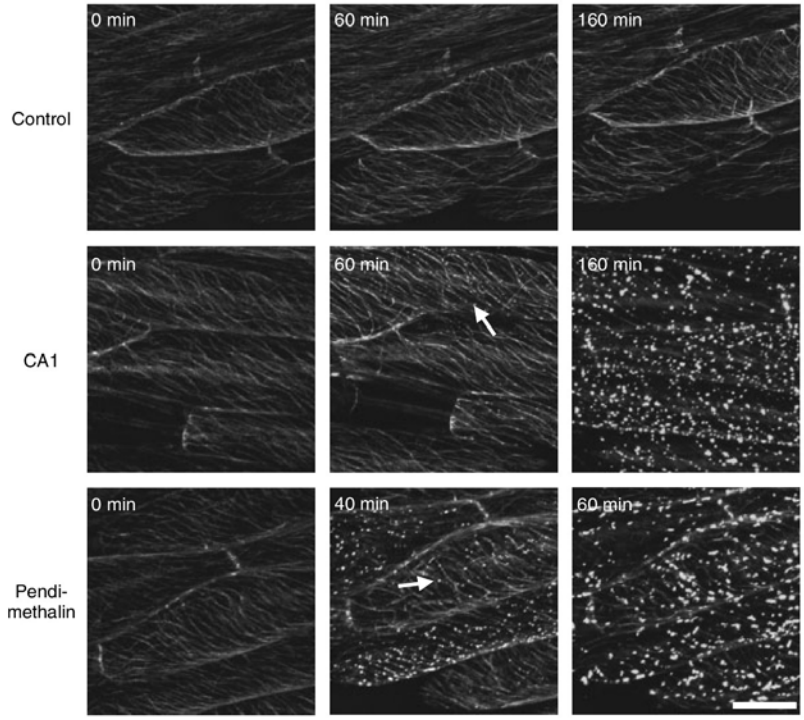

Figure 3. Effects of CA1 and pendimethalin on the arrangement of cortical microtubules in epidermal cells of hypocotyls in MAP4::GFP labelled *Arabidopsis* observed by confocal laser scanning microscopy. Collapse of microtubules and concomitant appearance of white spots were initially detectable at 40 and 60 min after application of pendimethalin or CA1, respectively (denoted by arrows). White spots are most likely a result of an aggregation of MAP4::GFP fusion proteins to small microtubule segments. Seedlings were treated with 10 μM of CA1 or pendimethalin in time-lapse studies. Bar = 10 μm.

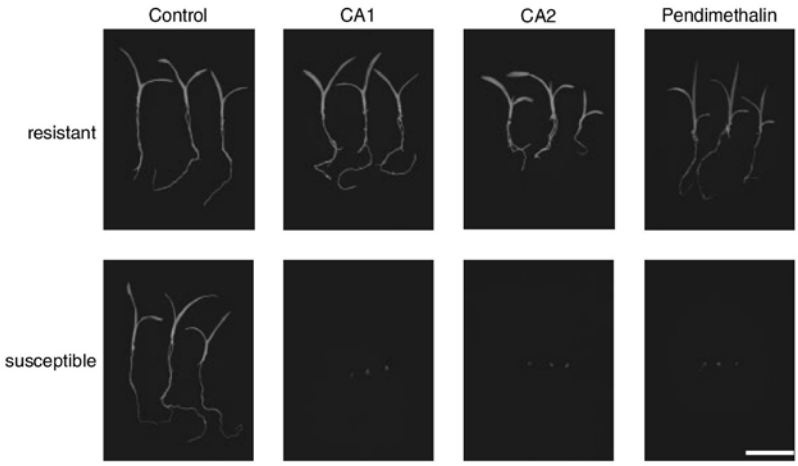

Figure 4. Effects of CA1 and CA2 and pendimethalin on seed germination and seedling development of dinitroaniline-resistant and -susceptible goosegrass (*Eleusine indica*). Seeds were treated with 5 μM of either herbicide for 11 days. Bar = 20 mm.

CA2, this dinitroaniline-resistant biotype of *Eleusine* was used to investigate whether the mutation also confers resistance to the cyanoacrylates. As shown in Fig 4, seed treatment with 5 μM pendimethalin, CA1 or CA2 only slightly influenced seed germination and seedling development of dinitroaniline-resistant *E indica*. Fresh weight of seedlings ($n = 24$ per treatment) changed from 10.3 (±0.7) mg in controls to 8.9 (±1.6) mg, 10.8 (±0.7) mg and 9.5 (±1.4) mg after application of pendimethalin, CA1 and CA2, respectively. In contrast, seed germination of dinitroaniline-susceptible *E indica* was completely inhibited by 5 μM pendimethalin, CA1 or CA2 (Fig 4). In addition, a biotype of green foxtail (*S viridis*) which has been found to be resistant to the dinitroaniline trifluralin[28] showed cross-resistance to the cyanoacrylates (Marianne K Pedersen, Oskar Schmidt; personal communication).

4 CONCLUSION

Mitotic (microtubule) disrupter herbicides belong to the most successful herbicides used in agriculture. Herbicides in this group include dinitroanilines, such as trifluralin and pendimethalin, phosphoric amides, and carbamates (see recent reviews by Molin and Khan,[29] and by Vaughn[21]). In addition to their value as herbicides, dinitroaniline-type compounds have been used as antimicrotubule agents for studying microtubule-dependent processes in higher plants. These compounds have been found to interfere with microtubule assembly by forming a tubulin–dinitroaniline complex that disrupts polymerization and microtubule stability (reviewed by Anthony and Hussey,[20] Vaughn[21]). Genetic data which implicate tubulin as the principal site of action for these herbicides came from studies in *Chlamydomonas* and particularly by using highly dinitroaniline-resistant biotypes of *E indica* and *S viridis*.[20,24] In the latter case, a specific base change in the coding sequence of the TUA1 gene causes an amino acid substitution in the α-tubulin.[20,27,30] A threonine at position 239, which is conserved in the deduced amino acid sequences of all known α-tubulins, was substituted by an isoleucine. This resulted in spatial reorganization of the α-tubulin surface which prevents dinitroaniline binding.[26,27,30] In contrast, genes of β-tubulin appeared not to be associated with dinitroaniline resistance in *Eleusine*.[31]

Taken together, the physiological profile, the characteristic club-shaped root tip swelling, the cytochemical observations and the microtubule mutant and GFP-labelled plant studies strongly indicate that the cyanoacrylates induce disruption of mitosis through the same antimicrotubule mechanism as dinitroaniline-type herbicides. This probably includes interaction with the same binding site in plant α-tubulin. In contrast, in mammalian HeLa-cells, the cyanoacrylates and pendimethalin do not affect mitosis and microtubule assembly (Stefan Tresch, Carola Gunkel, Thorsten Jabs, Klaus Grossmann; unpublished results). This suggests selectivity of the compounds between plants and mammals in influencing the microtubule system.

ACKNOWLEDGEMENTS

The authors thank Dr Jaideep Mathur (University of Cologne, Germany) for a gift of GFP-MAP4-labelled *Arabidopsis* seeds, Sigrid Hennig, Simone Huber and Anneliese Keller for technical assistance and Dr Rex Liebl for critical reading of the manuscript and valuable discussion.

REFERENCES

1 Huppatz JL, Phillips JN and Rattigan BM, Cyanoacrylates. Herbicidal and photosynthetic inhibitory activity. *Agric Biol Chem* **45**:2769–2773 (1981).

2 Phillips JN and Huppatz JL, Cyanoacrylate inhibitors of photosynthetic electron transport in atrazine susceptible and atrazine resistant *Brassica* chloroplasts. *Z Naturforsch* **42**:670–673 (1987).

3 Wang Q, Yonghong HL and Huang R, Synthesis and herbicidal activity of 2- cyano-3-(2-chlorothiazol-5-yl)methylamino-acrylates. *J Agric Food Chem* **52**:1918–1922 (2004).

4 Everson AC, Coughlin DJ, Guaciaro MA, Fleming LB, Maravetz LL and Huppatz JL, β-Amino-α-cyanoacrylates and their use as herbicides. PCT Int Appl WO 03 51,823 (2003).

5 Plath P, Goetz N, Rack M, Landes A, Zagar C, Witschel M and Grossmann K, Production of α-cyano-ß-aminoacrylates and their salts useful as herbicides. PCT Int Appl WO 03 51,824 (2003).

6 Grossmann K and Retzlaff G, Bioregulatory effects of the fungicidal strobilurin kresoxim-methyl in wheat (*Triticum aestivum*). *Pestic Sci* **50**:11–20 (1997).

7 Grossmann K, What it takes to get a herbicide's mode of action. Physionomics, a classical approach in a new complexion. *Pest Manag Sci* **61**:423–431 (2005).

8 Marc JM, Granger CL, Brincat J, Fisher DD, Kao T-H, McCubbin AG and Cyr RJ, A *GFP-MAP4* Reporter gene for visualizing cortical microtubule rearrangements in living epidermal cells. *Plant Cell* **10**:1927–1939 (1998).

9 Mathur J and Chua N-H, Microtubule stabilization leads to growth reorientation in *Arabidopsis* trichomes. *Plant Cell* **12**:465–477 (2000).

10 Grossmann K, Berghaus R and Retzlaff G, Heterotrophic plant cell suspension cultures for monitoring biological activity in agrochemical research. Comparison with screens using algae, germinating seeds and whole plants. *Pestic Sci* **35**:283–289 (1992).

11 Grossmann K, Tresch S and Plath P, Triaziflam and diamino-triazine derivatives affect enantioselectively multiple herbicide target sites. *Z Naturforsch* **56c**:559–569 (2001).

12 Avron M and Shavit N, A simple method for determination of ferrocyanide. *Anal Biochem* **6**:549–554 (1963).

13 Linsmaier EM and Skoog F, Organic growth factor requirements of tobacco tissue cultures. *Physiol Plant* **18**:100–127 (1964).

14 Scheltrup F and Grossmann K, Abscisic acid is a causative factor in the mode of action of the auxinic herbicide quinmerac in cleaver (*Galium aparine* L). *J Plant Physiol* **147**:118–126 (1995).

15 Ruzin SE. (Ed), *Plant Microtechnique and Microscopy*. Oxford University Press, Oxford (1999).

16 Tresch S and Grossmann K, Quinclorac does not inhibit cellulose (cell wall) biosynthesis in sensitive barnyard grass and maize roots. *Pestic Biochem Physiol* **75**:73–78 (2003).

17 Haseloff J, Dormand E-L and Brand AH, Life imaging of green fluorescent Protein, in *Methods in molecular biology: protocols in confocal microscopy*, ed by Paddock SW. Humana Press, Totowa, Chapter 17, pp 241–259 (1999).

18 Nick P, Control of plant shape, in *Plant microtubules. Potential for biotechnology*, ed by Nick P. Springer, Berlin, Heidelberg, pp 25–50 (2000).

19 Wasteneys GO, Progress in understanding the role of microtubules in plant cells. *Current Opinion in Plant Biology* **7**:651–660 (2004).

20 Anthony RG and Hussey PJ, Dinitroaniline herbicide resistance and the microtubule cytoskeleton. *Trends Plant Sci* **4**:112–116 (1999).

21 Vaughn KC, Anticytoskeletal herbicides, in *Plant microtubules. Potential for biotechnology*, ed by Nick P. Springer, Berlin, Heidelberg, pp 193–205 (2000).

22 Giani S, Campanoni P and Breviario D, A dual effect on protein synthesis and degradation modulates the tubulin level in rice cells treated with oryzalin. *Planta* **214**:837–847 (2002).

23 Sabba RP and Vaughn KC, Herbicides that inhibit cellulose biosynthesis. *Weed Sci* **47**:757–763 (1999).

24 Delye C, Menchari Y, Michel S and Darmency H, Molecular bases for sensitivity to tubulin-binding herbicides in green foxtail. *Plant Physiol* **136**:3920–3932 (2004).

25 Zeng L and Baird WV, Genetic basis of dinitroaniline herbicide resistance in an highly resistant biotype of goosegrass (*Eleusine indica*). *J Hered* **88**:427–432 (1997).

26 Anthony RG, Walden TR, Ray JA, Bright SWJ and Hussey PJ, Herbicide resistance caused by spontaneous mutation of the cytoskeletal protein tubulin. *Nature (London)* **393**:260–263 (1998).

27 Yamamoto E, Zeng L and Baird WV, α-Tubulin missense correlate with antimicrotubule drug resistance in *Eleusine indica*. *Plant Cell* **10**:297–308 (1998).

28 Beckie HJ and Morrison IN, Effective kill of trifluralin-susceptible and -resistant green foxtail (*Setaria viridis*). *Weed Tech* **7**:15–22 (1993).

29 Molin WT and Khan RA, Mitotic disrupter herbicides: recent advances and opportunities, in *Herbicide activity: toxicology, biochemistry and molecular biology*, ed by Roe RM, Burton JD and Kuhr RJ. IOS Press, Amsterdam, pp 111–141 (1997).

30 Blume YB, Nyporko AY, Yemets AI and Baird WV, Structural modeling of the interaction of plant α-tubulin with dinitroaniline and phosphoroamidate herbicides. *Cell Biol Int* **27**:171–174 (2003).

31 Yamamoto E and Baird WV, Molecular characterization of four ß-tubulin genes from dinitroaniline susceptible and resistant biotypes of *Eleusine indica*. *Plant Mol Biol* **39**:45–61 (1999).

3.2. Flamprop-m-methyl has a new antimicrotubule mechanism of action

The MoA of flamprop-m-methyl has not been studied in detail in the past. Only several papers have described more general effects of flamprop-m-methyl on membrane fluidity (Gauvrit, 1984; Rattermann and Balke, 1988) and cell division (Morrison *et al.*, 1979). Our initial phenotyping assays indicated a more specific MoA of flamprop-m-methyl on cell division. Therefore, the experiments described in Tresch *et al.* (2008) were designed to study the effect of flamprop-m-methyl on cell division in more detail. It was possible to demonstrate a direct influence of flamprop-m-methyl on the microtubule cytoskeleton different from the effect of typical microtubule assembly inhibitors such as dinitronanilines or cyanoacrylates. Nevertheless, it was not possible to identify the molecular target of flamprop-m-methyl, but the investigations led to the hypothesis that flamprop-m-methyl interacts with a signalling cascade to regulate the microtubule cytoskeleton. The description of the MoA in cytoskeletal or cell-cycle regulation is a good basis for further chemical genetic screens to unravel regulator components in cell division or cytoskeletal regulation.

Pest Management Science *Pest Manag Sci* **64**:1195–1203 (2008)

The herbicide flamprop-M-methyl has a new antimicrotubule mechanism of action

Stefan Tresch, Ricarda Niggeweg and Klaus Grossmann*
BASF Agricultural Centre Limburgerhof, D-67117 Limburgerhof, Germany

Abstract

BACKGROUND: The herbicidal mode of action of flamprop-M-methyl [methyl *N*-benzoyl-*N*-(3-chloro-4-fluorophenyl)-D-alaninate] was investigated.

RESULTS: For initial characterization, a series of bioassays was used, which indicated a mode of action similar to that of mitotic disrupter herbicides. Cytochemical fluorescence studies, which included monoclonal antibodies against polymerized tubulin, were applied to elucidate effects on mitosis and microtubule assembly in maize roots. When seedlings were root treated with 50 μM of flamprop-M-methyl, cell division activity in meristematic root tip cells ceased within 4 h. The compound severely disturbed the orientation of spindle and phragmoblast microtubules, leading to defective spindle and phragmoblast structures. Cortical microtubules were only slightly affected. In late anaphase and early telophase cells, phragmoblast microtubules were disorganized in multiple arrays that hampered regular cell plate deposition in cytokinesis. Microtubules of the spindle apparatus were found attached to chromosomal kinetochores, but did not show regular organization associated with a zone of microtubule-organizing centres at the opposite ends of the cell. On account of this loss of spindle organization, chromosomes remained in a condensed state of prometaphase or metaphase. Unlike known microtubule disrupter herbicides, flamprop-M-methyl and its biologically active metabolite flamprop did not inhibit soybean tubulin polymerization to microtubules *in vitro* at 50 μM. In contrast, soybean plants responded sensitively to the compounds.

CONCLUSION: The results indicate that flamprop-M-methyl is a mitotic disrupter herbicide with a new antimicrotubule mechanism of action that affects orientation of spindle and phragmoblast microtubules, possibly by minus-end microtubule disassembly.

Keywords: antimicrotubular herbicides; flamprop-M-methyl; cytochemical fluorescence; tubulin polymerization

1 INTRODUCTION

The herbicidal properties of the arylaminopropionic acid derivatives flamprop-M-isopropyl and flamprop-M-methyl were first reported by Jeffcoat and Harries in 1975.[1,2] The compounds were commercially introduced by Shell and American Cyanamid (now BASF) preferentially for the selective, post-emergence control of wild oats (*Avena* spp.) and blackgrass (*Alopecurus myosuroides* Huds.) in barley and wheat.[1,2] Herbicidal activity depends on hydrolytic conversion of the esters within the plant to the corresponding acid flamprop, which is the biologically active compound, transported to meristems in sensitive plants.[1,2] De-esterification was also found to be the basis for selectivity because this conversion occurs much more slowly in wheat and barley than in wild oats.[1,2] Histological studies showed that flamprop-M-methyl inhibited cell division and cell elongation in wild oats through a mode of action that has remained unknown to this day.[3] Flamprop-M-isopropyl was found to inhibit electron transfer in isolated rat liver mitochondria[4] and proton gradient development in membrane vesicles from oat root,[5] showing a potential to disrupt membrane function. However, the free carboxylic acid flamprop was far less effective than the esters,[4] indicating that disruption of membrane function is not the primary mode of action in plants.

Therefore, the aim of this study was to analyse the herbicidal mode of action of flamprop-M-methyl in more detail. By virtue of symptomology of plant damage exhibited by stunted shoot growth with intensified chlorophyll pigmentation, followed by tissue necrosis and histological studies,[3] it was hypothesized that flamprop-M-methyl primarily affects mitosis and cell expansion. This phenomenon might be achieved directly via disruption of microtubule formation or orientation, or indirectly via inhibition of very-long-chain fatty acid synthesis.

For initial characterization, an array of bioassays was used in a physionomics approach for comprehensive physiological profiling of flamprop-M-methyl effects.[6]

* Correspondence to: Klaus Grossmann, BASF Agricultural Centre, D-67117 Limburgerhof, Germany
E-mail: klaus.Grossmann@basf.com
(*Received 19 October 2007; revised version received 27 February 2008; accepted 7 April 2008*)
Published online 13 June 2008; DOI: 10.1002/ps.1618

The response pattern was compared with profiles of herbicides with known modes of action to classify the biological activity. Since similarities to mitotic (microtubule) disrupter herbicides such as dinitroanilines were found, the effects of flamprop-M-methyl on cell division processes were studied in maize roots by means of immunocytochemical fluorescence techniques. In addition, effects of flamprop-M-methyl and flamprop on *in vitro* polymerization of plant tubulin were investigated.

2 MATERIALS AND METHODS

2.1 Chemicals

Flamprop-M-methyl [methyl *N*-benzoyl-*N*-(3-chloro-4-fluorophenyl)-D-alaninate] (see Fig. 1), flamprop [*N*-benzoyl-*N*-(3-chloro-4-fluorophenyl)-DL-alanine] (see Fig. 1), pendimethalin [*N*-(1-ethylpropyl)-2,6-dinitro-3,4-xylidene] (see Fig. 2), CA2 [isopropyl (2*Z*)-3-amino-2-cyano-4-ethylhex-2-enoate] and metazachlor [2-chloro-*N*-(pyrazol-1-ylmethyl)acet-2′, 6′-xylidide] (see Fig. 2) were obtained from BASF SE, Ludwigshafen, Germany.

2.2 Bioassays and assay of acetyl-CoA carboxylase

The bioassays of the physionomics approach were carried out as described elsewhere.[6] In the heterotrophic cell suspension bioassay, freely suspended callus cells from *Zea mays* L. (DSM Collection of Plant Cell Cultures, Braunschweig, Germany) were cultivated in a modified Murashige–Skoog medium as described previously.[6] The cells were subcultured at 7 day intervals. Acetone solutions of the compounds were pipetted into plastic tubes, and the solvent was allowed to evaporate before adding 2 mL of exponentially growing cell suspensions. The tubes (three replicates) were shaken at 400 rpm and 25 °C in the dark on a rotary shaker. After incubation for 8 days, the conductivity of the medium was measured as the parameter for cell division growth.[6]

For the algae bioassay, cells of *Scenedesmus acutus* Pringsh (Culture Collection Göttingen, 276-3a, Göttingen, Germany) were propagated photoautotrophically.[6] The bioassay was carried out in plastic microtitre dishes containing 24 wells.[6] Before loading each well with 0.5 mL cell suspension, 0.5 mL medium and compound in acetone solution were added, allowing sufficient time for the organic solvent to volatilize. The 15 additional compartments between the wells were filled with sodium carbonate/bicarbonate buffer. The dishes were sealed with plastic lids and incubated on a shaker under continuous light at 23 °C. After 24 h, growth was measured photometrically.

For the *Lemna* bioassay, stock cultures of *Lemna paucicostata* (L.) Hegelm (Collection Prof. R Kandeler, University of Vienna, Austria) were propagated mixotrophically in an inorganic medium containing sucrose.[6] The bioassay was conducted under aseptic conditions in plastic petri dishes (5 cm diameter)

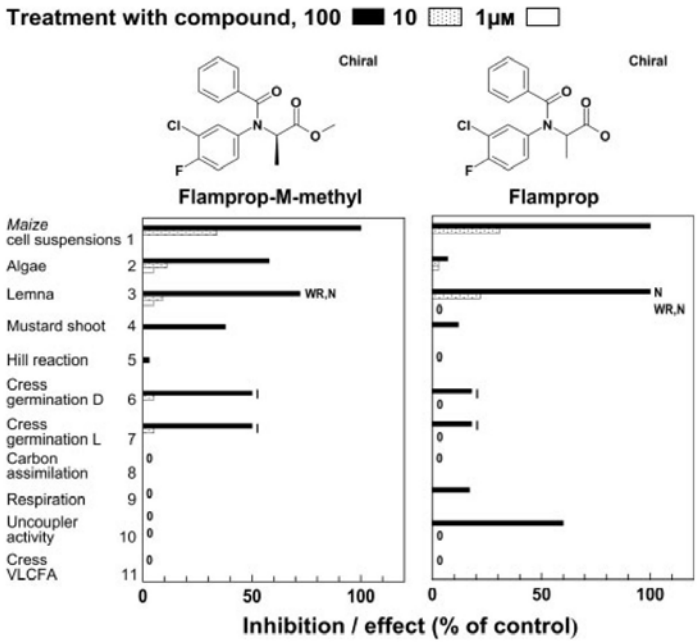

Figure 1. Effects of flamprop-M-methyl and flamprop in bioassays including maize and algal cell suspensions, duckweed, isolated mustard shoots, germinating cress seeds, the Hill reaction of isolated wheat thylakoids, respiration by measuring oxygen consumption in heterotrophic *Galium* cell suspensions, uncoupler activity in *Lemna* root mitochondria, carbon assimilation in *Galium* plants and toluidine-blue staining of cress hypocotyls on inhibition of very-long-chain fatty acid (VLCFA) synthesis. SE of the mean in all cases was less than 10%. Symptoms observed: I, root growth inhibition; N, necrosis; WR, intensified green leaf pigmentation.

Pest Manag Sci **64**:1195–1203 (2008)
DOI: 10.1002/ps

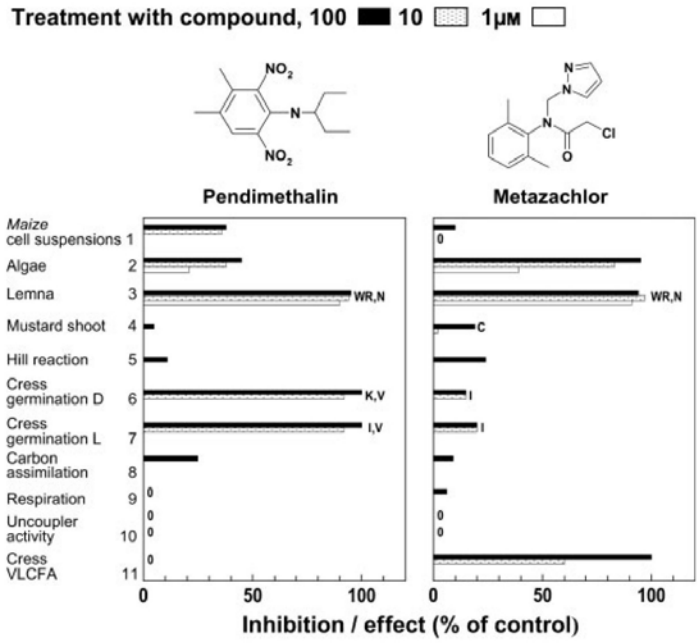

Figure 2. Effects of pendimethalin and metazachlor in bioassays including maize and algal cell suspensions, duckweed, isolated mustard shoots, germinating cress seeds, the Hill reaction of isolated wheat thylakoids, respiration by measuring oxygen consumption in heterotrophic *Galium* cell suspensions, uncoupler activity in *Lemna* root mitochondria, carbon assimilation in *Galium* plants and toluidine-blue staining of cress hypocotyls on inhibition of very-long-chain fatty acid (VLCFA) synthesis. SE of the mean in all cases was less than 10%. Symptoms observed: C, chlorosis; I, root growth inhibition; K, reduced seed germination; N, necrosis; V, root swelling; WR, intensified green leaf pigmentation.

which contained 15 mL medium without sucrose. The test compounds were added to the dishes in acetone solution, and the organic solvent was allowed to volatize before loading them with four fronds each. The culture dishes were then closed with plastic lids and incubated under continuous light (Philips TL white neon tubes, 40 µmol m^{-2} s^{-1} photon irradiance, 400–750 nm) in a growth chamber at 25 °C. Eight days after treatment, the increase in the area covered by the fronds in each dish was determined as the growth parameter using an image analysing system (LemnaTec Scanalyzer; LemnaTec, Würselen, Germany).

For the isolated shoot bioassay, seedlings of mustard (*Sinapis alba* L.) were grown under standardized greenhouse conditions. The shoots were removed, weighted and placed upright in plastic vials (25 mm diameter, 38 mm height; Greiner, Nürtingen, Germany) which contained 12 mL double-distilled water and the test compound added in acetone solution.[6] To avoid evaporation, the vials were closed with plastic covers with slits into which the shoots were fitted (three shoots per vial). The vials were cultivated in growth chambers with a 16:8 h light:dark photoperiod at 21 °C and 75% relative humidity (light: Osram krypton 100 W lamps and Osram universal white neon tubes, 200 µmol m^{-2} s^{-1} photon irradiance, 400–750 nm). After 3 days, changes in fresh weight were measured by weighing the shoots and subtracting the values from the initial weights.

To determine effects on the Hill reaction, thylakoids were isolated from shoots of young plants of *Triticum aestivum* L., and assay was performed as previously described.[6] Isolated thylakoids were suspended in a reaction medium (0.75 mL) that contained sucrose 0.1 M, tricine-NaOH (pH 8.0) 50 mM, magnesium chloride 5 mM and chlorophyll 41 µg mL^{-1}. The assay mixture included thylakoid suspension (0.23 mL), test compound dissolved in acetone + water (80 + 20 by volume; 0.05 mL) and ferricyanide (0.02 mL). During the subsequent illumination, ferrocyanide was formed in the Hill reaction. Then, in darkness, the ferrocyanide was allowed to react with ferric salt to form the ferrous salt, which produced a complex with phenanthroline. The complex was measured photometrically at 510 nm.

For the germination bioassay, seeds of cress (*Lepidum sativum* L.) were placed in glass petri dishes (5 cm in diameter) filled with a vermiculite substrate. Stock solutions of the test compounds in acetone were added together with 12 mL water.[6] Control seeds were moistened only with water and acetone. The dishes were incubated in a growth chamber at 25 °C in the dark for 3 days. Inhibition of germination and seedling development was evaluated visually (0 = no influence, 100 = total inhibition). Afterwards, the dishes were incubated for a further 3 days under light conditions (16:8 h light:dark at 25 °C and 75% relative humidity, 230 µmol m^{-2} s^{-1} photon irradiance, 400–750 nm), and seedling development and plant symptoms were

evaluated. For visualization of cuticular defects as an indication of compound-induced inhibition of very-long-chain fatty acid (VLCFA) synthesis in cuticular wax formation, seedling shoots were cut off and stained with toluidine-blue for 5 min, as described by Tanaka *et al.*[7] The epidermal surface of hypocotyl without a functional cuticle is permeable to the hydrophilic dye toluidine-blue, which leads to blue staining of hypocotyl tissue.

To determine carbon dioxide uptake as a parameter for carbon dioxide assimilation, plants of *Galium aparine* L. that had been raised under controlled conditions to the second whorl stage were cultivated hydroponically in illuminated glass chambers (four plants per chamber, three replications) which received a constant stream of air.[6] After foliar treatment, the amount of carbon dioxide assimilated per unit time was determined continuously from the difference between the carbon dioxide contents of the inflowing and outflowing air streams.

For the determination of respiration, cell suspensions of *Galium mollugo* L. (DSM Collection of Plant Cell Cultures, Braunschweig, Germany) were treated with compound in plastic vessels for 5 h in the dark on a rotary shaker. Samples of 5 mL cell suspension were then transferred to plastic tubes for measurement of oxygen consumption using the dissolved oxygen measuring system inoLab Oxi Level 3 with the oxygen sensor CellOx 325 (WTW, Weilheim, Germany).[6]

To determine the uncoupler activity of compounds, *Lemna* plants were pretreated with the mitochondrial potential sensor dye JC-1 (10 µg mL^{-1} medium; Molecular Probes Europe BV, Leiden, The Netherlands) for 30 min. JC-1 exhibits potential-dependent accumulation in mitochondria, indicated by a fluorescence emission shift from green to red.[6] Mitochondrial membrane depolarization is indicated by a decrease in the red/green fluorescence intensity ratio. After staining, *Lemna* plants were washed and loaded into 48-well plastic microtitre dishes, with each well containing four fronds, 0.5 mL medium and compound added in acetone solution. After treatment for 10 min, *Lemna* plants were transferred to slides for fluorescence microscopic observation of root mitochondria using an Olympus BX61 epifluorescence microscope (Hamburg, Germany).

The results were expressed as percentage inhibition. Mean values of three replicates are given as the percentage inhibition relative to the control. Individual standard errors were less than 10%. All experiments were repeated at least twice and proved to be reproducible. The results of a representative experiment are shown.

Determination of effects on acetyl-CoA carboxylase activity *in vitro* was based on a modified method described previously.[8] Coleoptiles from *Z. mays* (200 g frozen material) were homogenized in 400 mL of a medium containing tris(hydroxymethyl)aminomethane (Tris)/HCl buffer (pH 8.0) 100 mM, glycerol 200 mL L^{-1}, EDTA 2 mM, sodium bicarbonate 15 mM, mercaptoethanol 14 mM and phenylmethylsulfonylfluoride (PMSF) 0.4 mM. The extract was filtered, incubated with Dowex for 15 min at 4 °C and centrifuged. The ACCase activity was collected by adding solid ammonium sulfate to the supernatant up to a final concentration of 40% saturation. After centrifugation, the pellet was used for enzyme assays after desalting on a Sephadex G-25 column. In the test assay, the reaction mixture contained, in a total volume of 180 µL, Tris/HCl (pH 8.0) 100 mM, potassium chloride 50 mM, sodium bicarbonate 15 mM, magnesium chloride 2.5 mM, ATP 1 mM, dithiothreitol (DTT) 1 mM and up to 10 µL protein extract. For inhibitor studies the enzyme reaction was carried out in the presence of up to 250 µM flamprop-M-methyl or flamprop. The reaction was started by addition of 0.62 mM acetyl-CoA and stopped after 30 min incubation at 30 °C by adding perchloric acid. After removal of precipitated protein by centrifugation, the supernatant was neutralized by adding potassium hydroxide and analysed for production of malonyl-CoA by HPLC on a SunFire C_{18} 3.5 µm column (75 × 4.6 mm) (Waters, Eschborn, Germany) using a linear gradient from 100% buffer A (100 mM KH_2PO_4, pH 5.0, 80 mL L^{-1} methanol) and 0% buffer B (100 mM KH_2PO_4, pH 5.0, 500 mL L^{-1} methanol) to 30% buffer A and 70% buffer B in 13 min. The column eluant was monitored with a UV detector at 260 nm. The reaction product was identified by its chromatographic retention in comparison with malonyl-CoA standard.

2.3 Cultivation of plants in hydroponics

Uniformly developed plants of maize (*Zea mays* cv. Banguy, second leaf stage) and soybean [*Glycine max* (L.) Merr. cv. Oxford, first leaf stage] were transferred into 320 mL glass vessels containing 310 mL of half-strength Linsmeier–Skoog medium[9] and maintained at 16:8 h light (400 µmol m^{-2} s^{-1}, 400–750 nm):dark cycles, 22/20 °C and 75% relative humidity in climate chambers (three plants per vessel, four replications in randomized position). The solution was aerated throughout the experiments. After 2 days of adaptation, the compounds were added to the medium in acetone solution (1 mL L^{-1} final concentration of acetone). Controls received corresponding amounts of acetone alone, with no adverse effect on the growth of the plants. After incubation for 7 days, the fresh weights of root and shoot parts per plant were determined (mean values from 12 plant parts), and molar concentrations of compound required for 50% reduction of plant part (IC_{50}) were calculated.

2.4 Histochemical determinations

Histochemical studies were performed according to Tresch *et al.*[10] Uniformly germinated seedlings of *Z. mays* cv. Amadeo with a root length of 3 cm were transferred into 50 mL glass vessels

Pest Manag Sci **64**:1195–1203 (2008)
DOI: 10.1002/ps

(one seedling per vessel, three replications) in half-strength Linsmaier–Skoog[10] nutrient solution (16:8 h light:dark at 25 °C/20 °C and 75% relative humidity, 250 µmol m^{-2} s^{-1} photon irradiance, 400–700 nm; fluorescent lamps, radium HRLV). After 4 h of adaptation, flamprop-M-methyl was added to the medium in dimethyl sulfoxide (DMSO) solution (1 mL L^{-1} final concentration of DMSO). Controls received a corresponding quantity of DMSO alone, with no adverse effect on seedling growth. After 4 or 24 h treatment, primary root tips of 5 mm length with meristematic and elongation zones were harvested, fixed in 37 g L^{-1} paraformaldehyde in phosphate-buffered saline (PBS, pH 7.4), and embedded in paraffin as described elsewhere.[11] Longitudinal sections of 7 µm thickness were obtained with a rotary microtome (Leica RM 2165; Bensheim, Germany) and placed on Polysine™ slides (Menzel, Braunschweig, Germany).

Microtubules or tubulin were labelled with monoclonal antibodies against polymerized β-tubulin (Sternberger Monoclonals, Lutherville, MD). The primary antibodies were marked with fluorescent Alexa 488-conjugated secondary antibody (Molecular Probes Europe BV, Leiden, The Netherlands), as previously described.[10] Firstly, root tips were fixed in 40 g L^{-1} paraformaldehyde in microtubule-stabilizing buffer (MSTB, pH 6.9) which contained 60 mM PIPES [piperazine-*N*,*N*′-bis(2-ethanesulfonic acid)], 25 mM HEPES (*N*-2-hydroxyethylpiperazine-*N*′-2-ethanesulfonic acid), 10 mM EGTA [ethylenedioxy-bis(ethylenenitrilo)tetraacetic acid] and 0.2 g L^{-1} $MgSO_4.6H_2O$ for 14 h. Root tips were then subjected to a sequential series of sucrose infiltration, which contained 120, 140 and 160 g L^{-1} sucrose in MSTB buffer, for 1 h each step. Afterwards, they were frozen in liquid nitrogen. Longitudinal sections of 15 µm thickness were obtained with a cryostat (Frigocut-2800 E; Reichert-Jung, Leica, Bensheim, Germany) and placed on Polysine™ slides. The slides were incubated with DAKO antibody diluent (DAKO Cytomation, Hamburg, Germany) for 20 min. Incubation with tubulin antibodies and the secondary antibodies was carried out for 30 min. The primary and secondary antibodies were diluted with DAKO antibody diluent to 1:200 and 1:100 respectively. The labelled slides were mounted with ProLong Antifade (Molecular Probes) for microscopic observation.

Nuclear DNA was stained with Hoechst 33 342 (0.75 µg mL^{-1}) for 5 min. Microscopic observation was carried out using an Olympus BX61 epifluorescence microscope (Hamburg, Germany) and a confocal laser scanning microscope (Leica DMRXA TCS SP2) equipped with UV and krypton–argon laser.

2.5 Tubulin polymerization assay

Determination of compound effects on tubulin polymerization *in vitro* was studied using a microassay biochemical kit with soybean tubulin from Cytoskeleton, Inc. (Denver, CO) according to the standard protocol (tebu-bio, Offenbach, Germany). Soybean tubulin was isolated from seedlings in greater than 90% purity. The assay utilizes a fluorescent compound (DAPI) which binds to formed microtubules with higher affinity than tubulin.[12] The result is a fluorescence signal that closely follows microtubule formation. The microassay was performed in 384-well plates (three replications) at 25 °C, and fluorescence was measured continuously at an excitation of 360 nm and an emission wavelength of 405 nm using a temperature-controlled fluorescence plate reader (SpectraFluor Plus; Tecan Deutschland GmbH, Crailsheim, Germany).

3 RESULTS AND DISCUSSION

3.1 Physiological profiling using bioassays

In initial experiments, a set of bioassays was used to characterize and classify the mode of action of flamprop-M-methyl in a search for its biochemical target. These systems included heterotrophic maize (*Zea mays*) and photoautotrophic green alga (*Scenedesmus acutus*) cell suspensions, duckweed (*Lemna paucicostata*), isolated mustard (*Sinapis alba*) shoots and germinating cress (*Lepidum sativum*) seeds. The test panel was completed by assays for monitoring physiological processes, including the Hill reaction of isolated wheat thylakoids, respiration by measuring oxygen consumption in heterotrophic cleaver cell suspensions, membrane function/uncoupler activity determined in *Lemna* root mitochondria using the potential sensor JC-1, carbon gas-exchange measurements in cleaver (*Galium aparine*) plants and toluidine-blue staining of cress hypocotyls on inhibition of very-long-chain fatty acid (VLCFA) synthesis. In the latter test, activity of all known VLCFA synthesis inhibitors from chloroacetamide, oxyacetamide, phenylurea, benzofuran and thiocarbamate types can be detected (not shown). The response pattern represents a fingerprint of a compound, which has proved to be typical of its mode of action.[6] The results can be interpreted directly, or a library of response patterns of compounds with known modes of action can be screened for similarities to provide some clues that can be used as an aid to direct further investigations.[6]

The results showed that the inhibitory effects of flamprop-M-methyl on growth are most likely not triggered through an inhibition of photosynthesis (Fig. 1). Even at the high concentration of 100 µM, the compound had only a slight effect on the Hill reaction, carbon assimilation and green algae growth. Flamprop-M-methyl inhibited frond production and growth of *Lemna* (Fig. 1), which was accompanied with an intensified chlorophyll pigmentation, followed by necrosis of the meristematic leaf area. The compound also showed pre-emergence activity on germinating seeds of cress in darkness (Fig. 1). With increasing concentration, seed germination was reduced and hypocotyl and root growth of seedlings were stunted. In *Lemna* and cress, the symptoms

resembled those caused by mitotic disrupter herbicides. Accordingly, in heterotrophic cell suspension cultures of maize, cell division growth ceased at 10 μM (Fig. 1). This system offers an appropriate model system for cell division growth in meristematic tissue, as growth is governed in meristems and in cell suspension cultures mainly by cell division activity, and both cell species generally possess chloroplasts only as proplastids.[6] The results suggested that flamprop-M-methyl acts as a cell division inhibitor. Accordingly, in isolated mustard shoots, which show only low growth activity during incubation, only a slight response to compound treatment was observed (Fig. 1). The corresponding free acid, flamprop, induced similar effects, but with more intensified necrosis on *Lemna* fronds (Fig. 1). This additional necrosis can be explained by an uncoupling of oxidative phosphorylation, most likely due to a protonophore effect of the free acid (Fig. 1).

Overall, when compared with the effects of mitotic disrupter herbicides such as the dinitroaniline pendimethalin, flamprop-M-methyl and flamprop induced nearly the same type of physiological profile in the bioassays, which indicates a similar mode of action (Fig. 2). In contrast, a different type of physiological profile in the various bioassays was obtained with VLCFA synthesis inhibitors, such as metazachlor (Fig. 2). Cell division growth in heterotrophic maize cell suspensions and germinating seeds of cress were only slightly affected, whereas toluidine-blue staining of cress hypocotyls indicated inhibition of VLCFA synthesis. In the case of flamprop-M-methyl and flamprop, toluidine-blue staining of cress hypocotyls was not observed (Fig. 1), even at a concentration of 200 μM (not shown). In addition, the profiles of flamprop-M-methyl and flamprop did not resemble those of acetyl-CoA carboxylase (ACCase) inhibitors in early lipid biosynthesis.[6] Concomitantly, flamprop-M-methyl and flamprop did not inhibit acetyl-CoA carboxylase activity *in vitro* at concentrations up to 250 μM (not shown). This suggests that the primary mode of action of flamprop-M-methyl is most likely not based on inhibition of fatty acid synthesis.

3.2 Cytochemical observations

Mitotic (microtubule) disrupter herbicides, such as pendimethalin, affect cell division and expansion processes in plant growth by inhibiting microtubule assembly. This includes preprophase, spindle and phragmoplast microtubules in mitosis and cortical microtubules in controlling growth direction and cell wall formation.[13,14]

The effects of flamprop-M-methyl on cell division processes were studied in maize roots. Firstly, the appropriate concentration for treatment was studied in young plants of maize, which were tested for their sensitivity towards increasing concentration of flamprop-M-methyl or flamprop (5–100 μM) applied via the root hydroponically for 7 days. The molar concentrations of flamprop-M-methyl required for 50% reduction of root and shoot fresh weight (IC_{50} values) were 89 and 22 μM respectively. Similar sensitivity of maize was found with flamprop, with IC_{50} values for reduction of root and shoot fresh weight of 62 and 29 μM respectively.

Accordingly, maize seedlings were treated with 50 μM of flamprop-M-methyl for 4 and 24 h hydroponically. The tips of primary and adventitious roots were sampled, and serial longitudinal sections were processed for fluorescence microscopic examination. In order to investigate compound effects on mitosis and microtubules, nuclear DNA was stained with Hoechst 33 342, and microtubule arrays were visualized by means of fluorescence-labelled monoclonal antibodies against tubulin subunits.

After treating seedlings with 50 μM flamprop-M-methyl, cell division activity (mitosis and cytokinesis) in the apical root meristem ceased within 4 h (Fig. 3A and C). Treated cells were arrested in a condensed state of prometaphase or metaphase, or chromosomes were found disorganized (Fig. 3A and C). As observed using monoclonal antibody against polymerized β-tubulin, formation of spindle and phragmoplast microtubule arrays in meristematic cells was largely affected, whereas cortical microtubules were only slightly hampered (Fig. 3B and D). Spindle and phragmoblast microtubules present were not visibly changed in their length, but were severely disturbed in their orientation, leading to defective spindle and phragmoblast structures (Fig. 3B and D). The mitotic spindle was changed to a brush-like shape. Microtubules of the spindle apparatus were found attached to the chromosomes at their kinetochores, but did not show, at their minus ends, organization arising from, or in association with, microtubule-organizing zones of spindle poles at the opposite ends of the cell. The minus ends of spindle microtubules appeared to be free and disassembled. On account of this loss in organization of spindle microtubules, chromosomes could not move to the poles of the cell during mitosis. This resulted in mitotic root tip cells that were unable to progress further in the mitotic cycle because chromosomes remained in a condensed state of prometaphase or metaphase (Fig. 3A and C). In late anaphase and early telophase cells, phragmoblast microtubules did not form a regular, plate-like and uniform phragmoblast array that mediates cell plate deposition. Phragmoblasts were found disorganized and fragmented in multiple arrays in the cells, leading, consequently, to irregular and abnormal cell plates (Fig. 3B and D).

These effects are clearly different from those of microtubule disrupter herbicides of cyanoacrylate or dinitroaniline type, such as pendimethalin. These elicit a complete loss of microtubular structures, including cortical, preprophase, spindle and phragmoplast microtubules, and lead to mitotic root tip cells which are completely arrested in late prometaphase.[10,13,14] In addition, the loss of cortical microtubules results in irregular cell walls, which leads to isodiametric

Pest Manag Sci **64**:1195–1203 (2008)
DOI: 10.1002/ps

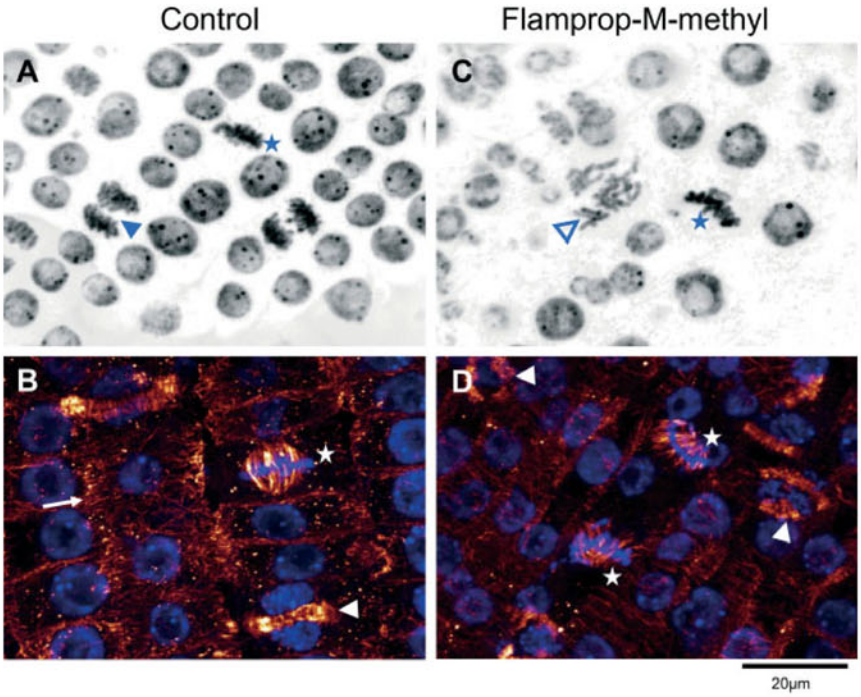

Figure 3. Effects of flamprop-M-methyl on mitosis and the microtubule cytoskeleton in meristematic maize root cells. Seedlings were treated with 50 µM of compound for 4 h hydroponically. Tips of primary and adventitious roots were sampled, and serial longitudinal sections were processed for fluorescence microscopic examination. A and C: Hoechst 33 342 staining of mitotic structures. Control root tip cells undergoing mitosis; metaphase (*) and telophase stages (▲) are shown. Flamprop-M-methyl-treated cells (C) are arrested in a condensed state of metaphase (*) or prometaphase, or chromosomes were found disorganized (△). B and D: Immunofluorescent staining of microtubules using monoclonal antibody against polymerized β-tubulin (in red). Nuclear DNA was stained with Hoechst 33 342 (in blue). Control cells (B) show cortical (arrow), spindle (*) and phragmoplast microtubules (▲). Flamprop-M-methyl-treated cells (D) show disorganized spindle in metaphase cells (*) and phragmoplast microtubules in telophase cells (▲). Microtubules of the spindle apparatus are attached to chromosomal kinetochores, but do not show an organization in the direction of, or association with, microtubule-organizing zones at spindle poles (*). Phragmoblast microtubules do not form an uniform phragmoblast array. Phragmoblasts are found fragmented in multiple arrays (▲).

cell growth and the phenomenon of root clubbing. This club-shaped swelling of root tips is typical of microtubule disrupter herbicides. However, flamprop-M-methyl did not induce isodiametric cell growth and root clubbing (not shown).

After 24 h treatment with flamprop-M-methyl, nuclear membranes reformed around the chromosomes, which resulted mostly in more than three micronuclei of different size and distance from the main nucleus in the cells. These micronuclei were often surrounded by a fuzzy band of microtubules.

3.3 Effects on tubulin polymerization *in vitro*

Microtubules are composed of polymers of the protein tubulin, which is a heterodimer of two polypeptide subunits, α- and β-tubulin. For analysis of compound effects on tubulin polymerization to microtubules *in vitro*, a microassay with purified tubulin from soybean was available. To test the usefulness of this assay specifically for analysis of flamprop effects, sensitivity of soybean to flamprop-M-methyl and flamprop was determined. Young plants of soybean were treated with increasing concentrations of flamprop-M-methyl or flamprop (5–300 µM) applied via the root hydroponically for 7 days. As is typical for mitotic disrupter herbicides,[14] shoot and root growth were stunted, accompanied with intensified green pigmentation of shoots (not shown). The molar concentrations of flamprop-M-methyl required for 50% reduction of root and shoot fresh weights (IC_{50} values) were <5 and 31 µM respectively. In the case of flamprop, IC_{50} values for reduction of root and shoot fresh weight of 36 and 60 µM respectively were determined. This indicates that soybean responds sensitively to flamprop-M-methyl and flamprop, with plant symptoms that suggest an antimicrotubule mechanism of action also in this species. Hence, soybean tubulin is useful for testing effects of flamprop or flamprop-M-methyl directly on polymerization to microtubules *in vitro*.

In the *in vitro* assay, the time course of the polymerization process of soybean tubulin was traced by an increasing fluorescence signal. This signal is generated by binding of the fluorescent compound DAPI to tubulin and microtubules with varying affinity.[12] There is a tenfold difference in the affinity of the fluorophore for microtubules compared with tubulin. In accordance with the reported mechanism,[13,14] the dinitroaniline

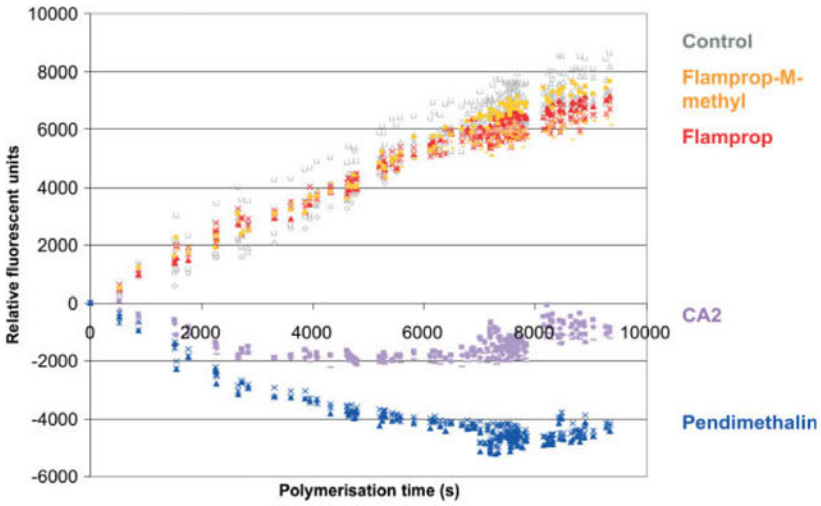

Figure 4. Effects of flamprop-M-methyl, flamprop, pendimethalin and CA2 on polymerization of soybean tubulin *in vitro*. The microassay was performed in three replications of each treatment with compound at 50 μM.

pendimethalin completely inhibited *in vitro* polymerization of soybean tubulin at 50 μM (Fig. 4). In the present test, the IC_{50} value of pendimethalin was 4 μM (not shown). The drop in fluorescence over the first period of incubation is due to aggregates of tubulin that are dissociated by the drug interactions and hence reduce the fluorescence (Cytoskeleton, Denver, CO). Likewise, the cyanoacrylate herbicide CA2, which has the same antimicrotubule mechanism of action as dinitroanilines,[10] completely blocked tubulin polymerization (Fig. 4). In contrast, flamprop-M-methyl and flamprop did not affect polymerization of plant tubulin *in vitro* (Fig. 4). This is in accordance with the cytochemical observations and indicates that flamprop-M-methyl is a mitotic (microtubule) disrupter herbicide that does not affect microtubule polymerization as dinitroaniline- or cyanoacrylate-type compounds do.

4 CONCLUSION

Compounds with an antimicrotubule mechanism of action belong to the most successful herbicides used in agriculture. Herbicides in this group include dinitroanilines, such as trifluralin, oryzalin and pendimethalin, phosphoric amides and carbamates.[10,14,15] These compounds and the newly discovered cyanoacrylates[10] have been found to interfere with microtubule assembly by forming a tubulin–compound complex that disrupts polymerization and microtubule stability.[13,14]

In contrast, flamprop-M-methyl and its biologically active metabolite flamprop induced disruption of mitosis and cytokinesis through a different mechanism of action that is not based on direct interference with the polymerization process of α- and β-tubulin heterodimers in microtubule assembly. The compound severely disturbed the orientation of spindle and phragmoblast microtubules and caused defective spindle and phragmoblast structures in mitotic cells. Phragmoblast was disorganized in multiple arrays, which led to hampered cell plate deposition for cell wall formation in cytokinesis. Microtubules of the spindle apparatus were attached to chromosomal kinetochores, but did not show an organization in the direction of, or in association with, microtubule-organizing zones at the spindle poles. The minus ends of spindle microtubules appeared to be disassembled and free. Consequently, the compound might interfere at the minus end of spindle and phragmoblast microtubules with organization processes including microtubule nucleation or minus-end release by breakage of existing microtubules. Recent work has shown that, in the acentrosomal nucleation and organization of microtubule arrays in plants, both existing microtubules and the presence of γ-tubulin play a central role.[16]

Taken together, the physiological profile, the cytochemical observations and tubulin polymerization studies revealed that flamprop-M-methyl is a mitotic disrupter herbicide with a new antimicrotubule mechanism of action that particularly affects orientation of microtubules in the formation of spindle and phragmoblast arrays in sensitive plants. In contrast, in mammalian HeLa cells, flamprop-M-methyl and flamprop did not affect mitosis and microtubule assembly at 100 μM (unpublished results). This suggests selectivity of the compounds between plants and mammals in influencing the microtubule system. In addition to its value as a herbicide, flamprop-M-methyl can be useful for studying the organization of spindle and phragmoblast microtubules in basic reseach.

ACKNOWLEDGEMENTS

The authors thank Guenter Caspar, Manuela Wetternach, Jacek Kwiatkowski and Michael Knapp for

technical assistance, and Dr John Speakman for critical reading of the English manuscript.

REFERENCES

1 Jeffcoat B and Harries WN, Selectivity and mode of action of flamprop-isopropyl, isopropyl (+-)-2-[*N*-(3-chloro-4-fluorophenyl)benzamido]propionate, in the control of *Avena fatua* in barley. *Pestic Sci* **6**:283–296 (1975).

2 Venis MA, The rational design of the optically active wild oat herbicide *L*-flamprop-isopropyl. *Pestic Sci* **13**:309–317 (1982).

3 Morrison IN, Hill BD and Dushnicky LG, Histological studies on the effects of benzoylprop-ethyl and flamprop-methyl on growth and development of wild oats. *Weed Res* **19**:385–393 (1979).

4 Gauvrit C, Effects of the herbicides benzoylprop-ethyl and flamprop-isopropyl on rat liver mitochondria: an alteration in membrane fluidity? *Pestic Biochem Physiol* **21**:377–384 (1984).

5 Ratterman DM and Balke E, Herbicidal disruption of proton gradient development and maintenance by plasmalemma and tonoplast vesicles from oat root. *Pestic Biochem Physiol* **31**:221–236 (1988).

6 Grossmann K, What it takes to get a herbicide's mode of action. Physionomics, a classical approach in a new complexion. *Pest Manag Sci* **61**:423–431 (2005).

7 Tanaka T, Tanaka H, Machida C, Watanabe M and Machida Y, A new method for rapid visualization of defects in leaf cuticle reveals five intrinsic patterns of surface defects in *Arabidopsis*. *Plant J* **37**:139–146 (2004).

8 Paul G, Activity and inhibition of acetyl-CoA carboxylase determined by HPLC, in *Target Assays for Modern Herbicides and Related Phytotoxic Compounds*, ed. by Böger P and Sandmann G. Lewis Publishers, Boca Raton, FL, pp. 161–166 (1993).

9 Linsmaier EM and Skoog F, Organic growth factor requirements of tobacco tissue cultures. *Physiol Plant* **18**:100–127 (1964).

10 Tresch S, Plath P and Grossmann K, Herbicidal cyanoacrylates with antimicrotubule mechanism of action. *Pest Manag Sci* **61**:1052–1059 (2005).

11 Ruzin SE (ed.) *Plant Microtechnique and Microscopy*. Oxford University Press, Oxford, UK (1999).

12 Bonne D, Heusele C, Simon C and Pantaloni D, 4′,6-Diamidino-2-phenylindole, a fluorescent probe for tubulin and microtubules. *J Biol Chem* **260**:2819–2825 (1985).

13 Anthony RG and Hussey PJ, Dinitroaniline herbicide resistance and the microtubule cytoskeleton. *Trends Plant Sci* **4**:112–116 (1999).

14 Vaughn KC, Anticytoskeletal herbicides, in *Plant Microtubules. Potential for Biotechnology*, ed. by Nick P. Springer, Berlin–Heidelberg, Germany, pp. 193–205 (2000).

15 Molin WT and Khan RA, Mitotic disrupter herbicides: recent advances and opportunities, in *Herbicide Activity: Toxicology, Biochemistry and Molecular Biology*, ed. by Roe RM, Burton JD and Kuhr RJ. IOS Press, Amsterdam, The Netherlands, pp. 111–141 (1997).

16 Eckardt NA, Function of γ-tubulin in plants. *Plant Cell* **18**:1327–1329 (2006).

3.3. Endothall, a protein phosphatase inhibitor acts on plant cell cycle regulation

The protein phosphatase inhibitor endothall is a well-known herbicide which was first reported in 1951 by Tischler *et al.*. Despite the fact that endothall was identified in a forward screen for inhibition of plant growth, the structure of endothall is similar to the natural product cantharidin, an ingredient of blister beetles that is toxic also in Mammalia. Therefore, cantharidin and endothall were the subject of a series of MoA studies, which finally described the inhibition of protein phosphatase 1 and protein phosphatase 2A as the molecular mechanism of action of both compounds (Li *et al.*, 1993; Ayaydin *et al.*, 2000). The experiments in Tresch *et al.* (2011) described the MoA of endothall with a phenotyping approach in more detail, in order to explain the processes leading to plant death. Based on the response in the physiological profile and the development of phenotypic symptoms in the bioassays suggests a MoA in the cell division process. Due to the fact that cell cycle processes are highly regulated also by protein phosphatases, detailed studies of the cytological effects caused by cantharidin and endothall were initiated. The phenotypic effects on the microtubule cytoskeleton and on DNA synthesis in combination with malformation of cell nuclei were similar to effects observed in *Arabidopsis thaliana ton1* / *ton2* mutants, suggesting an interaction between endothall and the TON1 signalling pathway. It is well known that protein phosphatases are involved in several processes in cell division, but also in primary biosynthesis pathways and photosynthesis related processes. The present study of endothall is an example of how to choose the appropriate model system to address specific aspects of the compound's MoA. The cytological experiments described in Tresch *et al.* (2011) do not explain the light-dependent effects of endothall.

Reprinted from Pesticide Biochemistry and Physiology, 99/1, Tresch S, Schmotz J, Grossmann K, Probing mode of action in plant cell cycle by the herbicide endothall, a protein phosphatase inhibitor, 86-95, Copyright (2011), with permission from Elsevier.

Pesticide Biochemistry and Physiology 99 (2011) 86–95

Contents lists available at ScienceDirect

Pesticide Biochemistry and Physiology

journal homepage: www.elsevier.com/locate/pest

Probing mode of action in plant cell cycle by the herbicide endothall, a protein phosphatase inhibitor

Stefan Tresch *, Jennifer Schmotz, Klaus Grossmann

BASF SE, Agricultural Research Centre, D-67117 Limburgerhof, Germany

ARTICLE INFO

Article history:
Received 18 August 2010
Accepted 9 November 2010
Available online 20 November 2010

Keywords:
BY-2 cells
Cell proliferation
Cantharidin
Endothall
Microtubules
Mitosis
Mode of action
Okadaic acid
Protein phosphatase inhibitor
S-phase detection

ABSTRACT

The mode of action of endothall, an herbicide which was reported to inhibit plant protein phosphatases 1 (PP1) and 2A (PP2A), was investigated. For initial characterization, a series of bioassays was used for comprehensive physiological profiling of endothall effects which suggested a phytotoxic mode of action similar to mitotic disrupter herbicides. Unlike known microtubule disrupters, endothall did not inhibit soybean tubulin polymerization *in vitro*. As shown in meristematic corn root tips, endothall distorted the orientation of cell division plane and microtubule spindle structures which led to cell cycle arrest in prometaphase. In tobacco BY-2 cells, malformed spindles together with prometaphase arrest of nuclei and abnormal perinuclear microtubule patterns were detected as early as 4 h of endothall treatment. These effects were also observed after treatment with other protein phosphatase inhibitors, cantharidin and okadaic acid, which phenocopied the mitotic changes described in *tonneau1* (*ton1*) and *tonneau2* (*ton2*) *Arabidopsis* mutants. These mutants are defective in TONNEAU2 (TON2) protein, a regulatory subunit of PP2A, which governs cell division plane and microtubule orientation. Therefore, PP2A/TON2 phosphatase complex is suggested to be an *in planta* molecular target of endothall. However, in BY-2 cells, additional effects of endothall, including inhibition of S-phase initiation and DNA synthesis, detected by 5-ethynyl-2′-deoxyuridine (EdU) incorporation, and condensed nuclei arrested in late mitosis were observed which were not reported in *Arabidopsis ton1* and *ton2* mutants. This result indicates that two additional checkpoints in cell cycle were blocked by endothall which are probably not associated with TON2-pathway inhibition. Possibly, inhibition of PP1 and/or other PP2A protein phosphatases are involved in the regulation of these cell cycle phenomena.

1. Introduction

The herbicidal properties of endothall (7-oxabicyclo[2.2.1]heptane-2,3-dicarboxylic acid) were first reported by Tischler et al. in 1951 [1]. The compound was commercially introduced by Sharples Chemical Corporation (now Cerexagri Inc.) for selective, postemergence control of several annual broadleaf and grass weeds in sugar beets [2]. Additionally, it can be applied as a preharvest desiccant in potatoes, alfalfa and clover seed crops [2]. Endothall is also used to control algae and several other aquatic weeds [2].

Early reports described cytological studies in cells of *Pisum sativum* which show effects of endothall on chromosome distribution within mitosis [3]. These effects of endothall, which included chromosome loss during metaphase, the presence of few micronuclei structures, and the absence of prometaphase, could be distinguished from other microtubule assembly inhibitors such as colchicine [3]. In other plant systems, endothall, applied at high concentrations, was found to increase leakage of electrolytes followed by tissue necrosis which suggested membranes as an early site of endothall injury [4]. Interference with plant lipid biosynthesis [5] and RNA and protein synthesis was also reported [6–8]. As a more specific effect, endothall and the structurally related cantharidin have been shown to inhibit mammalian protein phosphatase 1 (PP1) and protein phosphatase 2A activity (PP2A) *in vivo* [9,10]. Cantharidin is known as the toxic ingredient of a variety of blister beetles and was found to bind to mammalian PP2A [9,11]. Moreover, Li et al. [11] and Ayaydin et al. [12] have demonstrated that endothall and cantharidin also inhibit plant PP1 and more sensitive PP2A activity in cultured alfalfa cells and intact spinach leaves. In the latter tissue, inhibition of PP2A activity was accompanied by decreased light-induced activation of nitrate reductase [11]. However, the exact herbicidal mechanism and mode of action of endothall is not yet clarified.

Abbreviations: EdU, 5-ethynyl-2′-deoxyuridine; MI, mitotic index; MSTB, microtubule stabilizing buffer; PI, proliferation index; PP1, protein phosphatase 1; PP2A, protein phosphatase 2A; TBS, tris buffered saline.

* Corresponding author. Address: Speyerer Str. 2, D-67117 Limburgerhof, Germany. Fax: +49 621 6027176.
E-mail address: stefan.tresch@basf.com (S. Tresch).

0048-3575/$ - see front matter © 2010 Elsevier Inc. All rights reserved.
doi:10.1016/j.pestbp.2010.11.004

In order to study a possible causality between the known inhibition of protein phosphatases and processes leading to plant damage, we analyze the herbicidal mode of action of endothall in more detail. For initial characterization, an array of bioassays was used in a physionomics approach for comprehensive physiological profiling of endothall effects [13]. Cantharidin and the mitotic disrupter herbicide pendimethalin were included in this investigation. Since similarities to pendimethalin and cantharidin were observed, the effects of endothall on cell division processes were studied in corn root tips and tobacco BY-2 suspension cells in comparison to cantharidin and the known protein phosphatase inhibitor okadaic acid. Here, cytological and biochemical methods were used which include immunocytochemical fluorescence techniques and *in vitro* polymerization of plant tubulin. This is the first time detailed analysis of endothall effects has been done in plant tissue. The results suggest that effects of endothall on microtubule cytoskeleton arrangement and mitotic structures, possibly mediated by protein phosphatase inhibition, mainly contribute to the herbicidal mode of action.

2. Materials and methods

2.1. Chemicals

Endothall (7-oxabicyclo[2.2.1]heptane-2,3-dicarboxylic acid, CAS No. 62059-43-2), cantharidin (2,3-dimethyl-7-oxabicyclo[2.2.1] heptane-2,3-dicarboxylic anhydride, CAS No, 56-25-7) and okadaic acid (CAS No. 78111-17-8) were obtained from Sigma–Aldrich, Deisenhofen, Germany.

2.2. Bioassays

The bioassays of the physionomics approach were carried out as described elsewhere [13]. In the heterotrophic cell suspension assay, freely suspended callus cells from *Zea mays* L. (DSM Collection of Plant Cell Cultures, Braunschweig, Germany) were cultivated in a modified Murashige-Skoog medium as described previously [13]. The cells were subcultured at 7-day intervals. Acetone solutions of the compounds were pipetted into plastic tubes, and the solvent was allowed to evaporate before adding 2 ml of exponentially growing cell suspensions. The tubes (three replicates) were shaken at 300 rpm and 25 °C in the dark on a rotary shaker. After incubation for 8 days, the conductivity of the medium was measured as the parameter for cell division growth [13].

For the algae bioassay, cells of *Scenedesmus obliquus* Kützing 276-3a (Culture Collection Göttingen, Göttingen, Germany) were propagated photoautotrophically [13]. The bioassay was carried out in plastic microtitre dishes containing 24 wells. Before loading each well with 0.5 ml cell suspension, 0.5 ml medium and compound in acetone solution were added, allowing sufficient time for the organic solvent to volatilize. The 15 additional compartments between the wells were filled with sodium carbonate/bicarbonate buffer. The dishes were sealed with plastic lids and incubated on a shaker under continuous light with 60 µmol m^{-2} s^{-1} photon irradiance at 23 °C. After 24 h, cell density was measured photometrically.

For the *Lemna* bioassay, stock cultures of *Lemna paucicostata* (L.) Hegelm. (collection Prof. R Kandeler, University of Vienna, Austria) were propagated mixotrophically in an inorganic medium containing sucrose [13]. The bioassay was conducted under aseptic conditions in plastic petri dishes (5 cm diameter) which contained 15 ml medium without sucrose. The test compounds were added to the dishes in acetone solution, and the organic solvent was allowed to volatize before loading them with four fronds each. The culture dishes were then closed with plastic lids and incubated under continuous light (Philips TL white fluorescent tubes, 40 µmol m^{-2} s^{-1} photon irradiance, 400–700 nm) in a growth chamber at 25 °C. Eight days after treatment, the increase in the area covered by the fronds in each dish was determined as the growth parameter using an image analyzing system (LemnaTec Scanalyzer; LemnaTec, Würselen, Germany).

For the isolated shoot bioassay, seedlings of mustard (*Sinapis alba* L.) were grown under standardized greenhouse conditions. The shoots were removed, weighted and placed upright in plastic vials (25 mm diameter, 38 mm height; Greiner, Nürtingen, Germany) which contained 12 ml double-distilled water and the test compound added in acetone solution (1 ml l^{-1} final concentration of Aceton) [13]. To avoid evaporation, the vials were closed with plastic covers with slits into which the shoots were fitted (three shoots per vial). The vials were cultivated in growth chambers with a 16:8 h light:dark photoperiod at 21 °C and 75% relative humidity (light: Osram krypton 100 W lamps and Osram universal white fluorescent tubes, 200 µmol m^{-2} s^{-1} photon irradiance, 400–700 nm). After 3 days, changes in fresh weight were measured by weighing the shoots and subtracting the values from initial weights.

To determine effects on the Hill reaction, thylakoids were isolated from shoots of young plants of *Triticum aestivum* L., and assay was performed as previously described [13]. Isolated thylakoids were suspended in a reaction medium (0.75 ml) that contained sucrose 0.1 M, tricine–NaOH (pH 8.0) and 50 mM, magnesium chloride 5 mM and chlorophyll 41 µg ml^{-1}. The assay mixture included thylakoid suspension (0.23 ml), test compound dissolved in acetone + water (80 + 20 by volume; 0.05 ml) and ferricyanide (5 mM; 0.02 ml). During the subsequent illumination for 4 min with 1300 µmol m^{-2} s^{-1} photon irradiance, ferrocyanide was formed in the Hill reaction. Then, in the darkness, the ferrocyanide was allowed to react with ferric salt to form the ferrous salt, which produced a complex with phenanthroline. The complex was measured photometrically at 510 nm.

For the germination bioassay, seed of cress (*Lepidum sativum* L.) were placed in glass petri dishes (5 cm in diameter) filled with vermiculite substrate. Stock solutions of the test compounds in acetone were added together with 12 ml water (1 ml l^{-1} final concentration of aceton) [13]. Control seeds were moistened only with water and acetone. The dishes were incubated in a growth chamber at 25 °C in the dark for 3 days. Inhibition of germination and seedling development was evaluated visually (0 = no influence, 100 = total inhibition). Afterwards, the dishes were incubated for a further 3 days under light conditions (16:8 h light:dark at 25 °C and 75% relative humidity, 230 µmol m^{-2} s^{-1} photon irradiance, 400–700 nm), and seedling development and plant symptoms were evaluated.

To determine carbon dioxide uptake as a parameter for carbon dioxide assimilation, plants of *Galium aparine* L. that had been raised under controlled conditions to the second whorl stage were cultivated hydroponically in illuminated glass chambers (four plants per chamber, three replications) which received a constant stream of air [13] After foliar treatment with the compound, the amount of carbon dioxide assimilated per unit time was determined continuously for 24 h from the difference between the carbon dioxide contents of the inflowing and outflowing air streams.

For the determination of respiration, 18 ml cell suspensions of *Galium mollugo* L. (DSM Collection of Plant Cell Cultures, Braunschweig, Germany) were treated with compound in plastic vessels for 5 h in the dark on a rotary shaker (1 ml l^{-1} final concentration of aceton). Samples of 5 ml cell suspension were then transferred to plastic tubes for measurement of oxygen consumption using the dissolved oxygen measuring system inoLab Oxi Level 3 with the oxygen sensor CellOx 325 (WTW, Weilheim, Germany). Respiration inhibition was measured as oxygen consumption in µl l^{-1} per min in comparison to control. [13].

To determine the uncoupler activity of compounds, *Lemna* plants were pretreated with the mitochondrial potential sensor dye JC-1 (10 μg ml^{-1} in nutrient solution; Invitrogen Ltd., Paisley, United Kingdom) for 30 min. JC-1 exhibits potential-dependent accumulation in mitochondria, indicated by a fluorescence emission shift from green to red [13]. Mitochondrial membrane depolarization is indicated by a decrease in the red/green fluorescence intensity ratio. After staining, *Lemna* plants were washed and loaded into 48 well plastic microtitre dishes, with each well containing four fronds, 0.5 ml medium and compound added in acetone solution (1 ml l^{-1} final concentration of aceton). After treatment for 90 min, *Lemna* plants were transferred to slides for fluorescence microscopic observation of root mitochondria using an Olympus BX61 epifluorescence microscope (Hamburg, Germany).

The results were expressed as percentage inhibition. Mean values of three replicates are given as the percentage inhibition relative to control. Individual standard errors were less than 10%. All experiments were repeated at least twice and proved to be reproducible. The results of representative experiments are shown.

2.3. Histochemical determinations

Histochemical studies were performed according to [14]. Uniformly germinated seedlings of *Z. mays* cv. Amadeo with a root length of 3 cm were transferred into 50 ml glass vessels (one seedling per vessel, three replications) in half strength Linsmaier–Skoog [15] nutrient solution (16:8 h light:dark at 25 °C and 75% relative humidity, 250 μmol m^{-2} s^{-1} photon irradiance, 400–700 nm; fluorescent lamps, radium HRLV). After 4 h of adaption compound was added to the medium in dimethyl sulfoxide (DMSO) solution (1 ml l^{-1} final concentration of DMSO). Controls received a corresponding quantity of DMSO alone, with no adverse effect on seedling growth.

After 4 or 24 h treatment, primary root tips of 5 mm length with meristematic and elongation zones were harvested, fixed in 37 g l^{-1} paraformaldehyde in phosphate buffered saline (PBS, pH 7.4), and embedded in paraffin as described elsewhere [16]. For observation of nuclear DNA longitudinal sections of 7 μm thickness were obtained with a rotary microtome (Leica RM 2165; Leica, Wetzlar, Germany) and placed on Polysine™ slides (Menzel, Braunschweig, Germany). After deparaffinazing according to standard methods [16], nuclear DNA was stained with Hoechst 33342 (0.75 μg ml^{-1} in phosphate buffered saline, pH 7.5; Invitrogen Ltd.) for 5 min. To avoid fast fluorescence quenching, the stained slides were mounted with ProLong® Antifade (Invitrogen Ltd.).

Microtubules or tubulin were labeled with monoclonal antibodies against polymerized β-tubulin (Sternberger Monoclonals, Lutherville, MD, USA). The primary antibodies were marked with fluorescent Alexa Fluor® 488-conjugated secondary antibodies (Invitrogen), as previously described [14]. Firstly, root tips were fixed in 40 g l^{-1} paraformaldehyde in microtubule-stabilizing buffer (MSTB, pH 6.9) which contained 60 mM PIPES (piperazine-*N*,*N*′-bis(2-ethanesulfonic acid)), 25 mM HEPES (*N*-2-hydroxyethylpiperazine-*N*′-2-ethanesulfonic acid), 10 mM EGTA (ethylenedioxy-bis(ethylenenitrilo)tetraacetic acid) and 0.2 g l^{-1} $MgSO_4 \cdot 6H_2O$ for 14 h. Root tips were than subjected to a sequential series of sucrose infiltration, which contained 120, 140 and 160 g l^{-1} sucrose in MSTB buffer, for 1 h each step. Afterwards, they were frozen in liquid nitrogen. Longitudinal sections of 15 μm thickness were obtained with a cryostat (Frigocut-2800 E; Reichert-Jung, Leica) and placed on Polysine™ slides. The slides were incubated with DAKO antibody diluent (DAKO GmbH, Hamburg, Germany) for 20 min to block unspecific binding sites. Incubation with tubulin antibodies and secondary antibodies was carried out for 30 min. The primary and secondary antibodies were diluted with DAKO antibody diluent to 1:200 and 1:100, respectively. After staining of nuclear DNA with Hoechst 33342 (0.75 μg ml^{-1} in phosphate buffered saline, pH 7.5) for 5 min, labeled slides were mounted with ProLong® Antifade (Invitrogen) for microscopic observation.

Microscopic observations were carried out using an Olympus BX61 epifluorescence microscope with standard bandpass filter sets (Hamburg, Germany) and a confocal laser scanning microscope (Leica DMRXA TCS SP2) equipped with UV and krypton-argon laser.

2.4. Cytological investigations of BY-2 cells

For determination of distribution of mitotic phases, visualization of S-phase activity and observation of microtubules in cell culture, freely suspended cells of *Nicotiana tabacum* L., BY-2 cultures [17] were used. The cells were subcultured in Linsmaier and Skoog nutrient solution (including 3% sucrose, w/v, 1 μM 2,4-dichlorophenoxyacetic acid; [15]) at 7-day intervals and agitated on a rotary shaker at 115 rpm at 25 °C in the dark. For compound treatment 2 μl DMSO solutions were pipetted into plastic tubes before adding 2 ml of 3-day old cell suspensions. Control samples where treated with 2 μl DMSO alone. The tubes were shaken at 300 rpm and 25 °C in the dark on a rotary shaker. After incubation for 4 and 24 h, cells were fixed and stained with a modified method described by [18]. The cells were sedimented for 5 min and supernatant nutrient solution was discarded. Subsequently, 1 ml fixative solution (3.7% paraformaldehyd in MSTB) was applied to cells for at least 15 min at 4 °C. Afterwards cells were washed with 1 ml 0.05 mM tris buffered saline (TBS, pH 7.6) at 4 °C for 5 min and 1 ml acetone + methanol (1 + 1 by volume) solution was added at −20 °C for 15 min. Next to a washing step with TBS, the cell wall was digested for better antibody penetration with 0.5 ml enzyme solution in TBS (5 U ml^{-1} cellulase Onozuka R-10, w/v, SERVA Electrophoresis, Heidelberg, Germany and 0.05% pectolyase, v/v; Sigma–Aldrich; in TBS) for 15 min. Then, cells were treated for 5 min with 0.5 ml TBS containing 0.05% detergent Tween 20 and subsequently 0.5 ml DAKO antibody diluent for additional 20 min. For staining, cells were treated with 0.3 ml anti-β-tubulin antibody (Clone TUB 2.1; Sigma–Aldrich) solution as 1:100 dilution in DAKO antibody diluent (DAKO GmbH) for 25 min. After washing with TBS containing 0.05% Tween 20 for 5 min, cells were treated for 30 min with secondary antibody labeled with Alexa Fluor® 488 (Invitrogen). Subsequently, nuclear DNA was stained with Hoechst 33342 (10 μg ml^{-1} in 0.05 M TBS) for 10 min. All procedures after acetone + methanol treatment were done at room temperature. Labeled cells were pipetted on glass slides and mounted with ProLong® antifade (Invitrogen) prior to microscopic observation on Olympus BX61 microscope (Hamburg, Germany).

Effects on DNA synthesis in S-phase of proliferating BY-2 cells was studied using Click-iT® technology (Invitrogen) in combination with the nucleoside analog 5-ethynyl-2′-deoxyuridine (EdU, Invitrogen) as described by [19,20]. EdU is a nucleoside analog of thymidine and is incorporated into DNA during active DNA synthesis. Detection of EdU, which contains an alkyne group, was done with reactive Alexa Fluor® 488 dye which contained an azide group. Based on the principle of click chemistry, reactive Alexa 488 dye was used to detect incorporated EdU in proliferated nuclei. EdU (10 μM) was applied simultaneously to compound treatment for 4 and 24 h as described above. Control samples were treated with EdU, compound or solvent alone. After treatment, harvested cells were fixed as described above. After acetone + methanol treatment, cells were washed with phosphate buffer and EdU staining was performed according to standard protocol of Click-iT® EdU Imaging Kit (Invitrogen) as described by supplier. Total nuclear DNA was stained with Hoechst 33342 as described. Subsequently, cells were mounted on glass slide with ProLong® antifade and observed under epifluorescence microscope BX61 (Olympus).

Mitotic index (MI) was calculated as percent of cells in mitosis related to total counted cells. For classification of the mitotic phases, Hoechst 33342 stained nuclei were assigned by microscopic observation to interphase or a distinct mitotic phase. In addition, abnormal nuclei in cells were classified as prometaphase arrested, condensed, relaxed or multinuclear. Detection of DNA synthesis in S-phase of proliferating cells was carried out in a parallel experiment. Proliferation index (PI) was calculated as percent of cells showing nuclear DNA synthesis by EdU coupled Alexa Fluor® 488 fluorescence related to total counted cells. In each study, at least 500 cells were counted in two replicate samples. All experiments were replicated at least twice and proved to be reproducible.

2.5. Tubulin polymerization assay

Determination of compound effects on tubulin polymerization *in vitro* was studied using a microassay biochemical kit from Cytoskeleton Inc. (Denver, CO, USA) with soybean tubulin according to the standard protocol (Tebu-Bio, Offenbach, Germany) as described [21]. Soybean tubulin was isolated from seedlings in greater than 90% purity. The assay utilizes 4′,6-diamidino-2-phenylindole (DAPI) as fluorescent compound which binds to formed microtubules with higher affinity than tubulin heterodimers [22]. The result is a fluorescence signal that closely follows microtubule formation. The microassay was performed in 384-well plates (three replications) at 25 °C, and fluorescence was measured every 30 s during a time of 60 min at an excitation of 360 nm and an emission wavelength of 405 nm using a temperature-controlled fluorescence plate reader (SpectraFluor Plus; Tecan Deutschland GmbH, Crailsheim, Germany) The extent of polymerization in each assay was measured as mean of arbitrary fluorescence units during plateau phase of polymerization (range from 34 to 60 min of incubation). Inhibition of tubulin polymerization by compound treatment was expressed in percentage related to maximum polymerization of control assays.

3. Results

3.1. Physiological profiling using bioassays

In initial experiments, a set of established bioassays were used to characterize and classify the mode of action of endothall in the search for its inhibitory process leading to plant damage. These systems included heterotrophic corn (*Z. mays*) and photoautotrophic green alga (*S. obliquus*) cell suspensions, duckweed (*L. paucicostata*), isolated mustard (*S. alba*) shoots and germinating cress (*L. sativum*) seeds. The test panel was completed by assays for monitoring physiological processes, including the Hill reaction of isolated wheat thylakoids, respiration by measuring oxygen consumption in heterotrophic *G. aparine* cell suspensions, membrane function and uncoupler activity determined in *Lemna* root mitochondria using the potential sensor JC-1, carbon gas-exchange measurements in cleaver (*G. aparine*) plants. The response pattern represents a fingerprint of a phytotoxic compound, which has proved to be typical of its mode of action [13].

The response pattern of endothall (Fig. 1) shows strong inhibitory effects in bioassays with growth governed by high cell division activity including heterotrophic cell suspensions, *Lemna* and germinating seeds of cress. In the latter bioassay, in darkness, hypocotyl and root growth of cress seedlings were stunted and roots were swollen. In light, growth inhibition of cress seedlings, *Lemna* and isolated mustard shoots were accompanied by necrosis of shoot tissue. Light-dependent photosynthetic Hill reaction, carbon assimilation and green algae growth were less affected. Moderate effects were found on mitochondrial membrane potential (uncoupler activity) in all concentrations tested. No effects were observed on respiratory activity as measured through oxygen consumption in heterotrophic cell suspension. In summary, typical plant symptoms elicited by endothall were growth inhibition and swelling of roots on the one hand and tissue desiccation and necrosis on the other (Fig. 1).

The response pattern of cantharidin (Fig. 1) and pendimethalin (Fig. 1) in the bioassays were quite similar to endothall (Fig. 1).

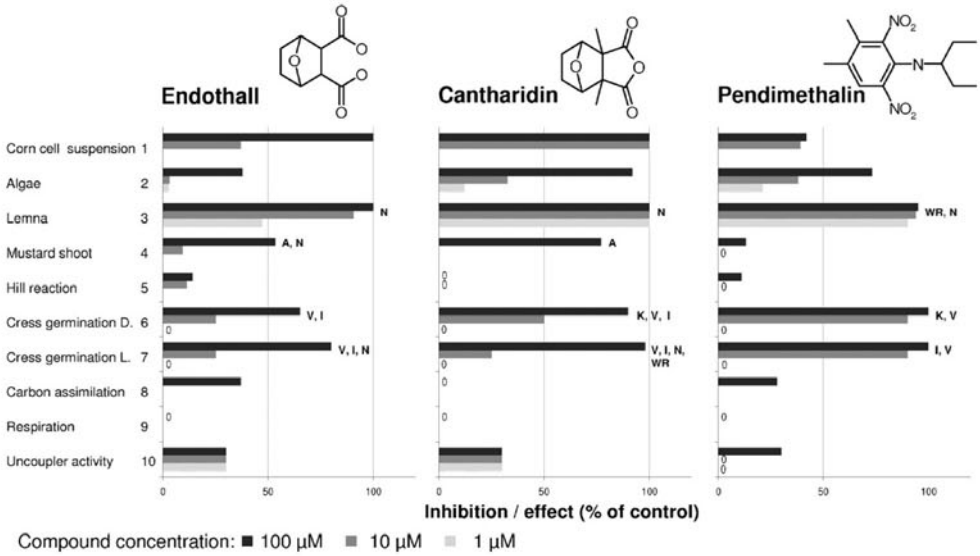

Fig. 1. Effects of endothall, cantharidin and pendimethalin in bioassays including corn and algal cell suspensions, duckweed, isolated mustard shoots, germinating cress seeds, the Hill reaction of isolated wheat thylakoids, respiration by measuring oxygen consumption in heterotrophic *Galium* cell suspensions, uncoupler activity in *Lemna* root mitochondria and carbon assimilation in *Galium* plants. SE of the mean in all cases was less than 10%. Symptoms observed: A, desiccation; I, root growth inhibition; K, reduced seed germination; N, necrosis; V, root swelling; WR, intensified green leaf pigmentation.

Particularly, root growth inhibition and swelling of root tips in dark-grown cress seedlings were typical of all compounds tested. However, the overall activity of cantharidin was higher than that of endothall. Here, cantharidin clearly shows higher activity in the algae bioassay than endothall. Different to endothall and cantharidin, the mitotic disrupter herbicide pendimethalin showed necrosis only at the meristematic leaf area in *Lemna*. In addition, slight uncoupler activity of pendimethalin was only observed at 100 μM.

3.2. Effects on tubulin polymerization in vitro

Induced root swelling into a club shape which was caused by endothall and cantharidin (Fig. 1) is very characteristic for mitotic disrupter herbicides such as pendimethalin, cyanoacrylates or flamprop-*m*-methyl [14,21,23]. Therefore, the effect of endothall on tubulin polymerization to microtubules *in vitro* was measured with purified tubulin from soybean (Table 1). It was shown for pendimethalin that tubulin polymerization was completely blocked at 50 μM and 10 μM. At 3 μM, pendimethalin inhibited polymerization by 48%, in comparison to control. In contrast, the *in vitro* polymerization of plant tubulin by endothall was minimal. At the highest concentration of 50 μM which could be tested in the assay, only 12% inhibition was measured.

3.3. Endothall influences cell division plane and mitotic spindle formation in tissue of corn root tips

To study effects on cell division processes *in vivo*, the effect of endothall on mitosis and microtubule cytoskeleton in meristematic tissue of corn root tips was analyzed (Fig. 2). Corn seedlings were treated hydroponically with 10 and 100 μM endothall for 4 and 24 h, respectively. The tips of primary and adventitious roots were sampled, and serial longitudinal sections were processed for microscopic examination. In order to investigate compound effects on mitosis and microtubules, nuclear DNA was stained with Hoechst 33342, and microtubule arrays were visualized by means of fluorescence-labeled monoclonal antibodies against β-tubulin.

After treatment with 10 μM endothall, cells with metaphase and prometaphase stages accumulated within 4 h (Fig. 2B), in comparison to control (Fig. 2A). As illustrated in Fig. 2B by arrows, endothall caused a change in the orientation of mitotic metaphase chromosomes. Most of the chromosomal metaphase plates showed a diagonal orientation and were not aligned transversally as in control tissue (Fig. 2A). Therefore, the cell division plane in endothall-treated tissue was disoriented. Prometaphase stages were also detected after endothall treatment (Fig. 2B, indicated by star). However, anaphase and telophase were not found which indicates cell cycle arrest in a condensed state of metaphase or prometaphase. Concomitantly, formation and orientation of spindle microtubule arrays were largely affected (Fig. 2D and E). Phragmoplast microtubule arrays were observed only scarcely and cortical microtubules decreased after 4 h of endothall treatment, dependent on concentration (Fig. 2D and E). Spindle microtubules were severely disorganized and unevenly oriented. Treatment with high endothall concentration (100 μM) led to a more condensed microtubule spindle array with shortened microtubule bundles, compared to control (Fig. 2E). Spindle microtubule length at 10 μM endothall treatment was not visibly changed (Fig. 2D). At both concentrations, the majority of microtubule spindle arrays were diagonally oriented and not longitudinally as in untreated cells. The arrays were unevenly arranged and apparent microtubule spindle poles showed malformations including condensed and twisted structure or widespread and disorganized appearance (Fig. 2D and E).

Table 1
Effect of endothall and pendimethalin on *in vitro* polymerization of soybean tubulin. The microassay was performed in three replications of each treatment. Inhibition of tubulin polymerization by compound treatment was expressed in percentage related to maximum polymerization in control assays.

Compound	(μM)	Inhibition of tubulin polymerization compared to control (%)
Endothall	50	12
	10	0
	3	0
Pendimethalin	50	100
	10	100
	3	48

3.4. Endothall influences mitotic spindle organization, causes unusual prometaphase arrest and reduces proliferation in BY-2 cells

To elucidate effects on mitosis and microtubule cytoskeleton in more detail, endothall was investigated in comparison to the structurally related cantharidin and the known phosphatase inhibitor okadaic acid [24] in tobacco BY-2 suspension cells, a powerful system to analyze cell cycle processes [17].

Staining of microtubules in endothall-treated BY-2 cells with monoclonal antibodies against β-tubulin (Fig. 3) showed comparable effects on spindle microtubules as observed in tissue of corn root tips (Fig. 2). Most of the spindle structures observed in endothall-treated BY-2 cells were unequally oriented and showed disoriented and multipolar spindles (Fig. 3B and J), compared to control (Fig. 3A and I). After only 4 h of treatment, microtubule spindle were asymmetrically dispersed and no longer oriented towards one spindle pole (Fig. 3B). In contrast to endothall, cells treated with cantharidin or okadaic acid showed strong accumulation of perinuclear microtubules (Fig. 3C and D). Abnormal mitotic spindle structures, similar to that observed in endothall-treated cells (Fig. 3B and J), could be found rarely in cantharidin (Fig. 3C and K) or okadaic acid (Fig. 3D and L) treated cells after 4 h (Fig. 3C and D) and 24 h (Fig. 3K and L).

In endothall-treated cells, malformed spindles ultimately led to disturbed chromosome arrangements which showed accumulation of prometaphase nuclei in mitosis as early as 4 h after treatment (Fig. 3F and N). Disturbed chromosome arrangement between prophase and metaphase is the dominant visual effect of endothall within 4 h of treatment (Fig. 4). The structure of arrested prometaphase were similar to abnormal, arched metaphases with single chromosomes outside the metaphase plane (Fig. 3F). This phenomenon is different to prometaphase arrest elicited by other mitotic disrupter herbicides, such as pendimethalin (Fig. 4) or cyanoacrylates (not shown), which induce prometaphase arrest by microtubule assembly inhibition and disrupting microtubule stability [14,25] Similar to endothall effects on mitotic nuclei, cantharidin and okadaic acid caused accumulation of prometaphase nuclei (Fig. 4). Additionally, strongly condensed nuclei, characterized by their compact and homogenous Hoechst 33342 stain, were observed particularly after treatment with the protein phosphatase inhibitors okadaic acid, cantharidin and endothall but not after treatment with the microtubule assembly inhibitor pendimethalin (Fig. 4). Strongest accumulations of condensed nuclei were elicited by okadaic acid and cantharidin treatment (Figs. 3G and H, 4 and 5). Both compounds also caused strong accumulations of nuclei with relaxed DNA structures (Figs. 3G, H and 5), whereas endothall was less effective (Fig. 5). In contrast, pendimethalin showed only accumulated prometaphase nuclei and cells with multinuclei, whereas cells with condensed nuclei or relaxed nuclei did not occur (Fig. 5).

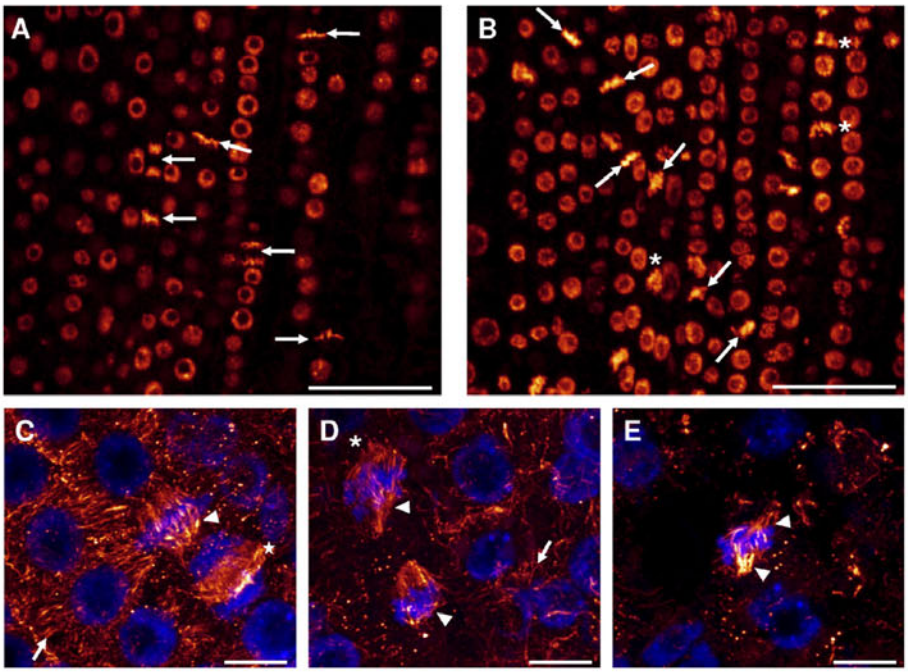

Fig. 2. Effects of endothall on orientation of division plane, mitosis and microtubule cytoskeleton in meristematic corn root cells. Seedlings were treated with 10 and 100 μM endothall for 4 h hydroponically. Tips of primary and adventitious roots were sampled, and serial longitudinal sections were processed for microscopic observation. (A) Control root tips and (B) 10 μM endothall treatment: Hoechst 33342 staining of mitotic structures. The orientation of the cell rows in the images is exactly longitudinal. The lower part of the images corresponds to the apical part of the root. Transversal (A) or diagonal (B) orientation of the division plane is denoted by arrow direction. Control cells (A) undergoing mitosis; metaphase and telophase stages (arrows) are shown. Endothall treated cells (B) showing disoriented metaphase stages (arrows) and malformed prometaphase stages (star). (C) Control cells, (D) 10 μM endothall, (E) 100 μM endothall treated cells: immunofluorescent staining of microtubules using monoclonal antibody against tubulin (red). Nuclear DNA was stained with Hoechst 33342 (blue). Control cells (C) show cortical (arrow), spindle (arrowhead) and phragmoplast microtubules (star). Endothall treated cells (10 μM) (D) show disorganized, uneven spindle (arrowhead) with spread microtubule spindle pole zone (star) and reduced cortical microtubules (arrow). Endothall treated cells (100 μM) (E) show accumulation of disorganized microtubule spindle and twisted or uneven spindle apparatus (arrowhead). Bar: 50 μm (A and B); 10 μm (C and D and E).

To determine if either the cells enter the S-phase or the cell cycle was blocked at G1/S transition by the compounds, cell proliferation rate was analyzed. DNA synthesis in proliferating cells was detected using a method based on the incorporation of the artificial nucleotide 5-ethynyl-2′-deoxyuridine (EdU) and its subsequent detection by a fluorescent azide, as described by [19]. BY-2 cells undergoing S-phase incorporate EdU into DNA during replication which results in a fluorescent signal after staining procedure (Fig. 3M–P). Proliferation index (PI) was determined as percent of fluorescent cells to total counted cells. As shown in Table 2, endothall decreased PI moderately after 4 h and strongly after 24 h of treatment in a dose dependent manner, respectively. Compared to endothall, cantharidin and okadaic acid caused a strong decrease of PI even at lower compound concentrations. No effect was observed by pendimethalin. A more detailed analysis of mitotic DNA stages after cantharidin and okadaic acid treatment revealed condensed nuclei which did not show DNA synthesis during 24 h of treatment (Fig. 3O and P). This effect was similar in endothall-treated cells. But different to cantharidin and okadaic acid, endothall additionally induced prometaphase nuclei which showed fluorescent staining for S-phase transition. Consequently, these cells were still able to enter G2/M transition during time of treatment (Fig. 3N). Accumulation of condensed nuclei without DNA synthesis in cantharidin, okadaic acid and endothall-treated cells clearly shows that nuclei, classified as condensed nuclei, did not undergo S-phase.

Shown as percent of affected nuclei in cell cycle to total counted cells (Fig. 5), the overall effect of endothall at 100 μM (15%) is lower compared to 10 μM cantharidin (34%), 10 μM okadaic acid (19%) or 10 μM of the microtubule assembly inhibitor pendimethalin (59%) after 24 h of treatment. Mitotic index (MI) as percent of cells in mitosis to total counted cells (Table 2) was only slightly changed 4 h after treatment with endothall, cantharidin and okadaic acid. In contrast, 10 μM pendimethalin increased MI from nearly 10% in control to 18% in treated cells (Table 2). After 24 h of treatment, endothall, cantharidin and okadaic acid mostly decreased MI, whereas pendimethalin showed an increase in MI from nearly 15% in control to 23% in treated cells (Table 2).

4. Discussion

The herbicide endothall was presented for the first time in 1951 [1]. However in spite of extensive research, the herbicide mode of action has not been clarified. The molecular interactions of endothall and the structurally related cantharidin with serine/threonine-specific plant protein phosphatases PP1 and PP2A have been shown and related to inhibitory effects on nitrate assimilation [11] and cell cycle processes [3,12].

To characterize the mode of action of endothall and the inhibitory process leading to plant damage, we used a set of bioassays for comprehensive physiological profiling of endothall and cantharidin effects. The results can be interpreted directly, or a library of response patterns of compounds with known modes of action can be screened for similarities to provide some clues that can be used as an aid to direct further investigations [13]. The overall response

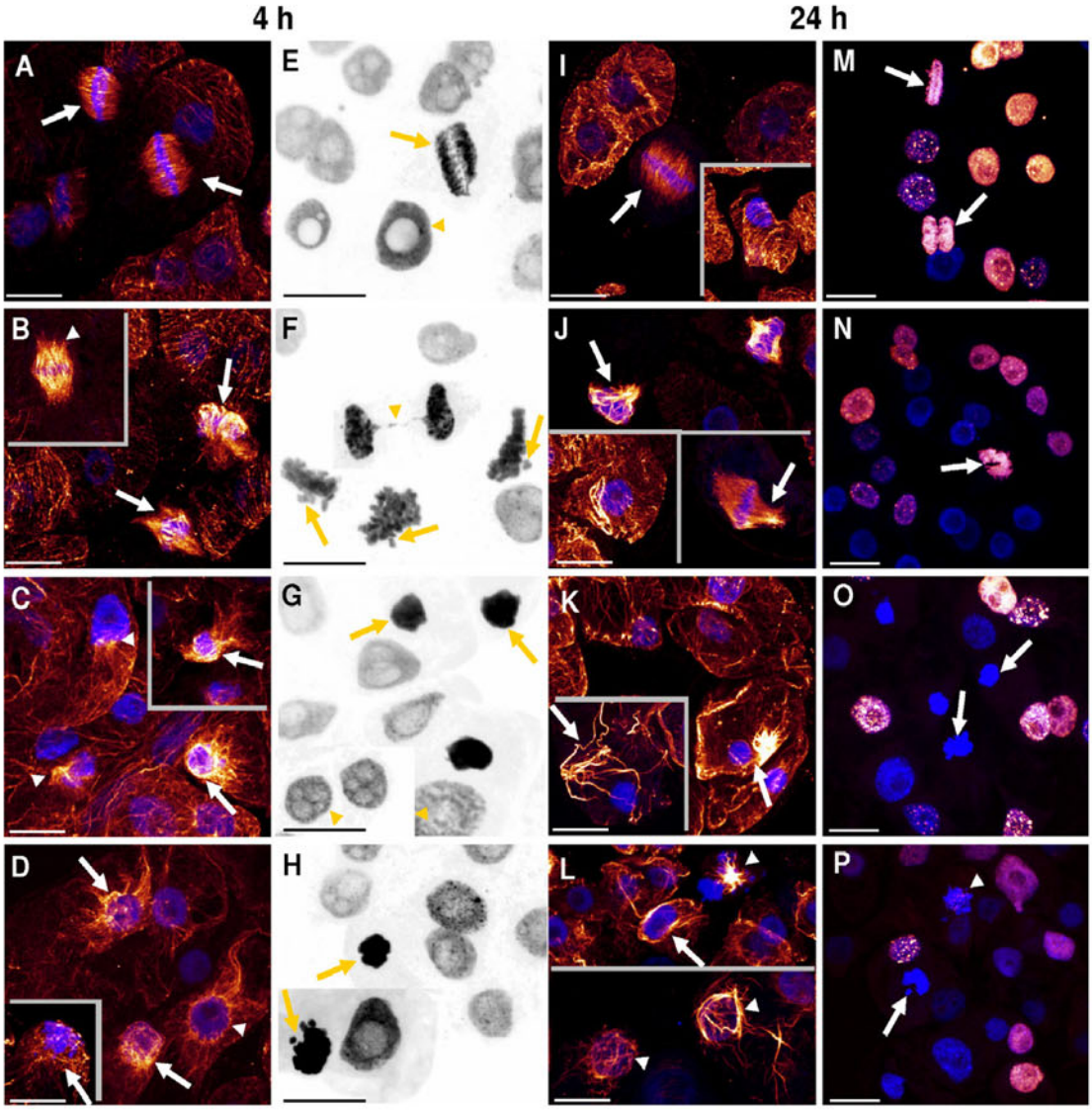

Fig. 3. Effects of endothall, cantharidin and okadaic acid on microtubule cytoskeleton and mitosis of tobacco BY-2 suspension cells. Exponentially growing BY-2 cells were treated with 10 μM compounds for 4 and 24 h and processed for fluorescence microscopic observations. (A–D) and (I–L) Immunofluorescent staining of microtubules using monoclonal antibody against β-tubulin (in red). Nuclear DNA was stained with Hoechst 33342 (in blue). Control cells (A, I) show typical mitotic phases (e.g. metaphase, arrows) and cortical microtubule patterns (I, inset). Endothall-treated cells (B), 4 h after treatment, show outspread spindle poles (inset, arrowhead) and uneven or asymmetrical mitotic spindle apparatus (arrows). Endothall-treated cells (J), 24 h after treatment, with affected spindle poles and deformed spindle apparatus (arrows). Cortical microtubules are reduced but still visible (J, inset). Cantharidin-treated cells (C), 4 h after treatment, show condensed microtubule patterns around the nucleus (C, arrows) or near by the nucleus (C, arrowheads). Cantharidin treated cells (K), 24 h after treatment, show strongly condensed and enlarged microtubule filaments often near by the nucleus, but also randomly distributed in the cell (arrows). Okadaic acid treated cells (D), 4 h after treatment, show similar changes in microtubule pattern than cantharidin. Nuclei are surrounded by condensed microtubules (D, arrows). Okadaic acid treated cells (L), 24 h after treatment, show condensed microtubule patterns in prophase or metaphase nuclei (L, arrowheads) and randomly distributed microtubules (L, arrow) in interphase cells. (E–H) and (M–P) Hoechst 33342 staining of nuclei. (M–P) Additional EdU labeling of nuclei (color coded in red) to visualize compound effects on cell proliferation. Characteristic structures of nuclei during cell cycle and mitosis are shown for each compound. Control cells (E), show distinct mitotic chromosome structures like anaphase (arrow). After 4 h of treatment, endothall-treated cells (F) show deformed chromosome structures (arrowhead), classified as prometaphase and incomplete distribution of chromosomes during mitosis (arrows). Cantharidin-treated cells (G) show strongly condensed nuclei (arrows) and relaxed nuclei structure (arrowhead). Okadaic acid (H) induces accumulation of strongly condensed nuclei (arrows) and few relaxed nuclei structures. Within 24 h, most of the control cells (M) entered or passed S-phase (red nuclei), including cells in mitotic phases. Metaphase and telophase nuclei show fluorescence which indicated EdU incorporation during S-phase (arrows). Endothall treated cells (N) show decreased S-phase transition and nuclei in mitosis with EdU incorporation (arrow). Cantharidin-treated cells (O) show few interphase nuclei with EdU incorporation, whereas strongly condensed nuclei do not show EdU mediated fluorescence (arrows). Okadaic acid-treated cells (P) also show no EdU mediated fluorescence (arrow). Prometaphase nuclei show only marginal EdU labeling (arrowhead).

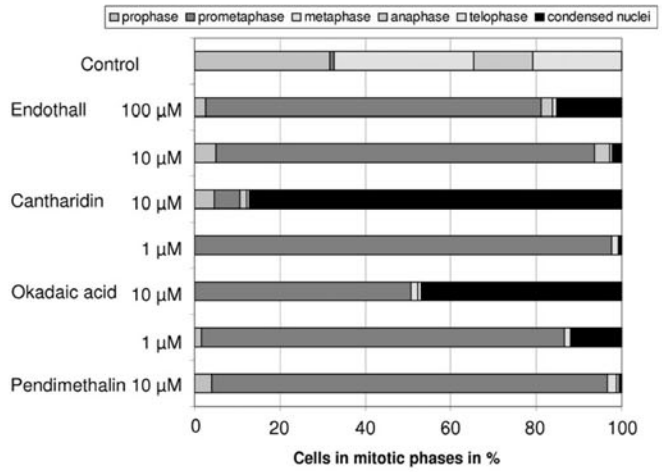

Fig. 4. Effects of endothall, cantharidin, okadaic acid and pendimethalin on the distribution of mitotic phases in tobacco BY-2 cells. Suspension cells were treated with compounds for 4 h. Hoechst 33342 stained nuclei of formalin fixed BY-2 cells were classified according to their cell cycle phase. Mitotic stages were categorized by microscopic observation of at least 500 cells per sample. Means of 4 biological replicates are shown. Cells in distinct mitotic phases were calculated as percent to total number of mitotic cells.

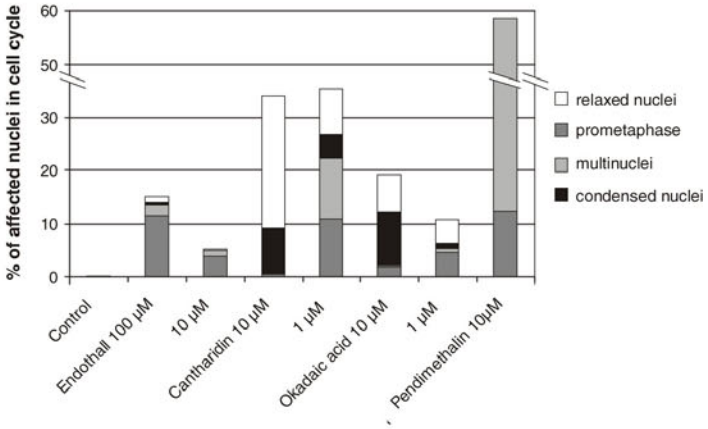

Fig. 5. Malformative effects on nucleus structure in different cell cycle phases induced by endothall, cantharidin, okadaic acid and pendimethalin in tobacco BY-2 cells. Hoechst 33342 stained nuclei of compound treated cells were classified as normal interphase, prophase, metaphase, anaphase or telophase nuclei. Malformed nuclei were classified as relaxed nuclei, prometaphase, multinuclei and strongly condensed nuclei. Relaxed nuclei were defined by their unusual Hoechst 33342 staining appearance and loosening of nucleus structure. Malformed nuclei of the distinct classes were calculated as percent to total number of affected nuclei and to total number of examined cells.

pattern of endothall and cantharidin in the bioassays together with typical plant symptoms like swelling of the meristematic root tip zone in cress seedlings showed strong similarity to inhibitors of microtubule assembly in mitosis such as pendimethalin (Fig. 1). The symptoms of tissue desiccation and necrosis which are, compared to pendimethalin, more dominant in endothall- or cantharidin-treated tissues are more typical for inhibitors which interfere with photosynthesis related processes and therefore induce reactive oxygen species, leading to cell death. These necrosis effects of endothall at high compound concentrations [4] could be based on inhibition of protein phosphatase regulated enzymes like nitrate reductase [11], sucrose phosphate synthase or hydroxymethylglutaryl-CoA reductase (reviewed by [26]). In addition, the observed slight uncoupler activity of endothall and cantharidin (Fig. 1) might contribute to membrane damage and leaf necrosis. However, further study is needed to clarify the mode of action behind the necrosis effects of endothall at high compound concentrations.

The relatively high endothall concentrations needed for induction of necrosis and the similarity of the physiological profile to mitosis inhibitors suggests that effects on cell division processes are the primary mode of action of endothall and cantharidin. Therefore, our advanced studies were focused on affected cell division processes. A direct interference of endothall in tubulin polymerization to microtubules does not appear to be the case, because endothall did not affect plant tubulin polymerization *in vitro* (Table 1). As shown in meristematic corn root tips, endothall has a strong distorting influence on the orientation of the cell division plane and microtubule spindle structures (Fig. 2). This effect was different to known microtubule assembly inhibitors such

Table 2
Changes in mitotic index (MI) and proliferation index (PI) in BY-2 tobacco suspension cells treated with endothall, cantharidin, okadaic acid and pendimethalin. Mitotic index was calculated as percent of cells in mitosis to total counted cells. Proliferation index was calculated as percent of fluorescent cells with EdU incorporation into DNA during S-phase to total counted cells.

	(μM)	4 h		24 h	
		MI	PI	MI	PI
Control		10.3 (±0.5)	24.1 (±1.4)	14.7 (±0.4)	86.0 (±5.0)
Endothall	100	12.3 (±1.1)	13.5 (±0.3)	16.4 (±1.0)	15.4 (±6.8)
	10	13.7 (±1.0)	17.1 (±3.6)	5.6 (±0.4)	47.1 (±1.6)
Cantharidin	10	14.4 (±1.0)	13.3 (±2.5)	8.5 (±0.6)	21.2 (±5.6)
	1	13.5 (±1.1)	18.8 (±2.0)	14.6 (±1.1)	17.6 (±1.0)
Okadaic acid	10	13.7 (±0.7)	14.1 (±2.9)	9.8 (±1.3)	8.0 (±3.4)
	1	14.0 (±1.7)	9.6 (±1.4)	6.1 (±0.5)	18.3 (±4.0)
Pendimethalin	10	17.9 (±1.5)	26.8 (±2.0)	22.9 (±1.2)	73.1 (±5.5)

as the dinitroaniline pendimethalin or flamprop-*m*-methyl [21,25]. Division plane orientation in corn cells has also been shown to be governed by DISCORDIA1 (DCD1) a homologue of the TONNEAU2 (TON2) protein in *Arabidopsis thaliana*, which functions as a regulatory subunit of protein phosphatases PP2As [27,28]. In accordance to microscopic observations in T-DNA inserted *A. thaliana ton1* and *ton2* mutants [28,29], most of the corn root cells undergoing mitosis were blocked by endothall in metaphase and chromosomal metaphase plates showed a diagonal orientation and were not aligned transversally as in untreated cells (Fig. 2). In addition, defective mitotic spindle microtubules oriented diagonally in the cell, similar to *ton1* and *ton2* mutant phenotypes, were observed in endothall treated plants. Studies in *ton1* and *ton2* mutants additionally revealed loss of preprophase band structures [28,29], which were also apparent in endothall-treated corn root cells (not shown). Walker et al. [30] described a relationship between TANGLED protein, which identifies the cell division plane throughout mitosis and cytokinesis, and TON2 pathway. Localization of TANGLED protein is disturbed in preprophase band defective *ton2* mutants. *tangled* mutants are affected in correct cell division plane orientation [30]. In conclusion, endothall-induced changes in microtubule cytoskeleton and cell division plane orientation resemble abnormalities observed in *Arabidopsis ton1* and *ton2* mutants [28,29]. Since endothall is an inhibitor of protein phosphatase PP2A *in vitro* [11,12], a direct effect of endothall on the functional protein complex of catalytic subunit PP2A and regulatory PP2A subunit TON2 could be expected to cause distorted microtubules and division plane orientation leading to mitotic disruption.

Further support of a causal relationship between protein phosphatase inhibition and effects on mitosis, is given by the observation of perinuclear microtubules patterns. This condensed pattern of microtubules around the nucleus was observed in *ton1* and *ton2* mutants [28,29] as well as in BY-2 tobacco suspension cells treated with endothall, cantharidin and the structurally different okadaic acid (Fig. 3). This effect was most pronounced in BY-2 cells treated with cantharidin and particularly with the more specific PP2A inhibitor okadaic acid. Mammalian PP2A responded 50 times more sensitive to okadaic acid than PP1 [31]. Endothall treatment elicited perinuclear microtubule patterns particularly at high concentration (100 μM). Treatment with 10 μM caused perinuclear microtubule patterns only occasionally. This could be due to less enzymatic inhibitor activity or PP2A sensitivity to endothall. Erdödi et al. [10] reported that, compared to PP1, mammalian PP2A responded only 3-fold and 1.8-fold more sensitive to cantharidin and endothall, respectively. This corresponds with data reported by [12] on the sensitivity of plant PP2A and PP1 to endothall.

Although the so far discussed effects of the protein phosphatase inhibitors including distorted microtubule and division plane orientation and perinuclear microtubule pattern correspond to the *ton1* and *ton2* phenotype, additional phenomena appear to be not based on TON2-pathway inhibition. These phenomena include especially the effects of the protein phosphatase inhibitors on distinct mitotic DNA phases and proliferation, which were not observed in *ton1* and *ton2* mutants. Nevertheless, induction of condensed nuclei in treated BY-2 cells appears to be also an effect based on PP2A inhibition. Snaith et al. [32] described *Drosophila* PP2A *mts* mutants with similar strongly condensed nuclei in embryos. In addition, condensed nuclei were also observed after endothall treatment of alfalfa cells [12]. However, it was difficult to evaluate in which cell cycle phase the condensed nuclei were arrested. In BY-2 cells, EdU labeling of nuclei revealed that none of the condensed nuclei contains artificial nucleotide EdU. This indicates that these nuclei have not entered S-phase with DNA replication during treatment with protein phosphatase inhibitors. It was speculated by [12] that these condensed nuclei are arrested in early prophase. This would implicate that protein phosphatase inhibitors interfere with mitosis and block S-phase entry and consequently, DNA replication. Based on our analysis of proliferation and detailed morphological evaluation of nuclei structure, it seems that the condensed nuclei are in late mitosis and are not able to undergo S-phase. This is supported by the observation of the fine structure of condensed nuclei. Whereas, chromosome like structures could be identified (Fig. 3O and H). Generally, BY-2 cells treated with endothall, cantharidin and okadaic acid showed strongly reduced proliferation activity, but EdU incorporation during DNA replication was not completely blocked. This suggests that S-phase transition from G1 is blocked, but ongoing DNA replication in S-phase cells is not or only less affected. Therefore, in addition to mitosis arrest, S-phase initiation might be an additional target site for protein phosphatase regulation.

Based on investigations in mammalian cells where PP1 activity was neutralized by an antibody, cells in mitosis where blocked at metaphase [33]. Derived from this effect, it could be speculated that the block during mitosis in BY-2 cells, characterized by condensed nuclei, could be based on PP1 inhibition by the compounds. This speculation is also supported by the observation that the strongest accumulation of condensed nuclei occurred after cantharidin treatment, which has a strong inhibitory effect on PP1 [10]. Okadaic acid was shown to possess a higher selectivity for PP2A inhibition and therefore, PP1 regulated processes should be less affected [31]. Endothall was found to be a 10-fold less potent protein phosphatase inhibitor than cantharidin *in vitro* [10,11]. This explains why endothall caused identical cell cycle phenomena to cantharidin in BY-2 cells, but, at higher compound concentration. The results suggest that, dependent on the protein phosphatase inhibitors used and their different potency and preference to PP1, PP2A or other phosphatases, slightly different phenotypes at the cytological level are induced. Additional experiments with inhibitors, such as fostriecin or tautomycetin [34,35], which act possibly more specific on the different protein phosphatases in plants, could clarify the distinct roles of the protein phosphatases in the cell cycle processes in more detail.

5. Conclusions

Supported by physiological and cytological investigations in comparison with known mitosis or protein phosphatase inhibitors,

the preferred phytotoxic mode of action of endothall appears to be based on changes in microtubule array formation and cell cycle regulation in meristematic cells, which lead to mitotic disruption, inhibition of cell division and, ultimately, to cell death. This suggests that endothall and cantharidin induced effects on cell cycle processes are mediated by protein phosphatase inhibition. Because of similarity of endothall-induced distorted microtubule array and division plane orientation, to phenomena observed in *ton1* and *ton2 Arabidopsis* mutants [28,29], we suggest that PP2A/TON2 protein phosphatase complex is an *in planta* molecular target of endothall. On the other hand, the endothall-induced phenomena of condensed nuclei, which indicate late mitosis arrest, and block of S-phase initiation in BY-2 cells, might be caused by inhibition of PP1 and/or other protein phosphatases related to PP2A.

Based on the mode of action discovery, endothall and cantharidin can be used in basic research as additional probes to unravel the function of the different types of protein phosphatases in plant cell cycle regulation.

Acknowledgments

We are grateful to Wolfgang Wernicke (University of Mainz, Germany) for kindly forwarded to us BY-2 cell cultures and valuable discussion. We also thank Günter Caspar and Manuela Wetternach for excellent technical assistance and Thomas Ehrhardt for critical reading the manuscript.

References

[1] N. Tischler, J.C. Bates, G.P. Quimba, A new group of defoliant-herbicidal chemicals, Proc. Ann. Meeting Northeastern Weed Control Conf. 4 (1951) 51–83.
[2] S.A. Senseman, Herbicide Handbook, ninth ed., Weed Sci. Soc. of Am., 2007.
[3] S.M. Wilson, A. Daniel, G.B. Wilson, Cytological and genetical effects of the defoliant endothal, J. Heredity 47 (1956) 151–155.
[4] A. Rikin, B. Rubin, Increase of cotton cotyledon resistance to the herbicide endothall by abscisic acid, Physiol. Plant. 59 (1983) 161–164.
[5] J.D. Mann, M. Pu, Inhibition of lipid synthesis by certain herbicides, Weed Sci. 16 (1968) 197–198.
[6] J.D. Mann, L.S. Jordan, B.E. Day, A survey of herbicides for their effect upon protein synthesis, Plant Physiol. 40 (1965) 840–844.
[7] D. Penner, F.M. Ashton, Influence of dichlobenil, endothall, and bromoxynil on kinin control of proteolytic activity, Weed Sci. 16 (1968) 323–326.
[8] R.-C. Tsay, F.M. Ashton, Effect of several herbicides on dipeptidase activity of squash cotyledons, Weed Sci. 19 (1971) 682–684.
[9] Y.-M. Li, J.E. Casida, Cantharidin-binding protein: identification as protein phosphatase 2A, Proc. Natl. Acad. Sci. USA 89 (1992) 11867–11870.
[10] F. Erdödi, B. Toth, K. Hirano, M. Hirano, D. J Hartshorne, P. Gergely, Endothall thioamide inhibits protein phosphatases-1 and -2A in vivo, Am. J. Physiol. 269 (1995) 1176–1184.
[11] Y.-M. Li, C. MacKintosh, J.E. Casida, Protein phosphatase 2A and its [^{3}H] cantharidin/[^{3}H]endothall thioanhydride binding site – inhibitor specifity of cantharidin and ATP analogues, Biochem. Pharmacol. 46 (1993) 1435–1443.
[12] F. Ayaydin, E. Vissi, T. Mesaros, P. Miskolczi, I. Kovacs, A. Feher, V. Dombradi, F. Erdödi, P. Gergely, D. Dudits, Inhibition of serine/threonine-specific protein phosphatases causes premature activation of cdc2MsF kinase at G2/M transition and early mitotic microtubule organisation in alfalfa, Plant J. 23 (2000) 85–96.
[13] K. Grossmann, What it takes to get a herbicide's mode of action. Physionomics, a classical approach in a new complexion, Pest Manage. Sci. 61 (2005) 423–431.
[14] S. Tresch, P. Plath, K. Grossmann, Herbicidal cyanoacrylates with antimicrotubule mechanism of action, Pest Manag. Sci. 61 (2005) 1052–1059.
[15] E.M. Linsmaier, F. Skoog, Organic growth factor requirements of tobacco tissue cultures, Physiol. Plant. 18 (1965) 100–127.
[16] S.E. Ruzin, Plant Microtechnique and Microscopy, Oxford University Press, Oxford, 1999.
[17] T. Nagata, Y. Nemoto, S. Hasezawa, Tobacco BY-2 cell line as the "HeLa" cell in the cell biology of higher plants, Int. Rev. Cytol. 132 (1992) 1–30.
[18] S. Hasezawa, T. Sano, T. Nagata, The role of microfilaments in the organization and orientation of microtubules during the cell cycle transition from M phase to G1 phase in tobacco BY-2 cells, Protoplasma 202 (1998) 105–114.
[19] A. Salic, T.J. Mitchison, A chemical method for fast and sensitive detection of DNA synthesis in vivo, Proc. Natl Acad. Sci. USA 105 (2008) 2415–2420.
[20] E. Kotogany, D. Dudits, G.V. Horvath, F. Ayaydin, A rapid and robust assay for detection of S-phase cell cycle progression in plant cells and tissues by using ethynyl deoxyuridine, Plant Methods 6:5 (2010).
[21] S. Tresch, R. Niggeweg, K. Grossmann, The herbicide flamprop-M-methyl has a new antimicrotubule mechanism of action, Pest Manag. Sci. 64 (2008) 1195–1203.
[22] D. Bonne, C. Heusele, C. Simon, D. Pantaloni, 4',6-Diamidino-2-phenylindole, a fluorescent probe for tubulin and microtubules, J. Biol. Chem. 260 (1985) 2819–2825.
[23] R.G. Anthony, P.J. Hussey, Dinitroaniline herbicide resistance and the microtubule cytoskeleton, Trends Plant Sci. 4 (1999) 112–116.
[24] S. Hasezawa, T. Nagata, Okadaic acid as a probe to analyse the cell cycle progression in plant cells, Bot. Acta 105 (1992) 63–69.
[25] J.C. Hoffman, K.C. Vaughn, Mitotic disrupter herbicides act by a single mechanism but vary in efficacy, Protoplasma 176 (1994) 16–25.
[26] R.D. Smith, J.C. Walker, Plant protein phosphatases, Annu. Rev. Plant Physiol. Plant Mol. Biol. 47 (1996) 101–125.
[27] A.J. Wright, K. Gallagher, L.G. Smith, *discordia1* and alternative *discordia1* function redundantly at the cortical division site to promote preprophase band formation and orient division planes in maize, Plant Cell 21 (2009) 234–247.
[28] C. Camilleri, J. Azimzadeh, M. Pastuglia, C. Bellini, O. Grandjean, D. Bouchez, The *Arabidopsis* TONNEAU2 gene encodes a putative novel protein phosphatase 2A regulatory subunit essential for the control of the cortical cytoskeleton, Plant Cell 14 (2002) 833–845.
[29] J. Azimzadeh, P. Nacry, A. Christodoulidou, S. Drevensek, C. Camilleri, N. Amiour, F. Parcy, M. Pastuglia, D. Bouchez, *Arabidopsis tonneau1* proteins are essential for preprophase band formation and interact with centrin, Plant Cell 20 (2008) 2146–2159.
[30] K.L. Walker, S. Müller, D. Moss, D.W. Ehrhardt, L.G. Smith, *Arabidopsis* TANGLED identifies the division plane throughout mitosis and cytokinesis, Curr. Biol. 17 (2007) 1827–1836.
[31] H. Fujiki, M. Suganuma, Tumor promotion by inhibitors of protein phosphatases 1 and 2A: the okadaic acid class of compounds, Adv. Cancer Res. 61 (1993) 143–194.
[32] H.A. Snaith, C.G. Armstrong, Y. Guo, K. Kaiser, P.T.W. Cohen, Deficiency of protein phosphatase 2A uncouples the nuclear and centrosome cycles and prevents attachment of microtubules to the kinetochore in Drosophila microtubule star (mts) embryos, J. Cell Sci. 109 (1996) 3001–3012.
[33] A. Fernandez, D.L. Brautigan, N.J.C. Lamb, Protein phosphatase type 1 in mammalian cell mitosis: chromosomal localization and involvement in mitotic exit, J. Cell Biol. 116 (1992) 1421–1430.
[34] A.H. Walsh, A.Y. Cheng, R.E. Honkanen, Fostriecin, an antitumor antibiotic with inhibitory activity against serine/threonine protein phosphatases types 1 (PP1) and 2A (PP2A), is highly selective for PP2A, FEBS Lett. 416 (1997) 230–234.
[35] S. Mitsuhashi, N. Matsuura, M. Ubukata, H. Oikawa, H. Shima, K. Kikuchi, Tautomycetin is a novel and specific inhibitor of serine/threonine protein phosphatase type 1, PP1, Biochem. Biophys. Res. Commun. 287 (2001) 328–331.

3.4. Mefluidide and perfluidone, selective inhibitors of 3-ketoacyl-CoA synthases in very-long-chain fatty acid synthesis

The paper by Tresch *et al.* (2012), describing the MoA of mefluidide and perfluidone, is an example of how to implement metabolic profiling studies in a MoA identification cascade. Previous studies described the effects of mefluidide or perfluidone as uncouplers of electron transport chains with influences on lipid concentrations, but detailed MoA descriptions are missing (Moreland, 1981; Valadon and Kates, 1984). Our initial characterisation of mefluidide and perfluidone by physiological assays indicated a MoA in the biosynthesis of lipids or fatty acids. Therefore, it appeared appropriate to investigate the effects in a metabolic profiling approach and to characterise the metabolite levels of the respective pathways in more detail. The described publication is an excellent example of how to direct the MoA studies in relation to the initial phenotypic characterisation. It also shows that a versatile methodical toolbox is needed to investigate the physiological effects of phytotoxic compounds. The interpretation of physiological assays, in correlation with metabolic profiling and biochemical characterisation of the inhibition potential on KCS proteins, shows the power of the phenotyping approach to identify the dominant mechanism of action leading to plant effects.

Phytochemistry 76 (2012) 162–171

Contents lists available at SciVerse ScienceDirect

Phytochemistry

journal homepage: www.elsevier.com/locate/phytochem

Inhibition of saturated very-long-chain fatty acid biosynthesis by mefluidide and perfluidone, selective inhibitors of 3-ketoacyl-CoA synthases

Stefan Tresch [a,*], Monika Heilmann [a,1], Nicole Christiansen [b], Ralf Looser [b], Klaus Grossmann [a]

[a] BASF SE, Crop Protection, Speyerer Str. 2, 67117 Limburgerhof, Germany
[b] Metanomics GmbH, Tegeler Weg 33, 10589 Berlin, Germany

ARTICLE INFO

Article history:
Received 22 September 2011
Received in revised form 7 December 2011
Accepted 31 December 2011
Available online 25 January 2012

Keywords:
Herbicide mode of action
Mefluidide
Perfluidone
Trifluoromethanesulphonanilide
3-Ketoacyl-CoA synthase
Very-long-chain fatty acid biosynthesis
Metabolic profiling
Physiological profiling

ABSTRACT

The trifluoromethanesulphonanilides mefluidide and perfluidone are used in agriculture as plant growth regulators and herbicides. Despite the fact that mefluidide and perfluidone have been investigated experimentally for decades, their mode of action is still unknown. In this study, we used a cascade approach of different methods to clarify the mode of action and target site of mefluidide and perfluidone. Physiological profiling using an array of biotests and metabolic profiling in treated plants of *Lemna paucicostata* suggested a common mode of action in very-long-chain fatty acid (VLCFA) synthesis similar to the known 3-ketoacyl-CoA synthase (KCS) inhibitor metazachlor. Detailed analysis of fatty acid composition in *Lemna* plants showed a decrease of saturated VLCFAs after treatment with mefluidide and perfluidone. To study compound effects on enzyme level, recombinant KCSs from *Arabidopsis thaliana* were expressed in *Saccharomyces cerevisiae*. Enzyme activities of seven KCS proteins from 17 tested were characterized by their fatty acid substrate and product spectrum. For the KCS CER6, the VLCFA product spectrum *in vivo*, which consists of tetracosanoic acid, hexacosanoic acid and octacosanoic acid, is reported here for the first time. Similar to metazachlor, mefluidide and perfluidone were able to inhibit KCS1, CER6 and CER60 enzyme activities *in vivo*. FAE1 and KCS2 were inhibited by mefluidide only slightly, whereas metazachlor and perfluidone were strong inhibitors of these enzymes with IC_{50} values in µM range. This suggests that KCS enzymes in VLCFA synthesis are the primary herbicide target of mefluidide and perfluidone.

1. Introduction

The plant growth regulator mefluidide and the herbicide perfluidone were developed and introduced in agriculture by 3 M Company as Embark and Destune, respectively (Tomlin, 2010). Both compounds belong to the class of trifluoromethanesulphonanilides which derived from a chemical synthesis and screening program in the 1970s (Friedinger, 1978). Because of their broad spectrum of effects on plant growth and development, studies on the mode of action of mefluidide and perfluidone were the objective of several reports in the 1980s (Moreland, 1981; Wilkinson, 1982; Valadon and Kates, 1984; Tautvydas and Hargroder, 1985). Due to the plant growth regulating activity of mefluidide, mode of action research was mainly focused on an interference of mefluidide in hormone biosynthesis and signaling. Glenn and Rieck (1985) found that the polar transport of auxin was influenced in corn coleoptiles after mefluidide application. Wilkinson (1982) suggested that mefluidide inhibits the synthesis of gibberellins. Since growth effects of mefluidide could not be reversed by adding of gibberellic acid A_3, an indirect interference of mefluidide in the production of gibberellins is most likely (Truelove et al., 1977; Tautvydas and Hargroder, 1985). In addition, effects of mefluidide on protein, DNA and RNA synthesis were reported, but not clarified if they are elicited by mefluidide directly or indirectly (Tautvydas and Hargroder, 1985). Investigations with perfluidone showed that the compound uncouples the electron transport of isolated thylakoid membranes as well as isolated mitochondria, but no evidence was obtained for a direct interaction between perfluidone and the redox components of the electron transport pathways (Moreland, 1981). Monitoring of changes in lipid classes and fatty acids showed that perfluidone affects the desaturation grade of fatty acids (Valadon and Kates, 1984). Valadon and Kates (1984) observed that the mol% distribution of linolenic acid (18:3) is decreased in comparison to saturated, mono- and di-unsaturated stearic acid. So far, no specific target site could be identified for mefluidide and perfluidone.

In order to characterize the growth-inhibiting effects of mefluidide and perfluidone and to identify the mode of action and target site, we initially used a set of bioassays for physiological profiling

* Corresponding author. Tel.: +49 621 6027317; fax: +49 621 6027176.
E-mail address: stefan.tresch@basf.com (S. Tresch).
[1] Present address: Institute of Molecular Cell and Systems Biology, University of Glasgow, Glasgow G128QQ, UK.

0031-9422/$ - see front matter © 2012 Elsevier Ltd. All rights reserved.
doi:10.1016/j.phytochem.2011.12.023

of the compound effects in a physionomics approach (Grossmann, 2005). In addition, metabolic profiling in treated *Lemna paucicostata* plants was performed to quantitate metabolite changes, relative to untreated controls. Physiological and metabolic profiling suggested a mode of action similar to inhibitors of very-long-chain fatty acid (VLCFA) biosynthesis such as the chloroacetamide-type herbicide metazachlor.

VLCFAs, fatty acids with more than 20 carbon atoms, have multiple functions in the plant. Primarily, they serve as precursors of cuticle wax biosynthesis and as components of storage lipids, sphingolipids and phospholipids (reviewed by Kunst and Samuels, 2003; Bach and Faure, 2010). An additional function in polar auxin transport has recently been identified (Roudier et al., 2010). Chloroacetamides have been shown to inhibit the plant VLCFA elongase complex, a four-step-catalytic system including a condensation, reduction, dehydration and a second reduction step (reviewed by Böger, 2003). Experiments with transgenic *Saccharomyces cerevisiae* strains expressing the plant 3-ketoacyl-CoA synthase (KCS) FAE1, which catalyzes the first, rate limiting step in the elongation of VLCFAs, identified this condensing enzyme as the primary target of chloroacetamides (Millar and Kunst, 1997; Böger, 2003). In plants, KCS enzymes are encoded by a gene family which contains 21 members in *Arabidopsis thaliana* (reviewed by Joubes et al., 2008) and similar number of genes in *Oryza sativa* (23), *Zea mays* (27), *Brachypodium distachyon* (23) and *Glycine max* (31) (Phytozome v6.0, 2011, http://www.phytozome.org). The different KCS genes vary in their tissue and ontogeny-specific expression patterns and the proteins show distinct substrate specificity (Joubes et al., 2008). The KCS isoenzymes are differentially inhibited by class K3 herbicides (according to HRAC, Herbicide Resistance Action Committee; Senseman, 2007), which include the chloroacetamide-type herbicides (Trenkamp et al., 2004).

In order to reveal direct effects of mefluidide and perfluidone on VLCFA synthesis, VLCFA contents in treated *L. paucicostata* plants and inhibition of enzyme activity *in vivo* of seven recombinant KCSs from *A. thaliana*, expressed in *S. cerevisiae* wildtype (InvSc1) and Δelo2 or Δelo3 knock out strains, were studied. The results suggest that the primary mode of action of mefluidide and perfluidone is based on the inhibition of KCSs involved in VLCFA biosynthesis.

2. Results

2.1. Physiological profiling using bioassays

The physiological and phenotypical plant response after a chemical treatment can be used to diagnose the mode of action of a compound (Grossmann, 2005). Therefore, we have used a set of bioassays for the comprehensive physiological profiling of plant effects elicited by mefluidide and perfluidone. The set of tests included heterotrophic corn (*Galium mollugo* L.) and phototrophic green algae (*Scenedesmus obliquus*) cell suspensions, duckweed (*L. paucicostata*), isolated mustard shoots (*Sinapis alba*) and germinating cress seeds (*Lepidium sativum*). The test panel was completed by assays for monitoring physiological processes including the Hill reaction of isolated wheat thylakoid, respiration activity measured by oxygen consumption in heterotrophic *Galium aparine* cell suspensions, membrane function and uncoupler activity determined in *Lemna* root mitochondria using the potential sensor JC-1, carbon gas-exchange measurement in *G. aparine* plants and toluidine-blue staining (TBO assay) of cress hypocotyls for determination of cuticle formation and function. The physiological profile represents a fingerprint of a phytotoxic compound, which has proved to be typical of its mode of action (Grossmann, 2005). The results can be interpreted directly, or response pattern of compounds with known mode of action can be screened for similarities as an aid to direct further studies.

The physiological profile of mefluidide (Fig. 1) shows the strongest inhibitory effects on *Scenedesmus*, *Lemna* (see also Table 4) and cress seedling growth. In *Lemna*, reduction of frond formation and growth, accompanied by intensified green frond pigmentation were observed. In cress seedlings, shoot and root growth were inhibited; the effects did not depend on light. Furthermore, treatment with mefluidide hampered proper formation of the plant cuticle which is indicated in the TBO assay (Fig. 1). When compared with the effects of standard herbicides, known inhibitors of VLCFA synthesis such as metazachlor induced a similar type of physiological profile as mefluidide; however, at a higher activity level in the bioassays. In comparison to mefluidide, the structurally related perfluidone showed similar, but stronger inhibitory effects particulary on growth of *Scenedesmus*, *Lemna* and cress seedlings as well as on cuticle functionality in the TBO assay (Fig. 1). However, at high concentrations (100 μM), perfluidone additionally elicited moderate uncoupling of oxidative phosphorylation in *Lemna* root mitochondria, which was accompanied by inhibition of respiration. Overall, the typical effects of mefluidide and perfluidone with inhibition of *Lemna* growth and intensified green frond pigmentation, and inhibition of cuticle formation and function were similar to those observed after treatment with metazachlor. These similarities indicate a mode of action for the compounds in VLCFA biosynthesis similar to metazachlor.

2.2. Metabolic profiling in Lemna

Metabolite changes induced by plant growth regulators and herbicides are a plant response which can provide information on affected metabolic and biochemical processes. Consequently, metabolic profiling is an opportunity to generate profiles which are diagnostic of a compound's mode of action (Sauter et al., 1991; Trenkamp et al., 2009; Grossmann et al., 2010; Aliferis and Jabaji, 2011). Recent studies using the model organism *Lemna* have shown that comparison of metabolic patterns after treatment with different compounds provide reliable and highly consistent results for mode of action classification (Grossmann et al., 2010). The small aquatic plant *Lemna* exhibits all organs of a higher vascular plant, is growing vegetatively with a doubling time of 24 h, and is therefore genetically uniform. The small space requirement for growth allows highly standardized experimental conditions and emphasizes *Lemna* as an excellent model organism for metabolic profiling studies.

Mode of action classification of metabolic changes induced by mefluidide or perfluidone was performed by cluster analysis based PAM. We searched against our reference metabolic profile database which consists of ca. 150 known herbicides and plant growth regulators from more than 60 different mode of action classes and several hundred new compounds. As shown in Table 1 for mefluidide as well as for perfluidone, PAM ranking assigned inhibition of 'VLCFA synthesis, elongase' at the first position with good maximum log likelihood (mll) values of −0.18 and −0.0064, respectively. This mode of action class contains alachlor, metazachlor, propachlor, mefenacet and dimethenamid, which are all described as inhibitors of KCSs (Trenkamp et al., 2004; Senseman, 2007). Close to the 'VLCFA synthesis, elongase' inhibitor mode of action class, mefluidide and perfluidone ranked at the second position to inhibitors 'VLCFA synthesis, not elongase' which consists of benfuresate, diallate, ethofumesate, methyldymron, molinate and triallate. These compounds are known inhibitors of VLCFA biosynthesis through a, so far, unknown mechanism (Senseman, 2007).

In the case of mefluidide, the relatively low distance value of 0.98 for the first ranking position indicates that the second ranking position could not be clearly separated from the first (Table 1). On

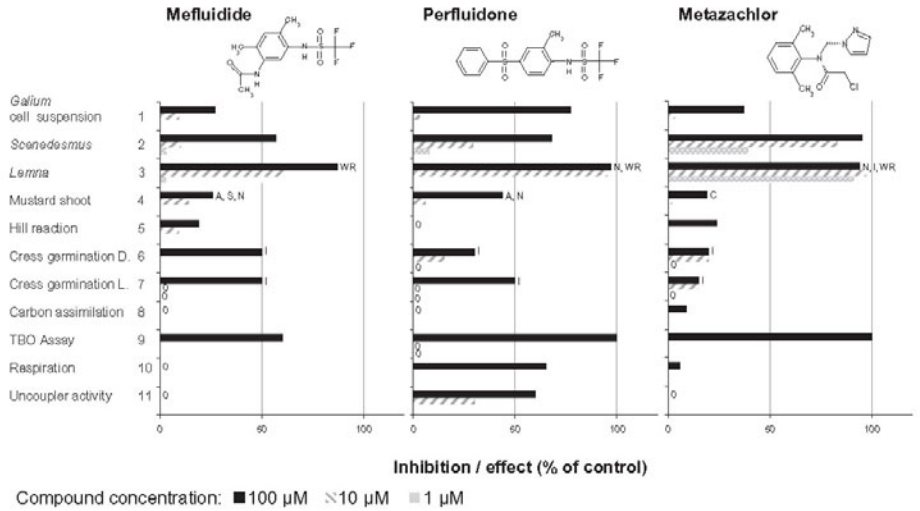

Fig. 1. Effects of mefluidide, perfluidone and metazachlor in bioassays including corn and *Scenedesmus* cell suspensions, duckweed (*Lemna paucicostata*), isolated mustard shoots, germinating cress seeds, the Hill reaction of isolated thylakoids, respiration by measuring oxygen consumption in heterotrophic *Galium aparine* cell suspensions, uncoupler activity in *Lemna* root mitochondria, test on cuticle function with toluidine-blue O (TBO) in cress hypocotyls and carbon assimilation in *G. aparine* plants. SE of the mean in all cases was less than 10%. Symptoms observed: A, desiccation; C, chlorosis; I, root growth inhibition; N, necrosis; S, swelling; WR, intensified green frond pigmentation.

Table 1
Mode of action classification by cluster analysis of metabolite changes with the use of prediction analysis of microarrays (PAM).

Ranking	Class	Distance	mll
Mefluidide			
1	Very-long-chain-fatty acid synthesis, elongase	0.908	−0.18
2	Very-long-chain-fatty acid synthesis, not elongase	10.69	−0.00014
3	HMG-CoA reductase	1.21	−0.68
4	Microtubule assembly	2.04	−0.085
Perfluidone			
1	Very-long-chain-fatty acid synthesis, elongase	7.15	−0.0064
2	Very-long-chain-fatty acid synthesis, not elongase	8.59	−0.0002
3	Acetyl-CoA-carboxylase	0.23	−2.4
4	Purine synthesis	0.41	−2.0

In *Lemna paucicostata* plants treated with mefluidide (10, 100 and 200 µM) and perfluidone (1, 10, 100 µM) for 48 and 72 h, changes of about 200 identified and about 300 unknown analytes, relative to control, were determined. PAM was applied for the ranking of profile changes elicited by the compounds. The profile classes for comparison were generated by herbicides with known MoA class membership. Ranking position of the best four modes of action from 60 is shown with their indicative statistical values. The ranking is based on the logarithmized probability indicated by mll. The distance value is an indicator for the degree of distinctness in the classification, with the highest value as the best, and results from the mll values of the two best ranks of the classes.

the other hand, the high distance value of 10.69 for the second ranking position separates the first two clearly from the consecutive mode of action classes 'HMG-CoA reductase' (3-hydroxy-3-methylglutaryl-coenzmye-A reductase) inhibitors and inhibitors of 'microtubule assembly'. For perfluidone the distance and mll values indicate the 'VLCFA synthesis, elongase' class as the most likely mode of action. The high distance value of 7.15 clearly separates the second possible mode of action 'VLCFA synthesis, not elongase' from the first one (Table 1).

For refinement of the mode of action classification to VLCFA synthesis inhibition, the supervised statistical clustering method PLS-DA was carried out (Fig. 2). The used mathematical model with a quality of prediction Q^2 (cum) of 80% separated inhibitors of the two mode of action classes 'VLCFA synthesis, elongase' and 'VLCFA synthesis, not elongase' (Fig. 2). As shown in Fig. 2A, PLS-DA revealed that mefluidide-induced metabolite changes cluster in and between the cluster of profiles of known 'VLCFA synthesis, elongase' and 'VLFCA synthesis, not elongase' inhibitors. However, most of the mefluidide profile samples cluster with 'VLCFA synthesis, elongase' inhibitor profiles. For perfluidone, PLS-DA clearly assigned metabolic profiles to the pre-defined cluster of profiles of known 'VLCFA synthesis, elongase' inhibitors (Fig. 2B). These results further support a primary mode of action of mefluidide and perfluidone in VLCFA biosynthesis, possibly based on the inhibition of elongation steps catalyzed by VLCFA elongases (KCSs).

2.3. Fatty acid analysis shows particularly a decrease in saturated very-long-chain fatty acids

To determine the effect of mefluidide and perfluidone in comparison to the known KCS inhibitor metazachlor on VLCFA biosynthesis in *Lemna* tissue, quantitative analyses of fatty acids were performed by GC/MS. As shown in Fig. 3, based on mol% of a fatty acid related to the total fatty acid content in *Lemna*, the saturated VLCFAs eicosanoic acid (20:0), docosanoic acid (22:0) and tetracosanoic acid (24:0) were strongly decreased by treatment with mefluidide, perfluidone and metazachlor, in a concentration dependent manner. Compared to control (100%), contents of saturated VLCFAs decreased to 36%, 53% and 52% after treatment with metazachlor (10 µM), perfluidone (10 µM) or mefluidide (100 µM), respectively. In contrast, the mol% of fatty acids with less then 20 carbon atoms showed only minor changes. Only tetradecanoic acid (14:0) showed an increase, particular after metazachlor treatment. Unsaturated VLCFAs, which account for 0.4 mol% of total fatty acids in *Lemna* tissue, were only slightly influenced. Only dodecanoid acid (22:1) showed a slight increase after metazachlor or perfluidone treatment.

Table 2
KCS proteins with their respective VLCFA elongation products.

Gene	Locus ID	C20	C22	C24	C26	C28	%VLCFA from total (SE)
FAE1 (KCS18)[a]	AT4G34520	20:0, 20:1*	22:0, 22:1				15.20 (±0.17)
KCS1	AT1G01120	20:0, 20:1	22:0				2.58 (±0.06)
KCS2	AT1G04220	20:0	22:0	24:0			6.21 (±0.18)
KCS20	AT5G43760	20:0	22:0*	24:0			9.20 (±0.19)
CER60 (KCS5)	AT1G25450			24:0	26:0*	28:0	5.95 (±0.09)
CER6 (KCS6)	AT1G68530			24:0	26:0*	28:0	8.73 (±0.21)
KCS17	AT4G34510			24:0			1.43 (0.05)

After expression of seven *Arabidopsis* KCSs in *S. cerevisiae* cells, the VLCFA products solely produced by the plant KCSs are shown. With the use of distinct *S. cerevisiae* strains (wildtype InvSc1, Δelo2, Δelo3), VLCFAs synthesized by the plant KCS proteins were differentiated from those produced by the endogeneous *S. cerevisiae* elo proteins. The identified plant-KCS-derived VLCFAs are listed and their summarized amount is given as %VLCFA from total content of fatty. The respective standard error (SE) was calculated from at least three biological replicates. Main VLCFA products with a share of more than 60% of the total amount of VLCFAs synthesized by the plant KCS proteins are indicated by asterisks.

[a] In KCS18 (FAE1), feeding of yeast cells with polyunsaturated C18 fatty acids resulted in additional accumulation of eicosadienoic acid (C20:2) and eicosatrienoic acid (C20:3) (not shown).

Table 3
Inhibition of activity of different plant KCS proteins by mefluidide and metazachlor.

Gene	Genetic background	%Inhibition at 100 μM	
		Mefluidide	Metazachlor
FAE1 (KCS18)	Δelo2	5.1 (±2.10)	95.7 (±0.27)
KCS1	Δelo2	91.0 (±1.41)	93.0 (±1.64)
KCS2	Wt	0.3 (±5.41)	82.4 (±1.73)
KCS20	Δelo2	26.9 (±1.07)	97.5 (±0.24)
CER60 (KCS5)	Δelo3	71.8 (±0.51)	100 (±0)
CER6 (KCS6)	Δelo3	51.2 (±1.54)	100 (±0)
KCS17	Δelo3	nd.	100 (±0)

Inhibition of KCS activity by mefluidide (100 μM) and metazachlor (100 μM) was demonstrated in transgenic *S. cerevisiae* cells which expressed different *Arabidopsis* KCS proteins. Inhibition of the different KCS enzyme activities were determined with the aid of wildtype (InvSc1) and Δelo2 and Δelo3 knock out strains to minimize influences of *S. cerevisiae* endogenous ELO-proteins on inhibition values. Inhibition values were calculated as percent inhibition of detected VLCFA products synthesized by a given KCS in comparison to untreated *S. cerevisiae* cells (nd.: not determined). The standard error was calculated from at least three biological replicates.

Table 4
Inhibition of activity of plant KCS FAE1 and CER6 and *Lemna* growth by mefluidide, perfluidone and metazachlor.

Compound	IC_{50} CER6 [μM]	IC_{50} FAE1 [μM]	*Lemna* growth inhibition IC_{50} [μM]
Metazachlor	0.032 (±0.002)	1.99 (±0.47)	0.12 (±0.03)
Mefluidide	114 (±12)	>500[a]	3.15 (±0.74)
Perfluidone	0.21 (±0.08)	7.60 (±0.74)	0.52 (±0.03)

Compound concentrations required for 50% inhibition (IC_{50}) of FAE1 and CER6 activities were determined in *S. cerevisiae* Δelo2 and Δelo3 strains, respectively, and for growth inhibition of *Lemna paucicostata* after seven days of treatment. Calculation of IC_{50} values were performed from at least four inhibitor concentrations with three biological replicates using a two-logistic regression model. Standard errors (SE) derived from the best fit.

[a] Mefluidide inhibited the activity of FAE1 by 30.3% (SE 3.4) at a concentration of 500 μM.

2.4. Heterologous expression of Arabidopsis KCS genes in S. cerevisiae

In order to investigate effects of mefluidide and perfluidone on KCS enzyme activity, we have cloned 17 *A. thaliana* KCS genes for recombinant expression in the galactose inducible expression vector pYES2.1. To determine the activity of expressed KCS isoenzymes in *S. cerevisiae*, the VLCFA content in the transgenic strain was analyzed in comparison to the wildtype (InvSc1).

This study showed functional expression of seven KCS gene products that were able to synthesize VLCFAs from substrates provided by *S. cerevisiae*. Due to the capability of the endogeneous *S. cerevisiae* elo2 and elo3 enzymes to synthesize the VLCFA hexacosanoic acid (26:0), clear differentiation between VLCFA products that were solely synthesized by expressed *Arabidopsis* KCS proteins or the *S. cerevisiae* ELO2/ELO3 enzymes was not possible. As illustrated in Fig. 4A, the ELO2 enzyme is capable of synthesizing eicosanoic (20:0) and docosanoic acid (22:0) using octadecanoic acid (18:0) as substrate, whereas the ELO3 protein is able to use docosanoic acid (22:0) as substrate to produce tetracosanoic (24:0) and hexacosanoic acid (26:0) as reported by Oh et al., (1997). Paul et al. (2006) showed that deletion of either the ELO2 or ELO3 gene is not lethal for *S. cerevisiae*. Therefore, in addition to the *S. cerevisiae* wildtype strain (InvSc1), elo2 and elo3 knock out mutants were used to differentiate the specific VLCFA product spectrum synthesized by the expressed *Arabidopsis* KCS proteins. Since the substrate and product spectrum of the CER6 protein (KCS6, AT1G68530) has not been shown before, this KCS activity is presented in more detail. After induction of CER6 protein expression with galactose for 48 h in wildtype *S. cerevisiae* cells (InvSc1), accumulations of hexacosanoic acid (26:0) and octacosanoic acid (28:0) were detected (Fig. 4B). In *S. cerevisiae* elo3 knock out mutant cells (Δelo3), accumulations of tetracosanoic acid (24:0), hexacosanoic acid (26:0) and octacosanoic acid (28:0) were detected after induction of CER6 protein expression with galactose for 72 h, whereas eicosanoic acid (20:0) and docosanoic acid (22:0) levels decreased (Fig. 4B). This indicates that the CER6 protein is most likely able to catalyze each elongation step from docosanoic acid (22:0) to octacosanoic acid (28:0). In total, Δelo3 CER6 *S. cerevisiae* cells accumulated 5.96% (SE 0.09) of total fatty acid content as plant-KCS-derived VLCFAs.

Also for the plant KCSs KCS1, KCS2, CER60 (KCS5), KCS17, FAE1 (KCS18) and KCS20, *S. cerevisiae* wildtype and elo2 and elo3 knock out mutants were used to differentiate between the VLCFA products that were solely synthesized by the expressed *Arabidopsis* KCS proteins or the endogenous *S. cerevisiae* enzymes. According to the identified plant KCS-derived VLCFAs, the KCSs could be grouped in three different classes of KCS enzymes (Table 2). FAE1 (KCS18) and KCS1 produced saturated and unsaturated VLCFAs with chain length up to 22 carbon atoms. KCS2 and KCS20 produced the saturated fatty acids eicosanoic (20:0), docosanoic (22:0) and tetracosanoic acid (24:0). The third type of KCS enzymes which includes of CER60 (KCS5), CER6 (KCS6) and KCS17 produced saturated fatty acids with chain length longer than or equal to 24 carbon atoms (Table 2).

2.5. Inhibition of activity of different plant KCSs by mefluidide, perfluidone and metazachlor

To study the effect of mefluidide and perfluidone in comparison to the known KCS inhibitor metazachlor, *S. cerevisiae* cells which

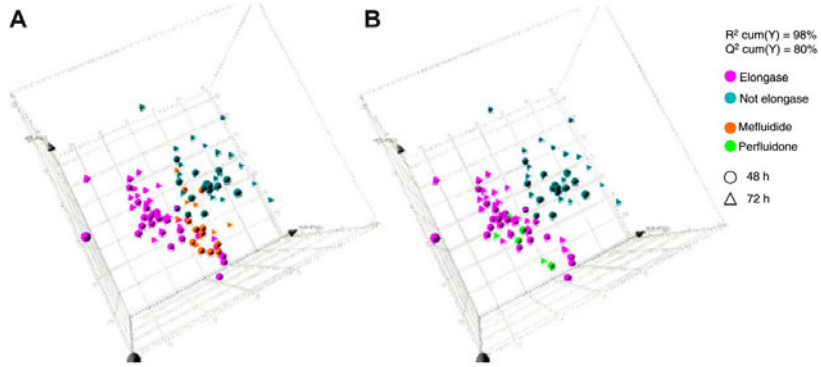

Fig. 2. Mode of action classification based on metabolite changes for mefluidide (A) and perfluidone (B) in comparison to VLCFA elongase and VLCFA non-elongase inhibitors by partial least square-discriminant analysis (PLS-DA). In *Lemna paucicostata* plants treated with different concentrations of mefluidide (10, 100, 300 µM) and perfluidone (1, 10, 100 µM) for 48 and 72 h, changes of approximately 200 identified and 300 unknown analytes were determined, relative to control plants. Testing for profile assignment to the mode of action classes of VLCFA elongase inhibitors (represented by alachlor, metazachlor, propachlor, mefenacet and dimethenamid) and VLCFA non-elongase inhibitors (represented by benfuresate, ethofumesate, diallate, methyldymron, molinate and triallate) were performed using PLS-DA. PLS-DA constructs an empirical model which relates treatment, as observation (class variable) with analytes, as x-type variable. The model is visualized as a score plot where each point represents an individual sample. The high quality of the model is indicated by low unexplained variability in the data set (R^2 (cum) = 98%) and good prediction Q^2 (cum) value of 80% for mode of action classification. The predicted scores of the three components (tPS[i]) were plotted on the axes *x*, *y* and *z*.

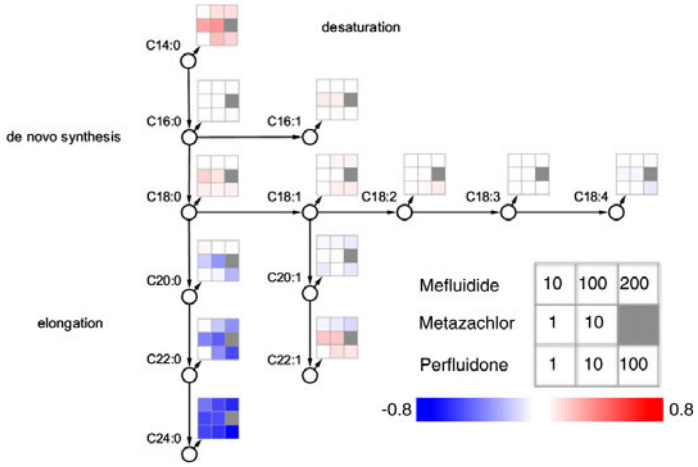

Fig. 3. Levels of fatty acids based on mol% (Δmol%) in *Lemna paucicostata* treated with different concentrations of mefluidide (10, 100, 200 µM), perfluidone (1, 10, 100 µM) or metazachlor (1, 10 µM) for 48 h, relative to untreated samples. The Δmol% values of each fatty acid were normalized on a scale of 1 to −1 for heatmap visualization in Cytoscape. For example, a value of −0.8 (dark blue) indicates 80% decrease of a fatty acid in a treated *Lemna* versus a control sample. Numerical values used for visualization and respective standard errors from at least three biological replicates are available as *Supplementary* Table 2.

expressed different *Arabidopsis* KCS enzymes were treated with the test compounds. Inhibition of different KCS enzyme activities were determined with the aid of wildtype (InvSc1) and Δelo2 and Δelo3 knock out strains to minimize influences of *S. cerevisiae* endogeneous ELO-proteins on inhibition values. In control experiments, it was shown that the tested compounds did not affect *S. cerevisiae* cell suspension growth at highest concentrations applied (100 µM, data not shown). In addition, the compounds did not inhibit the activity of the endogeneous *S. cerevisiae* ELO proteins, especially VLCFA production, which was determined by comparison of the fatty acid profile from treated and untreated *S. cerevisiae* wildtype (InvSc1) cells (data not shown). Inhibition values were calculated as percent inhibition of detected VLCFA products synthesized by a given KCS in comparison to untreated *S. cerevisiae* cells. As shown in Table 3, the activity of the investigated KCS enzymes was strongly inhibited by metazachlor applied at a concentration of 100 µM. In contrast, mefluidide (100 µM) inhibited CER60 (KCS5), CER6 (KCS6) and KCS1 activities by more than 50%, whereas KCS20 and FAE1 (KCS18) were only slightly inhibited by 26.9% and 5.1%, respectively. For a detailed inhibitor study, effects

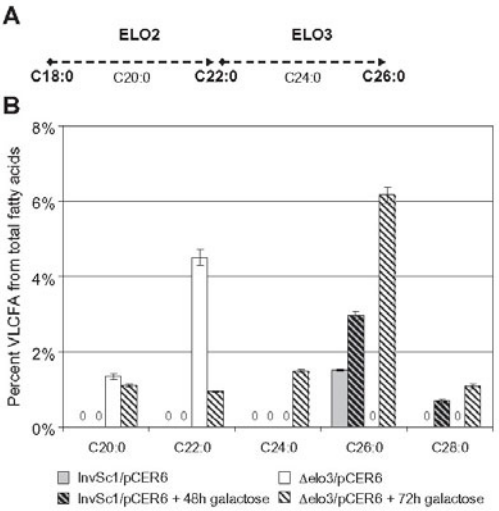

Fig. 4. Simplified pathway of hexacosanoic acid (C26:0) biosynthesis from octadecanoic acid (C18:0) by the *S. cerevisiae* ELO2 and ELO3 proteins with their typical substrates is shown in panel A. It is also known that ELO3 can have some minor activity on C18:0 and C20:0 fatty acids (A). Very-long-chain fatty acid product spectra of transgenic *S. cerevisiae* wildtype (InvSc1) and Δelo3 strains expressing the *A. thaliana* CER6 (AT1G68530) protein is shown (InvSc1/pCER6; Δelo3/pCER6; B). Based on percent share of distinct VLCFAs relative to the total amount of fatty acids (100%), *S. cerevisiae* endogenous VLCFA and additional VLCFA produced by the expressed CER6 protein, with (diagonal striped) and without (monochrome) galactose induction are shown. Standard errors were calculated from three biological replicates.

of mefluidide, perfluidone and metazachlor were tested on CER6 (KCS6) and FAE1 (KCS18) activity at different concentrations. Both KCS enzymes were used, because they produced, expressed in *S. cerevisiae* cells, high amounts of plant-KCS derived VLCFAs which accumulated to 8.73% and 15.20% of total fatty acid contents for CER6 (KCS6) and FAE1 (KCS18), respectively (Table 2). In addition, the VLCFA spectrum is different between CER6 (KCS6) and FAE1 (KCS18) (Table 2). This could clarify differences in inhibitor quality between mefluidide and perfluidone and metazachlor.

As shown in Table 4, CER6 (KCS6) activity was inhibited by metazachlor (IC_{50}: 0.032 μM) and perfluidone (IC_{50}: 0.21 μM) in the submicromolar range. Mefluidide showed clearly lower inhibition of CER6 (IC_{50}: 114 μM). FAE1 (KCS18) responded with similar preference to the inhibitors, but with less sensitivity compared to CER6. Metazachlor (IC_{50}: 1.99 μM) and perfluidone (IC_{50}: 7.60 μM) inhibited FAE1 activity with IC_{50} values in the micromolar range, whereas mefluidide showed only low enzyme inhibition (30% inhibition at 500 μM). Overall, enzyme inhibition correlated with the phytotoxic activity of the compounds to affect *Lemna* growth. Here, *Lemna* showed the highest sensitivity against metazachlor (IC_{50}: 0.12 μM), followed by perfluidone (IC_{50}: 0.52 μM) and mefluidide (IC_{50}: 3.15 μM) (Table 4).

3. Discussion

Mefluidide and perfluidone, both trifluoromethanesulphonanilides, were developed as plant growth regulator or herbicide, respectively (Tomlin, 2010). Several studies in the 1980s investigated the mode of action, but could not unravel a specific target site for this class of compounds. The physiological profiling approach revealed that both compounds induce growth inhibition with symptoms of intensified green frond pigmentation in *Lemna* followed by tissue necrosis particularly in the case of perfluidone (Fig. 1). These symptoms are typical of inhibitors of fatty acid synthesis and cell division (Grossmann, 2005). Additionally, treatment of cress seeds with mefluidide and perfluidone caused staining of developed hypocotyls with toluidine blue O. This indicates a defect of cuticle function, which is typical especially of inhibitors of VLCFA synthesis for cuticular wax formation like the chloroacetamide metazachlor (Fig. 1), the oxyacetamide flufenacet or the tetrazolinone fentrazamide (Tresch et al., 2008). Overall, the effects on *Lemna* growth and cuticular function suggested a mode of action of mefluidide and perfluidone in VLCFA synthesis. In addition, the physiological profile of perfluidone confirmed studies of Moreland (1981) that the compound has moderate uncoupler activity at high concentrations and can act as a protonophore to alleviate proton gradients across membranes. This effect was not observed after mefluidide treatment. It could be speculated that the uncoupler effect is most likely based on the acidic proton at the nitrogen atom in the trifluoromethanesulphonate moiety which is easily released because of the electron acceptor group in *para* position at the phenyl-ring. This is in contrast to mefluidide that is substituted with a methyl group at the phenyl-ring which functions as an electron donor. However, the uncoupler activity of perfluidone appears to be a secondary effect which was observed in *Lemna* only at high concentrations. Herbicides with uncoupler activity are known to cause rapid necrosis on plant tissues accompanied by inhibition of respiration (Grossmann, 2005). However, strong growth inhibition in *Lemna* already occurred at 1 μM perfluidone (Fig. 1). Accordingly, cluster analysis of metabolite changes induced by perfluidone and mefluidide in *Lemna* indicated inhibition of VLCFA biosynthesis as the primary mode of action (Table 1). The metabolic profile of perfluidone is typical for known inhibitors of KCS-catalyzed elongation steps like metazachlor (Fig. 2B). In the case of mefluidide, metabolite changes cluster in and between the cluster of profiles of known KCS and "not elongase" inhibitors in VLCFA synthesis (Fig. 2A). Detailed analysis of fatty acids in *Lemna* revealed that both, perfluidone and mefluidide, elicited changes in VLCFAs which were identical to this induced by the KCS inhibitor metazachlor (Fig. 3).

In order to investigate the effects of mefluidide and perfluidone on possible KCS target enzymes, 17 *A. thaliana* KCS genes were expressed in *S. cerevisiae* and their activity determined by VLCFA analysis according to Trenkamp et al. (2004). With the use of wildtype (InvSc1) and Δelo2 and Δelo3 knock out strains of *S. cerevisiae* that lack the activity of the endogenous VLCFA elongases elo2 or elo3, VLCFA products of seven plant KCS enzymes were identified (Table 2). The product spectrum of six from these seven KCS proteins were already described (Trenkamp et al., 2004; Blacklock and Jaworski, 2006; Paul et al., 2006). In addition, we have shown here the activity of the KCS protein CER6. CER6 is expressed in the epidermal cells of all shoot tissues (Hooker et al., 2002) and is involved in wax production of the stem and in pollen development (Fiebig et al., 2000). CER6 recombinantly expressed in *S. cerevisiae* produced VLCFAs with chain length of 24, 26 and 28 carbons. Studies with *Arabidopsis* plants lacking the CER6 protein were found to accumulate C24 VLCFAs, accompanied by decreased levels of C28 and C30 (Millar et al., 1999). It was suggested that CER6 catalyzes the elongation of C24 to C28 and C30 VLCFAs. According to our results, CER6 catalyzes the elongation, beginning one step earlier in the path, of C22 to C24, C26 and C28 VLCFAs (Table 2). It could be speculated that *in planta*, due to the functional redundancy of different KCS isoforms, the production of C24 VLCFAs is not solely based on CER6 activity. The activities of the KCS20 or even KCS2 enzymes might be additionally involved because they are also able to produce C24 VLCFAs (Table 2) and are transcribed particularly in plant stem, flowers and siliques (Joubes et al., 2008).

It has been previously shown that most herbicides listed in the HRAC K3 mode of action group including metazachlor (Senseman, 2007) are inhibitors of VLCFA biosynthesis (Böger, 2003; Yang et al., 2010). These herbicides inhibit specifically the first process step in the elongation of VLCFAs, the condensation of acyl-coenzyme A with malonyl-coenzyme A, catalyzed by KCS enzymes (Trenkamp et al., 2004). Accordingly, we showed for the first time that mefluidide and perfluidone are also inhibitors of KCS enzyme activities in the micromolar range (Tables 3 and 4). While metazachlor was shown to inhibit the activities of FAE1, KCS1, KCS2, KCS20, CER60, CER6 and KCS17 (Table 3), mefluidide inhibited KCS1, CER60, CER6, and only slightly KCS20 and FAE1. As particularly shown for the inhibition of CER6 and FAE1, perfluidone was more active than mefluidide, but inferior to metazachlor (Table 4). Accordingly, inhibitor effects on KCS enzyme activities correlated well with the induced growth inhibition in *Lemna* (Table 4). This is also in accordance to the use of mefluidide as growth regulator and perfluidone and metazachlor as herbicides. In addition, the plant phenotype (intensified green frond pigmentation) which is induced after mefluidide treatment of *Lemna* is very similar to that described for the mutant cer6–1 which is defective in CER6 (Koornneef et al., 1989). The cer6–1 plant phenotype exhibits reduced growth and intensified green leaf pigmentation ((The Arabidopsis Information Resource (TAIR), http://www.arabidopsis.org/servlets/TairObject?id=137221type=locus, on www.arabidopsis.org, December 4th, 2011).

In *Lemna* tissue, mefluidide and perfluidone strongly decreased the level of tetracosanoic acid (C24:0), accompanied by moderate reductions in docosanoic acid (C22:0) (Fig. 3). In comparison, metazachlor additionally reduced the level of eicosanoic acid (C20:0). The levels of unsaturated fatty acids were not reduced by mefluidide, perfluidone or metazachlor treatment. Only the levels of docosenoic acid (C22:1) slightly increased after treatment with metazachlor or perfluidone.

In conclusion, our results suggest that the plant growth-regulating and herbicidal activity of mefluidide or perfluidone is based on the inhibition of distinct KCS isoenzymes in VLCFA synthesis. Consequently, the trifluoromethanesulphonanilides mefluidide and perfluidone represent a new chemical class of KCS inhibitors. It is assumed that, dependent on the affected KCS isoenzymes and the intensity of inhibition, plant phenotypes are induced by mefluidide and perfluidone which are characterized by shoot stunting with intensified green pigmentation or strong growth inhibition followed by tissue necrosis and plant death, respectively.

4. Experimental procedures

4.1. Chemicals

Metazachlor (2-chloro-*N*-(2,6-dimethylphenyl)-*N*-(1H-pyrazol-1-ylmethyl)acetamide, Fig. 1) were purchased from Sigma–Aldrich (Deisenhofen, Germany). Perfluidone (1,1,1-trifluoro-*N*-(4-phenylsulphonyl-o-tolyl)methanesulphonamide, Fig. 1) and mefluidide (5′-(1,1,1-trifluoromethanesulfonamido)aceto-2′4′-xylidide, Fig. 1) were obtained from Dr. Ehrenstorfer GmbH (Augsburg, Germany) or from BASF SE (Ludwigshafen, Germany).

4.2. Physiological profile

The bioassays of the physionomics approach were carried out as described in Grossmann (2005) and Tresch et al. (2008). In the heterotrophic cell suspension assay with callus cells from *G. mollugo* L., cell suspensions (2 ml) were treated with compound in plastic tubes for 8 days and the conductivity of the nutrient solution was measured as the parameter for cell division growth. For the algae bioassay, photoautotrophically growing cells of *S. obliquus* were incubated in microtitre dishes with 24 wells (1 ml per well) and growth was measured photometrically 24 h after test compound treatment. For the *Lemna* bioassay, *L. paucicostata* plants were treated with compound in petri dishes which contained 15 ml nutrient solution for 8 days and the increase of the area covered by the fronds in each dish was measured by digital image analysis. For the isolated shoot bioassay, shoots of *S. alba* plants, 10 days after sowing, were placed in vials which contained 12 ml water and test compound. After 3 days of treatment, the changes in fresh weight were measured by weighing the shoots. To measure compound effects on Hill reaction, isolated thylakoids from shoots of *Triticum aestivum* were used and after illumination, formation of a complex of ferrous salt with phenanthroline was measured in the assay photometrically. For the germination bioassay, seeds of *L. sativum* were incubated in petri dishes which contained a vermiculite substrate moistened with aqueous compound solution. After 3 days in the dark and subsequent 3 days in the light, compound effects on seed germination and seedling development were evaluated. To determine CO_2 uptake as a parameter for CO_2 assimilation, young *G. aparine* plants were foliar-treated with test compound and incubated in illuminated glass chambers for 24 h under controlled air conditions. The amount of CO_2 assimilated per unit time was determined from the difference between the CO_2 contents of the inflowing and outflowing air streams. For determination of respiration, the oxygen consumption of *G. mollugo* cell suspensions (5 ml) in plastic tubes was measured after 5 h of compound treatment with an oxygene sensor. The determination of uncoupler activity, in roots of *L. paucicostata* plants, the membrane potential of mitochondria was visualized by the potential sensor dye JC-1. Uncoupler activity was evaluated visually by fluorescence microscopy after 90 min of compound treatment. For evaluation of compound effects on VLCFA synthesis in cuticular wax formation, induced cuticular defects of cress seedlings were used as an indicator. Five days after seed treatment, shoots of cress seedlings (*L. sativum*) were cut off and immersed in toluidine-blue O (TBO) staining solution (0.05% in water) for 5 min. The epidermal surface of hypocotyl without a functional cuticle is permeable to the hydrophilic dye toluidine-blue O, which leads to blue staining of the hypocotyl tissue with staining intensities related to the cuticular defects Tanaka et al. (2004).

The results were expressed as percentage inhibition or effect and mean values of three replicates are given relative to the control. Individual standard errors were less than 10%. The effect on cuticle function and uncoupler effect was visually evaluated by grouped values (0%, 30%, 60% and 100%). All experiments were repeated at least twice and proved to be reproducible. The results of representative experiments are shown.

4.3. Metabolic profile

Metabolic profiling was performed as described in Grossmann et al. (2010). Duckweed (*L. paucicostata*) plants were cultivated and treated with test compounds in plastic petri dishes (three replicates) under continuous light (80 μmol Phot m^{-2} s^{-1}) in a growth chamber at 25 °C as described (Grossmann, 2005). Compounds, dissolved in acetone, were added to the dishes containing 15 ml *Lemna* nutrient solution without sucrose (Pirson and Seidel, 1950). Organic solvent was allowed to volatilize before the dishes were loaded with about 120 fronds each. Controls (nine replicates) received corresponding amounts of acetone alone. After 48 h and 72 h of treatment with mefluidide (10, 100, 300 μM) or perfluidone (1, 10, 100 μM), plants from three replicates were washed with distilled water, rapidly dried with filter paper, sampled (approximately 200 mg fresh weight), and immediately frozen in liquid nitrogen. After freeze drying, the metabolites were extracted with

the use of accelerated solvent extraction (ASE) with polar (methanol:water, 4:1, v:v) and nonpolar (methanol:dichlormethan, 2:3, v/v) solvents. Subsequent analyses of metabolites were performed by gas chromatography-mass spectrometry (GC–MS) and liquid chromatography-mass spectrometry (LC–MS/MS) were performed as described (Roessner et al., 2000; Walk et al., 2007; Niessen, 2003; Gergov et al., 2003).

After GC–MS and LC–MS/MS analyses, data normalization and data validation, significance between treatment-group values per time and metabolite and respective untreated control-group values were tested with the use of the Student's *t* test (two-sided with inhomogeneous variance; Mead et al., 1993). Overall, changes in the levels of about 200 identified metabolites and 300 unknown analytes were determined and calculated as numerical ratios, relative to control samples. Known mode of action assignment was performed by comparing the metabolic profile of mefluidide and perfluidone, including total changes of known and unknown analytes, with those of about 150 previously characterized herbicides and growth regulators representing a range of about 60 mode of action. For mode of action cluster analysis, prediction analysis of microarrays (PAM, described in Tibshirani et al., 2002) and partial least square-discriminant analysis (PLS-DA, described in Ramadan et al., 2006 and van Ravenzwaay et al., 2007) were used as multivariate statistical data analysis. PAM was applied for ranking profile changes elicited by a new compound to profile classes generated by compounds with known mode of action class membership with the use of the nearest-shrunken-centroid methodology. The quality of the classification can be estimated by the distance values (dist) and maximum log likelihood values (mll). The ranking is based on the logarithmized probability indicated by mll. The mll values are always below or, in the best case, equal to 0, because *p* values lie between 0 and 1. The dist value is an indicator for the degree of distinctness in the classification, with the highest value as the best, and results from the mll values of the two best ranks of the classes. PLS-DA, which was performed with the use of Simca-P + Version 12 (Umetrics AB, Umea, Sweden), is a supervised regression method. It is used to construct an empirical model relating *y*-type variables (e.g. treatments) with *x*-type variables (e.g. analytes) when the variables are many and highly correlated. By applying PLS-DA, a model is obtained that describes maximum separation among predefined classes, whereas the model quality value R^2 (cum) indicates the coverage of the sample variability by the PLS-DA model and Q^2 (cum) indicates the prediction power of the model (Holmes and Antti, 2002).

4.4. Recombinant expression of A. thaliana KCS genes in S. cerevisiae

Seventeen from 21 KCS genes (Joubes et al., 2008) were cloned into pYES2 (Invitrogen, Karlsruhe, Germany) vector for galactose inducible expression in *S. cerevisiae* with standard cloning techniques described in Sambrook et al., (2001). The genes were selected because of their expression pattern analyzed with Genevestigator (Hruz et al., 2008), presence of cysteine at active site (Joubes et al., 2008) and availability of full length cDNA clones at *Arabidopsis* Biological Resource Stock Center. Plasmids with full length cDNA clones of 13 KCS genes (TAIR ID: AT1G01120, TAIR ID: AT1G68530, TAIR ID: AT2G15090, TAIR ID: AT5G04530, TAIR ID: AT1G04220, TAIR ID: AT1G19440, TAIR ID: AT1G71160, TAIR ID: AT2G26250, TAIR ID: AT2G26640, TAIR ID: AT2G28630, TAIR ID: AT5G43760, TAIR ID: AT1G07720, TAIR ID: AT3G52160) were received from the *Arabidopsis* Biological Resource Stock Center (ABRC, The Ohio State University, Columbus, USA) and either directly cloned into pYES2 or PCR amplified with suitable restriction sites for subsequent cloning into pYES2. The protein coding sequences of TAIR ID: AT1G25450, TAIR ID: AT2G16280 and TAIR ID: AT4G34510 were codon optimized for expression in *S. cerevisiae* and made synthetically (febit synbio GmbH, Heidelberg, Germany) with respective 5′ and 3′ restriction sites added for subcloning into pYES2. The pYES2 expression vector containing TAIR ID: AT4G34520 (FAE1) was kindly provided by O. Rowland (University of British Columbia, Vancouver, Canada). For detailed cloning strategy see Supplementary Table 1.

S. cerevisiae cells are capable to synthesize eicosanoic, docosanoic, tetracosanoic and hexacosanoic acid with its endogenous elo2 and elo3 proteins (Paul et al., 2006). In order to differentiate between the *S. cerervisiae* endogenous elongase activity and the plant KCS activity we introduced the KCS plasmids in wildtype INVSc1 strain (Invitrogen, Karlsruhe, Germany) as well as Δelo2 (acc. No.: Y05736; Euroscarf, University of Frankfurt, Germany) and Δelo3 (acc. No.: Y15281; Euroscarf) deletion mutants. *S. cerevisiae* strains were transformed with S.c.EasyComp™ transformation kit (Invitrogen) as described in the manufacturers manual. Transformants were selected on SC minimal medium agar plates (Amberg et al., 2005) lacking uracil. Before induction, transformed cells were grown overnight on a rotary shaker at 30 °C with 180 rounds per minute in SC minimal medium lacking uracil and supplemented with 2% glucose as the only carbon source. Expression of recombinant protein was induced by transferring cells to SC minimal medium lacking uracil and supplemented with 1% raffinose and 2% galactose for 72 h at 24 °C. Supplementation studies were used to examine the utilization of polyunsaturated octadecanoic fatty acids by KCS1 and FAE1 (KCS18) proteins expressed in transgenic *S. cerevisiae* strains (InvSc1). Therefore, induction medium was supplemented by addition of respective fatty acids, dissolved in acetone, to a final concentration of 200 μM and of 0.2% Tergitol (Sigma–Aldrich). For inhibitor experiments the test compounds, dissolved in dimethylsulfoxide (DMSO), were added to the *S. cerevisiae* cell suspensions simultaneously with the induction of the KCS expression for 48 h (InvSc1, Δelo2) or 72 h (Δelo3). In order to analyze the fatty acid composition, 2×10^7 *S. cerevisiae* cells were harvested by centrifugation (5 min, 4 °C, 6000*g*), washed one time with *aqua dest.* and lyophilized prior to subsequent extraction of fatty acids.

4.5. Fatty acid extraction of S. cerevisiae

To determine total fatty acid composition, fatty acid methyl esters were prepared according to a modified protocol described in Browse et al. (1986). For transesterification 2×10^7 lyophilized cells of *S. cerevisiae* were resuspended in 2.44 ml BCl_3:methanol (9.8%, v/v; Sigma–Aldrich, Deisenhofen, Germany) including 1.7% 2,2-dimethoxypropane and 15 μg internal standard pentadecanoic acid. After incubation for 4 h at 80 °C, samples were cooled down, 1 ml 0.9% NaCl (w/v) was added and fatty acid methyl esters were extracted in liquid hexane for two times. After evaporation of hexane under nitrogen at 50 °C, the fatty acid methyl esters were dissolved in 100 μl heptane containing 15 μg quantitation standard heptadecanoic acid methyl ester and subsequently analyzed by GC/MS.

4.6. GC/MS analysis of fatty acid methyl esters

Fatty acid methyl esters from either *S. cerevisiae* cells or *Lemna* tissue were injected in an Agilent 5973 N gas chromatograph (Agilent, Waldbronn, Germany) and separated on a DB-5 MS column (Agilent; length: 20 m; film thickness: 0.18 μm). The column was operated with helium carrier gas (flow: 7.1 ml/min) and 4:1 split injection (injection temperature: 250 °C). The oven temperature was increased constantly from 120 to 190 °C with 6 °C per min and further up to 260 °C with 3.5 °C per min. Subsequent to the detection of the mass fragments in a mass spectrometer detector (detector temperature: 230 °C), the analytes were identified by their mass spectra (Wiley Registry of Mass Spectral Data, 8th edi-

tion, 2006, John Wiley & Sons, Inc., Hoboken, NJ, USA) and confirmed by analytical fatty acid methyl ester standards (Supelco® 37 Component FAME Mix; Sigma–Aldrich).

4.7. Determination of fatty acid content and KCS inhibition in S. cerevisiae cells

Each detected fatty acid analyte was integrated and evaluated as percent amount of total detected fatty acid analytes. Each sample from transgenic *S. cerevisiae* was compared to their respective untreated or non-induced control and identified plant-KCS-derived VLCFAs were calculated as %VLCFA from total content of fatty acids. Inhibition of KCS activity after compound treatment was calculated by comparison of %VLCFA of treated versus untreated cells. IC_{50} calculations, based on inhibition values of five different compound concentrations with three parallel samples, were executed with a two-logistic regression model by SAS statistical analysis tool (Version 9.2; SAS Institute Inc., Cary, NC, USA).

4.8. Fatty acid extraction and analysis of L. paucicostata tissue

L. paucicostata plants were cultivated and treated with compounds in plastic petri dishes (three replicates) with 15 ml *Lemna* nutrient solution without sucrose (Pirson and Seidel, 1950) under continuous light (40 μmol Phot $m^{-2} s^{-1}$) in a growth chamber at 25 °C. Compounds in DMSO solution (final DMSO concentration 0.1%) were added to dishes which contained about 25 *Lemna* fronds each. Control samples received corresponding amounts of DMSO alone. After 48 h of treatment with mefluidide (10, 100, 200 μM), metazachlor (1, 10 μM) or perfluidone (1, 10, 100 μM) about 50 mg of plant tissue per replicate were collected, dried with filter paper and lyophilized after freezing on dry ice. Fatty acid extraction was done according to a modified protocol described in Browse et al. (1986). Lyophilized tissue was mixed with 2.44 ml BCl_3:methanol (9.8% v/v; Sigma–Aldrich, Deisenhofen, Germany) including 1.7% 2,2-dimethoxypropane and 15 μg pentadecanoic acid as transesterification standard. Afterwards the tissue was homogenized for 2 min with a frequency of 25 Hz in a mixer mill MM400 (Retsch, Haan, Germany). Subsequently, homogenized tissue was incubated for 4 h at 80 °C for direct transesterification. After samples were cooled down to 20 °C, 1 ml 0.9% NaCl (w/v) was added and fatty acid methyl esters were extracted in hexane for two times. After evaporation under nitrogen at 50 °C, fatty acid methyl esters were dissolved in 100 μl heptane containing 15 μg quantitation standard heptadecanoic acid methyl ester and subsequently analyzed by GC/MS as described herein.

For quantitation of fatty acids, the molar fraction (mol%) of analytes were calculated based on the peak area compared to an analytical standard for each fatty acid species. In addition, two internal standards (pentadecanoic acid, heptadecanoic acid methyl ester) were used to eliminate the extraction and injection variability. For comparison of changes in fatty acid content of treated versus control *Lemna*., each fatty acid was normalized to a scale from −1 and 1 using Δmol% = (mol% treated − mol% control)/(mol% treated + mol% control). With this normalization, a value of −1 indicates that a fatty acid is completely vanished, whereas values close to one indicate strong increase compared to control. Accordingly, a value of 0.5 means an increase of about three times compared to control. The Δmol% values plotted on a fatty acid biosynthesis pathway scheme with Cytoscape software package (Cline et al., 2007).

Acknowledgments

The authors thank Dr. O. Rowland (University of British Columbia, Vancouver, Canada) for kindly proving the pYES2.1-FAE1 plasmid, Dr. Jens Lerchl (BASF SE), Dr. Martin Lohr (University of Mainz) and Dr. Jörg Bauer (Metanomics GmbH) for their expert comments, and critical reading of the manuscript. We also thank Thomas Mietzner (BASF SE) for support in statistical analysis and Guenter Caspar, Simone Huber, Jennifer Schmotz and Manuela Wetternach for excellent technical assistance.

Appendix A. Supplementary data

Supplementary data associated with this article can be found, in the online version, at doi:10.1016/j.phytochem.2011.12.023.

References

Aliferis, K.A., Jabaji, S., 2011. Metabolomics – A robust bioanalytical approach for the discovery of the modes-of-action of pesticides: a review. Pesticide Biochem. Physiol. 100, 105–117.
Amberg, D.C., Burke, D.J., Strathern, J.N., 2005. Methods in yeast genetics. Cold Spring Harbor Laboratory Press, Cold Spring Harbor.
Bach, L., Faure, J., 2010. Role of very-long-chain fatty acids in plant development, when chain length does matter. C. R. Biol. 333, 361–370.
Blacklock, B.J., Jaworski, J.G., 2006. Substrate specifity of *Arabidopsis* 3-ketoacyl-CoA synthases. Biochem. Biophys. Res. Commun. 346, 583–590.
Böger, P., 2003. Mode of action for chloroacetamides and functionally related compouonds. J. Pestic. Sci. 28, 324–329.
Browse, J., McCourt, P.J., Somerville, C.R., 1986. Fatty acid composition of leaf lipids determined after combined digestion and fatty acid methyl ester formation from fresh tissue. Anal. Biochem. 152, 141–145.
Cline, M.S., Smoot, M., Cerami, E., Kuchinsky, A., Landys, N., Workman, C., Christmas, R., et al., 2007. Integration of biological networks and gene expression data using Cytoscape. Nat. Protoc. 2, 2336–2382.
Fiebig, A., Mayfield, A., Miley, N., Chau, S.R., Preuss, D., 2000. Alterations in CER6, a gene identical to CUT1, differentially affect long-chain lipid content on the surface of pollen and stems. Plant Cell 12, 2001–2008.
Friedinger, T.L., 1978. The trifluoromethanesulphonanilide class of herbicides and plant growth regulators. In: Geissbuehler, H., Brooks, G.T., Kearney, P.C. (Eds.), Advances in pesticide science Vol 2. Pergamon Press, Oxford, pp. 261–270.
Gergov, M., Ojanperä, I., Vuori, E., 2003. Simultaneous screening for 238 drugs in blood by liquid chromatography–ionspray tandem mass spectrometry with multiple-reaction monitoring. J. Chromatogr. B 795, 41–53.
Glenn, D.S., Rieck, C.E., 1985. Auxinlike activity and metabolism of mefluidide in corn (*Zea mays*) and soybean (*Glycine max*) tissue. Weed Sci. 33, 452–456.
Grossmann, K., 2005. What it takes to get a herbicide's mode of action. Physionomics, a classical approach in a new complexion. Pest Manag. Sci. 61, 423–431.
Grossmann, K., Niggeweg, R., Christiansen, N., Looser, R., Ehrhardt, T., 2010. The herbicide saflufenacil (Kixor™) is a new inhibitor of protoporphyrinogen IX oxidase activity. Weed Sci. 58, 1–9.
Holmes, E., Antti, H., 2002. Chemometric contributions to the evolution of metabolomics: mathematical solutions to characterising and interpreting complex biological NMR spectra. Analyst 127, 1549–1557.
Hooker, T., Millar, A.A., Kunst, L., 2002. Significance of the expression of the CER6 condensing enzyme for cuticular wax production in *Arabidopsis*. Plant Physiol. 129, 1568–1580.
Hruz T., Laule O., Szabo G., Wessendrop F., Bleuler S.O., Widmayer P., Gruissem W., Zimmermann P., 2008. Genevestigator V3: a reference expression database for the meta-analysis of transcriptomes. Adv. Bioinformatics 2008, Article ID 420747, 5 pages.
Joubes, J., Raffaele, S., Bourdenx, B., Garcia, C., Laroche-Traineau, J., Moreau, P., Domergue, F., et al., 2008. The VLCFA elongase gene family in *Arabidopsis thaliana*: phylogenetic analysis, 3D modelling and expression profiling. Plant Mol. Biol. 67, 547–566.
Koornneef, M., Hanhart, C.J., Thiel, F., 1989. A genetic and phenotypic description of eceriferum (cer) mutants in *Arabidopsis thaliana*. J. Hered. 80, 118–122.
Kunst, L., Samuels, A.L., 2003. Biosynthesis and secretion of plant cuticular wax. Prog. Lipid Res. 42, 51–80.
Mead, R., Curnow, R.N., Hasted, A.M., 1993. Statistical methods in agriculture and experimental biology. 2nd ed. Chapman and Hall, London.
Millar, A.A., Kunst, L., 1997. Very long chain fatty acid biosynthesis is controlled through the expression and specificity of the condensing enzyme. Plant J. 12, 121–131.
Millar, A.A., Clemens, S., Zachgo, S., Giblin, M., Taylor, D.C., Kunst, L., 1999. CUT1, an *Arabidopsis* gene required for cuticular wax biosynthesis and pollen fertility, encodes a very-long-chain fatty acid condensing enzyme. Plant Cell 11, 825–838.
Moreland, D.E., 1981. Interaction of perfluidone with mitochondrial, thylakoid, and liposome membranes. Pesticide Biochem. Physiol. 15, 21–31.
Niessen, W.M., 2003. Progress in liquid chromatography–mass spectrometry instrumentation and its impact on high-throughput screening. J. Chromatogr. A 1000, 413–436.

Oh, C., Toke, D.A., Mandala, S., Martin, C.E., 1997. ELO2 and ELO3, homologues of the *Saccharomyces cerevisiae* ELO1 gene, function in fatty acid elongation and are required for sphingolipid formation. J. Biol. Chem. 272, 17376–17384.

Paul, S., Gable, K., Beaudoin, F., Cahoon, E., Jaworski, J., Napier, J.A., Dunn, T.M., 2006. Members of the *Arabidopsis* FAE1-like 3-ketoacyl-CoA synthase gene family substitute for the elop proteins of *Saccharomyces cerevisiae*. J. Biol. Chem. 281, 9018–9029.

Pirson, A., Seidel, F., 1950. Zell – und Stoffwechselphysiologische Untersuchungen an der Wurzel von *Lemna minor* L. Unter besonderer Berücksichtigung von Kalium – und Kalziummangel. Planta 38, 431–473.

Ramadan, Z., Jacobus, D., Grigorov, S., Kochhar, S., 2006. Metabolic profiling using principal component analysis, discriminant partial leat squares, and genetic algorithms. Talanta 68, 1683–1691.

van Ravenzwaay, B., Coelho-Palermo, C.G., Leibold, E., Looser, R., Mellert, W., Prokoudine, A., Walk, T., Wiemer, J., 2007. The use of metabolomics for the discovery of new biomarkers of effect. Toxicol. Lett. 172, 21–28.

Roessner, U., Wagner, C., Kopka, J., Tretheway, R.N., Willmitzer, L., 2000. Simultaneous analysis of metabolites in potato tuber by gas chromatrography-mass spectrometry. Plant J. 23, 131–142.

Roudier, F., Gissot, L., Beaudoin, F., Haslam, R., Michaelson, L., Marion, J., Molino, D., Lima, A., Bach, L., Morin, H., Faure, J., 2010. Very-long-chain fatty acids are involved in polar auxin transport and developmental patterning in *Arabidopsis*. The Plant Cell 22, 364–375.

Sambrook, J., Russel, D.W., Irwin, N., Janssen, K.A., 2001. Molecular cloning – A Laboratory manual, third ed. Cold Spring Harbor Laboratory Press, Cold Spring Harbor.

Sauter H., Lauer M., Fritsch H., 1991. Metabolic profiling of plants – a new diagnostic technique, in: Baker D.R., Fenyes J.G., Moberg M.K., (Eds.), Synthesis and chemistry of Agrochemicals II. ACS Symposium Series Vol 443, Washington, pp. 288–299.

Senseman, S.A., 2007. Herbicide handbook, 9th ed. Weed Sci. Soc. Am, Lawrence.

Tanaka, T., Tanaka, H., Machida, C., Watanabe, M., Machida, Y., 2004. A new method for rapid visualization of defects in leaf cuticle reveals five intrinsic patterns of surface defects in *Arabidopsis*. Plant J. 37, 139–146.

Tautvydas, K.J., Hargroder, T.G., 1985. Mode of action of the plant growth regulator mefluidide. Proc. of the Plant Growth Regulator Society of America, 13–16.

Tibshirani, R., Hastie, T., Narasimhan, B., Chu, G., 2002. Diagnosis of multiple cancer types by shrunken centroids of gene expression. Proc. Natl. Acad. Sci. USA 99, 6567–6572.

Tomlin, C.D., 2010. The e-pesticide manual version 5.1. British Crop Production Council, Hampshire.

Trenkamp, S., Martin, W., Tietjen, K., 2004. Specific and differential inhibition of very-long-chain fatty acid elongases from *Arabidopsis thaliana* by different herbicides. Proc. Natl. Acad. Sci. USA 101, 11903–11908.

Trenkamp, S., Eckes, P.B., Fernie, A.R., 2009. Temporally resolved GC–MS-based metabolic profiling of herbicide treated plants treated reveals that changes in polar primary metabolites alone can distinguish herbicides of differing mode of action. Metabolomics 5, 277–291.

Tresch, S., Niggeweg, R., Grossmann, K., 2008. The herbicide flamprop-M-methyl has a new antimicrotubule mechanism of action. Pest Manag. Sci. 64, 1195–1203.

Truelove, B., Davis, D.E., Pillai, C.G., 1977. Mefluidide effects on growth of corn (*Zea mays*) and the synthesis of protein by cucumber (*Cucumis sativus*) cotyledon tissue. Weed Sci. 25, 360–363.

Valadon, L.R., Kates, M., 1984. Effect of perfluidone on metabolism of lipids in maize (*Zea mays* L.) and sunflower (*Helianthus annuus* L.). J. Plant Growth Regul. 3, 111–120.

Walk T., Looser R., Bethan B., Herold M.M., Kamlage B., Schmitz B., van-Ravenzwaay B., Mellert W., Coelho P.C., Ehrhardt T., Wiemer J., Proukoudine A., Krennrich .G., 2007. Means and methods for analyzing a sample by means of chromatography-mass spectrometry. International Patent Application No. WO2007/012643.

Wilkinson, R.E., 1982. Mefluidide inhibition of sorghum growth and gibberellin precursor biosynthesis. J. Plant Growth Regul. 1, 85–94.

Yang, X., Guschina, I.A., Hurst, S., Wood, S., Langford, M., Hawkes, T., Harwood, J.L., 2010. The action of herbicides on fatty acid biosynthesis in barley and cucumber. Pest Manag. Sci. 66, 794–800.

4. Discussion

An in-depth knowledge of the MoA is the key to interpreting plant responses to phytoactive compounds. In the past, accurate analyses of plant phenotypes and targeted analyses of selected pathways of interest were the main approach to studying the MoA of a compound. In order to define the most powerful approach for MoA identification, the literature on plant active compounds was analysed based on the methodology used for MoA identification.

4.1. Successful MoA studies confirming the target sites of compounds using plant systems

Compounds or compound classes that were initially identified in a plant screen or as a plant active natural product and with a description of the target site are listed in Table 1. With the 37 compounds or compound groups listed in Table 1 with a detailed understanding of the MoA in plants, it was possible to describe the respective target sites for 25 compounds by the use of a phenotyping approach (Figure 3). It is characteristic for this approach, that a broad range of different organisms is used to study the compound-induced phenotype. There is no principle prerequisite of what kind of organism can be used in a phenotyping approach, except for the sensitivity of the organisms to the compound. Two examples showed the importance of the right model system. It had been demonstrated that arylphenoxypropionates (fops) and cyclohexanediones (dims) selectively act on grass species and do not inhibit growth of dicot species (reviewed by Sasaki and Nagano, 2004). This observation was translated by several research groups to choose sensitive monocot species and tolerant dicot species as model systems to study the MoA of fops and dims. With these models four groups described simultaneously the inhibition of homomeric ACCase in plastids of grass species as the primary MoA of fops and dims (Burton *et al.*, 1987; Focke and Lichtenthaler, 1987; Rendina and Felts, 1988; Secor and Ceske, 1988). In another example, the use of a less appropriate model system hindered straight forward target identification in higher plants. The group of Böger investigated the MoA of chloroacetamides intensively (reviewed in Schmalfuß *et al.*, 1998; Matthes *et al.*, 1998) and used the algae *Scenedesmus acutus* as a model because of their high inhibitor sensitivity. Couderchet *et al.* (1996) detected the inhibition of sporopollenin synthesis as the most sensitive effect of chloroacetamides on algae. Despite the fact that this effect could not explain the phytotoxicity in higher plants, they started to reinvestigate the chloroacetamide effects in seedlings of *Cucumis sativus*, *Hordeum vulgare* and *Zea mays* (Matthes *et al.*, 1998). These studies led to the hypothesis that the primary chloroacetamide MoA was based on the inhibition of the fatty acid elongation complex. Finally, the 3-ketoacyl-CoA-synthase, which catalysed the first elongation step of VLCFA synthesis, was identified as the primary target by Trenkamp *et al.* (2004). Selection

of the appropriate model system and the use of various models to study the MoA of phytotoxic compounds is one of the criteria for straight-forward MoA identification.
A comparison of the types of targets with respect to the classification mentioned in section 2.2.2 reveals that most of the target sites identified by a phenotyping approach belong to a group of inhibitors with target enzymes in primary and secondary metabolism. There are several examples of enzymatic targets of inhibitors in a primary pathway that were identified in a straight-forward way by a combination of physiological studies with metabolic feeding or metabolic profiling (Grossmann *et al.*, 2012a). Most of the targets identified in primary metabolism (e.g., amino acid, nucleotide or biotin biosynthesis) were proposed by metabolite feeding studies and finally confirmed by biochemical studies.
Limitations of this fast strategy are obvious when dealing with processes in fatty acid or pigment biosynthesis. Intermediates of these pathways could not be used in metabolite feeding experiments because of their poor uptake properties in *in vivo* studies. Therefore, targeted analytics was used to nominate a target protein in a specific pathway. After initial physiological characterisation of CPTA (Hsu and Yokoyama, 1972; Bouvier *et al.*, 1997), LS80707 (Sandmann *et al.*, 1985) or Norflurazon (Mayer *et al.*, 1989; Sandmann *et al.*, 1989), pigment biosynthesis was identified as the most affected pathway. Detailed analyses of carotenoid precursors indicated specific accumulation of intermediates and allowed hypothesis generation for target enzymes, which were confirmed in biochemical assays. Also, target sites in fatty acid biosynthesis and sterol biosynthesis are hard to address with feeding studies, and similar to pigment biosynthesis, targeted analytics to detect all intermediates of the specific pathway allows the generation of target hypotheses.

Only for six out of the 37 compound classes in Table 1, the mechanism of action was identified by a genetic approach. All genetic studies were published after 2000 and used *Arabidopsis thaliana* as a model system (Scheible *et al.*, 2001; Walsh *et al.*, 2006, Walsh *et al.*, 2007; Rojas-Pierce *et al.*, 2007; Park *et al.*, 2009; Sheard *et al.*, 2010). Interestingly, three out of six target sites identified by a genetic approach belong to a group of targets in signalling pathways and one belongs to a group of targets that is involved in establishment of the cytological architecture. This shows the power of genetic screens to identify target proteins in signalling cascades or proteins involved in cytological architecture. Auxin herbicides were studied for more than 60 years with physiological approaches (see review by Grossmann, 2010), but the final description of the TIR proteins as molecular targets of auxin herbicides resulted from a genetic screening approach (Walsh *et al.*, 2006; Tan *et al.*, 2007). Similarly, for herbicides inhibiting cell wall biosynthesis, many compound classes are known (Table 1, Table 3), but a target protein has been defined only for isoxaben (Scheible *et al.*, 2001). The application of genetic screens is actually limited by the number of appropriate model species. Additional limitations in performing a genetic screen are the availability of

space to cultivate and screen several thousands of individuals, the genetic tractability and the possibility to generate a large population of mutants or the public availability thereof. Actually, only *Arabidopsis thaliana* and *Chlamydomonas reinhardtii* are available for this kind of screen. Because of the huge efforts to establish a monocot model system (Mur *et al.* 2011; Brkljacic *et al.*, 2011), it is very likely that additional species such as *Brachypodium distachyon* will be available for genetic screens in the near future.

Based on the evaluation of the 37 compounds or compound classes in Table 1 with a defined target protein, only one target protein was identified by a biochemical screen. For such a biochemical screen, the compound of interest needs an affinity group (e.g., azido moiety) to covalently bind the compound to the target protein and a detection group (e.g., radioactive label) to visualise the compound in a mixture of proteins. In the case of atrazine, azido-atrazine with a photoaffinity group was combined with a radioactive ^{14}C label. The fact that azido-atrazine shows the same physiological effects as atrazine (Gardner, 1981), led to the hypothesis that it interacts with the same target and, therefore, the application of a biochemical screen made sense (Pfister *et al.*, 1981). To apply a biochemical screen, some knowledge on the structure-activity-relationship (SAR) is needed to synthesise a compound with a photoaffinity label that influences the same physiological target site as the original hit compound. Also some knowledge of the metabolism within the cell is needed, e.g., if the parent compound is a prodrug and has to be activated. In such a case the photoaffinity label could be lost or conjugated to the metabolising enzyme. For *in vivo* biochemical screens, the affinity group should not have an influence on the uptake towards the cell wall and distribution within the cell. Therefore, only small affinity groups are allowed for *in vivo* screens. The ease of use of azide and alkyne groups for *in vivo* labelling of target proteins was recently shown by Kaschani *et al.* (2009). Because of the use of inhibitors that covalently react with their target protein, Kaschani *et al.* used only one molecule label, either an alkyne or an azide group. With that strategy it was possible to identify protease targets of E-64, a cysteine protease inhibitor *in planta* (Kaschani *et al.*, 2009).

Some of the compounds or compound classes described in Table 1 were initially identified in HTS enzyme assays in a reverse screen or by *in silico* modelling. The target site of these compounds is known per definition of a reverse screen, or can be proposed in the case of *in silico* modelling (Figure 3). To use such a compound in basic research as a chemical probe, to specifically block a biochemical process, or to use the initial hit as lead compound in crop protection, it is important to confirm the *in vivo* MoA by applying the methods from the MoA toolbox. Sirtinol (Table 2), for example, was first identified as a specific inhibitor of NAD-dependent deacetylases, named sirtuins, in yeast and mammalian cells (Grozinger *et al.*, 2001). Therefore, it was speculated that the effects induced in *Arabidopsis thaliana* are

caused by the inhibition of plant sirtuins, but detailed investigations showed that the active principle in plants is a cleavage product of sirtinol, the auxin mimic 2-hydroxy-1-naphthoic acid (Dai *et al.*, 2005). The final oxidation is most probably catalysed by an aldehyde oxidase (Dai *et al.*, 2005).

It can be summarised that the appropriate methodologies can be chosen, based on initial characterisation in physiological studies, which is equivalent to 1st-level studies (Figure 2). For compounds with an indication for interaction in primary metabolism the phenotyping approach using feeding studies and detailed analytics is most appropriate. If cytological studies suggest an interaction of the inhibitor with the cell architecture or physiological studies indicate an interaction with the hormone system or plant development, a genetic screening approach is suggested. The biochemical approach strongly depends on the availability of active compounds with a photoaffinity group or a click chemistry-compatible group (section 4.6). These compounds must have the same physiological characteristics as the initial lead compound, which has to be proven in physiological studies.

Table 1: Compounds identified in plant screens with their respective MoA

Compound source: Forward screen (FS), Reverse screen (RS), *In silico* design (ISD); Compound type: synthetic (S), natural product (NP), synthetic compound derived from natural product (SND); Strategy: Phenotyping (P), Genetic screen (G), Biochemical screen (B), Target based (T); [1] compounds from a company proprietary library; [2] Publicly available compound library (for details see Toth and van der Hoorn, 2010); [3] Year of first market introduction (Phillips McDougal, 2011).

		Source of compound				Mode of Action			
Structure	Compound	Source	Cpd. Type	Origin	Reference	Organism for plant MoA studies	Pathway Target	Strategy	Reference
see review by Singh and Shaner, 1995	various classes (e. g. sulfonylureas & imidazolinone herbicides)	FS	S	Du Pont, *et al.* [1] Am. Cyanamide, *et al.* [1] 1982[3]		*Zea mays* (suspension culture)	amino acid biosynthesis Acetolactate synthase	P	LaRossa and Schloss, 1984 Shaner *et al.* , 1984
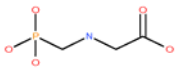	**Glyphosate**	FS	S	Monsanto[1]	Baird *et al.* , 1971	*Lemna gibba*	amino acid biosynthesis Enolpyruvylshikimate synthase	P	Jaworski, 1972 Steinbrücken and Amrhein, 1980
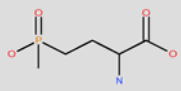	**Glufosinate** (Phosphinotricine)	FS	NP	*Streptomyces viridichromogenes*	Bayer *et al.* 1972	Pisum sativum (enzyme assay)	amino acid biosynthesis Glutamine synthase	P	Leason *et al.* ,1982
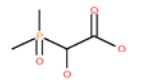	**Hoe 704**	FS	S	Hoechst AG[1]	Schulz *et al.* , 1988	*Lemna gibba, Klebsiella pneumoniae*	amino acid biosynthesis ketol-acid reductoisomerase	P	Schulz *et al.* , 1988
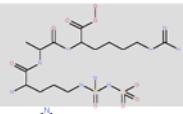	**Phaseolotoxin**	Extract	NP	*Pseudomonas syringae*	Mitchell, 1976 Moore *et al.* 1984	various plants	amino acid biosynthesis (Arg) Ornithine Carbamoyltransferase	P	Ferguson and Johnston, 1980
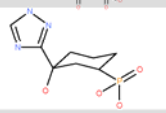	**IRL1803**, IRL1856 (triazole phosphonates) pyrrole aldehydes	ISD	S	Ciba-Geigy[1] Monsanto[1]	Mori and Fonne-Pfister, 1995 Schweitzer *et al.* ,	*Ocymum basilicum* (cell culture), *Arabidopsis thaliana*	amino acid biosynthesis (His) Imidazoleglycerolphosphate dehydratase	T	Mori and Fonne-Pfister, 1995
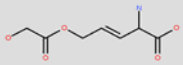	**Rhizobitoxine**	Extract	NP	*Rhizobium japonicum*	Owens and Wright, 1965	*Spinacia oleracea* *Zea mays*	amino acid biosynthesis (Met) β-Cystathionase	P	Giovanelli *et al.* , 1971 Giovanelli *et al.* , 1972
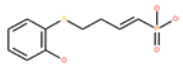	Arylsulfide phosphonates (e. g. **Cpd1**)	ISD	S	American Cyanamid[1]	Finn *et al.* , 1999	*Salmonella typhimurium* Tsa enzyme *Arabidopsis thaliana* (reversal)	amino acid biosynthesis (Trp) Tryptophan synthase	T	Finn *et al.* , 1999
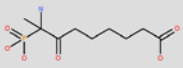	**8-Amino-7-oxo-8-phosphononanoic acid** Triphenyltin acetate	ISD	S	targeted synthesis	Ploux *et al.* , 1999 Hwang *et al.* , 2010	*Arabidopsis thaliana*	biotin synthesis 7-keto-8-aminopelargonic acid synthase	T	Ploux *et al.* , 1999 Hwang *et al.* , 2010
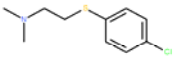	**CPTA** (2-(4-chlorophenylthio)-triethylamine HCl	FS	S		Porter and Lincoln, 1950	*Blakeslea trispora*	Carotenoid biosynthesis Lycopene synthase	P	Hsu and Yokoyama, 1972 Bouvier *et al.* , 1997
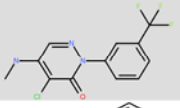	Pyridazinone (**Norflurazon**, 1971) Fluridone (1981)	FS	S	Syngenta, *et al.* [1]	1971[3]	*Narcissus pseudonarcissus*	carotenoid biosynthesis Phytoenedesaturase	P	Mayer *et al.* , 1989 Sandmann *et al.* , 1989
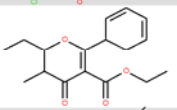	**LS80707**, J852	FS	S	Rhone-Poulenc[1]	Vial and Borrod, 1984	*Aphanocapsa* (blue-green algae)	Carotenoid biosynthesis ζ-Carotene-Desaturase	P	Sandmann *et al.* , 1985
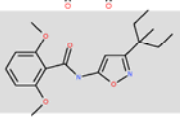	**Isoxaben**, Thiazolidinone	FS	S	Dow Agro Science[1]	1984[3]	*Arabidopsis thaliana*	cell wall biosynthesis Cellulose synthase	G	Heim *et al.* , 1989 Scheible *et al.* , 2001
see review by Hao *et al.* , 2011	various classes, eg. diphenyl ether herbicide Bifenox	FS	S	Bayer, et al.[1]	1969[3]	*Zea mays, Solanum tuberosum*	chlorophyll biosynthesis Protoporphyrinogen IX Oxidase	P	Matringe *et al.* , 1989

Table 1: continued

Structure	Compound	Source of compound: Source	Cpd. Type	Origin	Reference	Mode of Action: Organism for plant MoA studies	Pathway	Target	Strategy	Reference
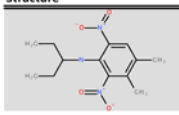	**Pendimethalin** and other Dinitroanilines	FS	S	Dow, *et al.* [1]	1964*	*Chlamydomonas*	cytoskeleton	α-Tubulin	P	Strachen and Hess, 1983 Morejohn et al., 1987 Anthony et al., 1998
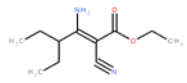	**Cyanoacrylates**	FS	S	BASF[1]	Tresch *et al.* , 2005	*Zea mays, Eleusine indica* , various model systems	cytoskeleton	α-Tubulin	P	Tresch *et al.* , 2005
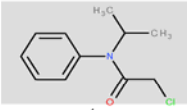	Chloroacetamides (e. g. Propachlor)	FS	S	Monsanto, *et al.* [1]	1965[3]	*Arabidopsis thaliana*	fatty acid biosynthesis	3-Ketoacyl-CoA synthase	P	Trenkamp *et al.* , 2004
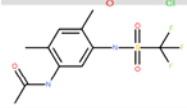	Trifluoromethan-sulfonanilides (e. g. **Mefluidide**)	FS	S	3M Company[1]	Friedinger, 1978	*Lemna paucicostata* , various model systems	fatty acid biosynthesis	3-Ketoacyl-CoA synthase	P	Tresch *et al.* , 2012
see Rendina *et al.* , 1990	various classes (e. g. aryloxyphenoxy-propionates (fop's) & cyclohexanediones (dim's))	FS	S	Bayer, *et al.* [1]	1975[3]	*Zea mays* (seedlings), *Hordeum vulgare* (chloroplasts)	fatty acid biosynthesis	Acetyl-CoA-Carboxylase	P	Burton *et al.* , 1987 Focke *et al.* , 1987 Rendina and Felts, 1988 Secor and Ceske, 1988
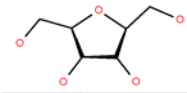	Anhydro-D-glucitol	Extract	NP	Fusarium solani, NRRL 18883 Tanaka *et al.* , 1996		*Spinacia oleracea, Lactuca sativa*	Glycolysis	Fru-1,6-bisP aldolase	P	Dayan *et al.* , 2002
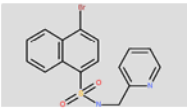	Pyrabactin	FS	S	DiverSet NT488, LOPAC, Spectrum[2] Zhao *et al.* , 2007		*Arabidopsis thaliana*	hormone (abscisic acid signal perception)	Pyrabactin resistance 1	G	Park *et al.* , 2009
see review by Grossmann, 2010	various classes (e. g. phenoxycarboxylic acids)	FS	S	Dow Agro Science, et al.[1] 1945[3]		*Arabidopsis thaliana*	hormone (auxin signal perception)	Transport inhibitor response factors	G	Dharmasir *et al.* , 2005 Kepinski and Leyser, 2005 Walsh *et al.* , 2006 Tan *et al.* , 2007
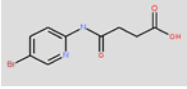	Bikinin	FS	S	DiverSet[2] Rybel and Audenaert, 2009		*Arabidopsis thaliana*	hormone (brassinosteroid signaling)	GSK3 like kinases in brassinolide signaling	P	Rybel and Audenaert, 2009
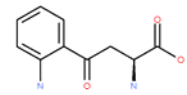	Kynurenine	FS	NP	Microsource Spectrum Collection[2] He *et al.* , 2011		*Arabidopsis thaliana* (ctr1-1, eto1-2)	hormone (ethylene signalling)	Tryptophan aminotransferase	P	He *et al.* , 2011
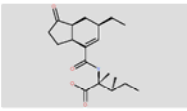	Coronatin	Extract	NP	*Pseudomonas syringae* Ichihara *et al.* , 1977		*Arabidopsis thaliana*	hormone (jasmonate signal perception)	Coronatin insensitive 1	G	Feys *et al.* , 1994 Xie *et al.* , 1998 Sheard *et al.* , 2010
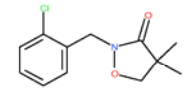	Clomazone	FS	S	FMC Corporation[1] 1986[3]		*Spinacia oleracea; Scenedesmus obliquus, Sinapis alba, Narcissus sp.*	isoprenoid biosynthesis	Deoxyxylulose-5-phosphate-synthase	P	Ferhatoglu, 2006
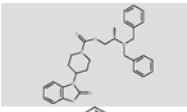	Galvestine-1	RS	S	Cerep diversity based library[2] Botte and Deligny, 2011		*Arabidopsis thaliana* MGD1 enzyme (*in vitro*)	lipid synthesis	MGDG-synthase	T	Botte and Deligny, 2011
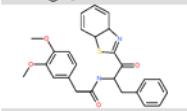	5 compound classes (e. g. **G, H**)	RS	S	Monsanto[1] Duff *et al.* , 2007		*Spinacia oleracea* CtpA enzyme (*in vitro*)	photosynthesis	Carboxyterminal processing protease of D1	T	Chen *et al.* , 2007
see Trebst, 2007	various classes (e. g. urea & triazine herbicides)	FS	S	MAI, *et al.* [1] 1954[3]		*Amaranthus hybridus* (susceptible, resistant) *Rhodopseudomonas*	photosynthesis	D1 protein (psbA gene)	B & P	Wessels and Vanderveen, 1956 Pfister *et al.* , 1981 Michel *et al.* , 1986
see van Almsick, 2009	various classes (e. g. pyrazolones & triketone herbicides)	FS	SND	Sankyo *et. al.* [1] 1979[3]		*Lemna gibba*	plastoquinone biosynthesis	Hydroxyphenylpyruvate Dioxygenase	P	Schulz *et al.* , 1993 Barta and Böger, 1996

Table 1: continued

		Source of compound			Mode of Action			
Structure	Compound	Source	Cpd. Type	Origin Reference	Organism for plant MoA studies	Pathway Target	Strategy	Reference
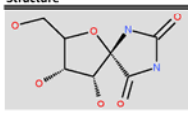	Hydantocydin	Extract	NP	*Streptomyces hygroscopicus* Nakahima *et al.* , 1991	*Ocymum basilicum* (cell culture), *Arabidopsis thaliana*, *Zea mays*	purine biosynthesis Adenylosuccinate synthase	P	Heim *et al.* , 1995 Fonne-Pfister *et al.* , 1996 Cseske et al., 1996 Siehl *et al.* , 1996 Walters *et al.* , 1997
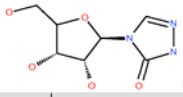	Ribofuranosyl triazolone	Extract	NP	*Actinomadura madurae* Schmitzer *et al.* , 2000	*Arabidopsis thaliana*	purine biosynthesis Adenylosuccinate synthase	P	Schmitzer *et al.* , 2000
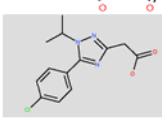	DAS734	FS	S	Dow Agro Science[1] Walsh *et al.* , 2007	*Arabidopsis thaliana*	purine biosynthesis Glutamine Phospho-ribosylpyrophosphate Amidotransferase	G	Walsh *et al.* , 2007
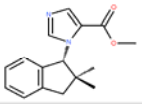	CGA214372	FS	S	*Ciba-Geigy* [1] *Monsanto* [1] Streit *et al.* , 1991	*Zea mays* (seedlings), *Nicotiana tabacum* (BY-2)	sterol biosynthesis Obtusifoliol 14α demethylase	P	Streit *et al.* , 1991 Salmon *et al.* , 1992
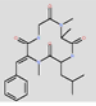	Tentoxin	Extract	NP	*Alternaria tenuis* *Alternaria alternata* Meyer *et al.* , 1971	*Spinacia oleracea* (biochemistry) *Arabidopsis thaliana*	photosynthesis chloroplast F1-ATPase	P	Arntzen, 1972 Steele *et al.* , 1976 Groth, 2002 Sobolev *et al.* , 2002
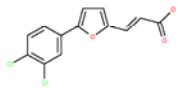	Gravacin	FS	S	ChemBridge, DiverSet library[2] Surpin *et al.* , 2005	*Arabidopsis thaliana*	- P-glycoprotein19	G	Surpin *et al.* , 2005 Rojas-Pierce *et al.* , 2007
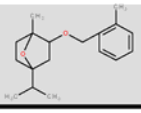	Cinmethylin	FS	S	BASF[1] Grossmann *et al.* , 2012	*Lemna paucicostata* , various model systems	- Tyrosine aminotransferase	P	Grossmann *et al.* , 2012b

4.2. Successful MoA studies of phytoactive compounds with confirmation of target sites using bacterial, fungal or animal systems

Some of the compounds intensively investigated in plants were originally described in studies of bacterial, fungal or animal cells (Table 2). The activity in bacteria or fungi allowed the application of a broader panel of model systems and methods to study compound MoA. Triclosan was identified as a broad-spectrum antibacterial and antifungal agent, but is also active in plant cells (Serrano *et al.*, 2007; Dayan *et al.*, 2008). The target protein for triclosan, enoyl-acyl carrier protein reductase, was identified by a genetic screen in *Escherichia coli* for the selection of triclosan-resistant clones. Afterwards, the causative mutation was identified by transformation of a genomic library from the resistant strain to susceptible *E. coli* cells (McMurry *et al.*, 1998). With the knowledge of the target protein in bacteria, Serrano *et al.* (2007) showed that triclosan also inhibited the plant enoyl-acyl carrier protein reductase. This was confirmed also by physiological studies that showed a decrease in linoleic acid and α-linolenic acid in *Arabidopsis thaliana* plants after treatment with triclosan, but also by cyperin, a natural product produced by pathogenic fungi (Dayan *et al.*, 2008). The structural similarity of cyperin to triclosan and the knowledge of the MoA of triclosan in bacteria led to a fast confirmation of the MoA of cyperin (Dayan *et al.*, 2008).

This example shows, that model systems in addition to plants can be used for MoA identification of plant active compounds, and that single-cell bacteria or fungi do have the potential to accelerate MoA identification. A prerequisite is to clarify that the *in vivo* MoA in plants is most likely the same as in the species where the activity or target protein was originally described.

There are three main questions to guide the MoA identification strategy if a compound acts on a decribed target in bacteria, fungi or animals:

1. Is the described target or pathway present in plant cells?

If plants share the same target or pathway that is inhibited by the compound of interest in bacteria, fungi or animals, then the compound could act in the same manner as in the originally described species. This is the case for the enoyl-acyl carrier protein reductase inhibitor triclosan and for asulam (Guerineau *et al.*, 1990), which inhibits the dihydropteroate synthase.

2. Does the target belong to a large protein family?

Compounds that inhibit enzymes belonging to a large enzyme class or protein family could induce completely different effects on plant metabolism, compared to bacteria, fungi or animals. This is the case for gabaculin, which generally blocks aminotransferase enzymes. In mammalian cells, the most dominant effect is the inhibition of 4-aminobutyrate aminotransferase (Mishima *et al.*, 1976). In plants, however, it was shown that inhibition of glutamate 1-semialdehyde aminotransferase (GSA) is the most sensitive process blocked by gabaculin. This was supported by feeding studies with 5-aminolevulinate showing a reversal of the inhibitory effect (Anderson and Gray, 1991) and the use of transgene overexpression of a mutated form of the *Medicago sativa* GSA gene (Giancaspro *et al.*, 2012). Another example is the azole class of fungicides. Initially, they were discovered as antifungal compounds, but some derivatives also showed activity on plant growth. Their MoA in fungi was described as inhibitors of the cytochrome P450-dependent 14α-lanosterol demethylase in sterol biosynthesis (reviewed in Ghannoum and Rice, 1999). They act not only as specific sterol biosynthesis inhibitors, but also with other cytochrome P450-dependent enzymes. Depending on the specific derivative, effects in plants were primarily caused by the inhibition of cytochrome P450 enzymes in gibberelin (e.g., Paclobutrazole; Hedden and Graebe, 1985) or brassinolide biosynthesis (e.g., Brassinazole; Asami *et al.*, 2001). To use a compound with a described target in other organisms as a probe to study physiological processes in plants, it is important to correlate the plant response with the expected physiological changes.

3. Is the parent compound active in plant cells or does the phytoactivity rely on a possible metabolite?

The third question pays attention to the fact that plants, compared with animals, do have a more diverse pool of enzymes that can potentially metabolise a compound to a novel phytoactive metabolite (reviewed in Hatzios, 2005). If that is the case, the target protein

within plants could be different from the described mechanism of action in bacteria, fungi or animals. Also, for compounds with a described target in bacteria, fungi or animals, the strategy for MoA identification in plants has to start with a basic physiological characterisation in order to confirm the target or apply appropriate techniques for further investigation.

Table 2: Compounds with a described MoA, identified by cross-fertilisation from antibiotic, fungicide, or pharma research.

Compound source: Forward screen (FS), Reverse screen (RS), *In silico* design (ISD); Compound type: synthetic (S), natural product (NP), synthetic compound derived from natural product (SND); Strategy: Phenotyping (P), Genetic screen (G), Biochemical screen (B), Target based (T); [1] Compound from a company proprietary library; [2] Publicly available compound library (for details see Toth and van der Hoorn, 2010); [3] Year of first market introduction (Phillips McDougal, 2011).

		Source of compound				Mode of Action			
Structure	Compound	Source	Cpd. Type	Origin	Reference	Organism for plant MoA studies	Pathway / Target	Strategy	Reference
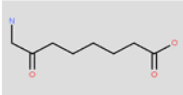	**Desmethyl-KAPA**	ISD		*Streptomyces lavendulae*	Nudelman *et al.*, 2004 Ashkenazi *et al.*, 2005		biotin synthesis 7,8-diaminopelargonic acid aminotransferase		Sandmark *et al.*, 2002 Ashkenazi *et al.*, 2005
	Amiclenomycin	Extract	S		Okami *et al.*, 1974	-		P	Mann *et al.*, 2009
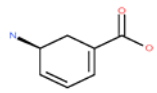	**Gabaculin**	Extract	NP	*Streptomyces toyocaenis*	Mishima *et al.* 1976	*Pisum sativum, Z. mays, Avena sativa Hordeum vulgare Chlamydomonas,*	chlorophyll biosynthesis Glutamate 1-semialdehyde aminotransferase	P	Gardner and Gorton, 1985 Kannangara and Schouboe, 1985 Kahn and Kannangara, 1987
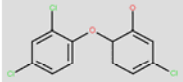	**Triclosan**	FS	S	Ciba-Geigy[1]	Zinkernagel and König, 1967	*Arabidopsis thaliana*	fatty acid biosynthesis enoyl-acyl carrier protein reductase	G	McMurry *et al.*, 1998 Heath *et al.*, 1999
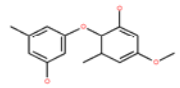	**Cyperin**	Extract	NP	*Preussia fleischhakii*	Weber and Gloer 1988 Stierle *et al.* 1991	*Arabidopsis thaliana*	fatty acid biosynthesis enoyl-acyl carrier protein reductase	P	Dayan *et al.*, 2008
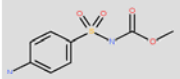	Sulfamethoxazole, **Asulam**	FS	S	Bayer[1]	1965[3]	*Triticum aestivum* (shoot tips), *Avena fatua*	Folate biosynthesis Dihydropteroate synthase	P	Veerasekarana *et al.*, 1981 Guerineau *et al.*, 1990
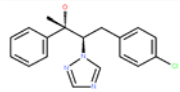	**Brassinazole**	FS	S	small set of synthesized compounds	Asami and Yoshida, 1999	*Arabidopsis thaliana*	hormone (brassinolide synthesis) cytochrom P450 monooxygenase	P	Asami *et al.*, 2001
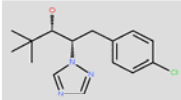	**Paclobutrazol**	FS	S	Syngenta (former ICI)[1]	Lever *et al.* 1982	*Cucurbita maxima, Malus pumila*	hormone (Gibberelin synthesis) ent-Kaurene oxidase	P	Hedden and Graebe, 1985
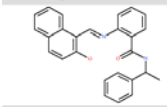	**Sirtinol**	FS	S	ICCB diversity set of compounds, ICCB Chem-Bridge Library[2]	Grozinger *et al.*, 2001	*Saccharomyces cerevisiae*	hormone perception (auxin); cell cycle re sirtuin family of NAD-dependent deacetylases; acts auxin like after metabolisation	G	Grozinger *et al.*, 2001 Zhao *et al.*, 2003 Dai *et al.*, 2005
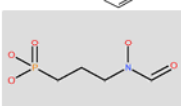	**Fosmidomycin**	Extract	NP	*Streptomyces lavendulae*	Okuhara *et al.* 1980	*Lemna gibba, Hordeum vulgare*	isoprenoid biosynthesis 1-Deoxy-D-xylulose-5-phosphate reductoisomerase	P	Zeidler *et al.*, 1998 Kuzuyama *et al.*, 1998
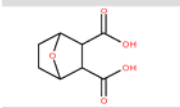	**Endothall**	FS	SND	Sharples Chemicals Inc.[1]	Tischler *et al.*, 1951	various model systems, *Nicotiana tabacum* (cell culture), *Arabidopsis thaliana*, *Lemna paucicostata*	signaling cascades serine / threonin protein phosphatases	P	Tresch *et al.*, 2011 Bajsa *et al.*, 2012
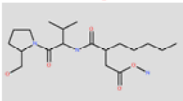	**Actinonin**	Extract	NP	*Streptomyces sp.* CUTTER c/2 NCIB 8845	Gordon *et al.* 1962	*Nicotiana tabacum*	translation Peptide deformylase	P	Attwood, 1969 Chen *et al.*, 2000 Hou *et al.*, 2007

4.3. Status of MoA studies of phytoactive compounds with undescribed target sites

For several compound classes that have been intensively studied in plant science, preliminary descriptions of their MoAs are available, but their target sites are still unidentified (Table 3). MoA studies indicated that most of them act on signalling pathways or structural targets. Cytological investigations and the inhibition of ^{14}C-glucose incorporation in cell wall fractions indicated that four compounds (dichlobenil, thaxtomin A, flupoxam and phthoxazolin) and members of the compound group of fluoroalkyltriazines (e.g., CGA325615 and related compounds; Table 3) inhibit the biosynthesis of the cell wall. Cross-resistance studies using isoxaben-resistant (*ixr*) mutants showed that none of them had the same target site as isoxaben. Therefore, a different target in cell wall biosynthesis or at least a different binding site at cellulose synthase has been proposed for the mentioned compounds.

Similarly, a target site has rarely known for compounds interacting with the plant cytoskeleton. Compounds like cobtorin, flamprop-m-methyl or morlin affect the functionality of the cytoskeleton, but it could only be hypothesised that either proteins supporting the function of microtubules or proteins involved in cytoskeleton signalling were blocked. Flamprop-m-methyl, for example, disrupts microtubule spindle formation in a manner different to classical microtubule assembly inhibitors, like dinitroanilines (Tresch *et al.*, 2008). The *in vitro* assembly of microtubules formed by α/β-tubulin dimers is not affected by flamprop-m-methyl. Therefore, an effect of flamprop-m-methyl on the regulation of the plant cytoskeleton is proposed (Tresch *et al.*, 2008). Equal to the compounds listed in Table 1 with a described target site, the effects of compounds interacting with cell wall biosynthesis or the cytoskeleton can be described in detail; however, except for isoxaben (Scheible *et al.*, 2001), dinitroanilines (Anthony *et al.*, 1998) and cyanoacrylates (Tresch *et al.*, 2005) a molecular target could not be described. These examples show the limitation of the phenotypical approach. Inhibitors that block structural targets could hardly be addressed using analytical or biochemical methods. Most of the proteins involved in cell wall biosynthesis are membrane bound, and some of them are active as large protein complexes like cellulose synthase. Both facts limit the use of biochemical methods to confirm a target hypothesis. Also, for inhibitors interacting with the cytoskeleton, biochemical assays to analyse inhibitor-protein interactions with microtubule-associated proteins or other signalling proteins modulating the cytoskeleton are challenging. The only assay on a target level is to measure tubulin assembly *in vitro*. It is difficult to establish biochemical assays to analyse interactions between inhibitors and regulatory proteins.

In several *in vivo* reporter system screens, compounds could be identified that specifically affect the reporter system (Hayashi *et al.*, 2001; Armstrong *et al.*, 2004; Yamazoe *et al.*, 2004; Gendron *et al.*, 2008; Hayashi *et al.*, 2009). The most common system is based on

either the DR5::GUS or BA3::GUS reporter line. In both lines, the β-glucuronidase gene (GUS) is under the control of a primary auxin-inducible promoter (Ulmanov *et al.*, 1997; Oono *et al.*, 1998). The chemical screens used either extracts of microorganisms (Hayashi *et al.*, 2001; Yamazoe *et al.*, 2004; Hayashi *et al.*, 2009) or libraries of diverse compounds (Armstrong *et al.*, 2004). The screens were designed to identify compounds that inhibit auxin signalling, which leads to blocking of auxin-induced transcription of the GUS reporter. These negative screens, however, rely on the functionality of RNA transcription and protein translation after compound treatment. This is one of the principal challenges of *in vivo* screens to identify compounds inducing a phenotype of interest. If active transcription or translation is required to induce the desired phenotype, compounds blocking these processes also occur as hit compounds. Hayashi *et al.* (2009) presented toyocamycin as a specific inhibitor of auxin signalling in plants, but it was formerly also described as an inhibitor of RNA synthesis (Sverak *et al.*, 1970). With the use of different reporter lines, Hayashi *et al.* (2009) showed that toyocamycin inhibits the transcription of the GUS reporter under the control of various auxin-inducible promoters, but not if GUS expression is under the control of the tobacco parB promoter, which is known as a general stress promoter, or the cytokinin-inducible promoter ARR5. The specific response of toyocamycin on auxin signalling, in contrast to cytokinin or the general stress response, insinuates the specificity of toyocamycin on auxin signalling.

A system that was used as a positive reporter screen is described by Gendron *et al.* (2008). They have used a brassinosteroid-repressed reporter system (CPD::GUS) to identify compounds that induce the expression of the GUS reporter gene. With the identification of brassinopride, they found a compound that induces the CPD::GUS reporter and inhibits the hypocotyl length, which is normally controlled by brassinosteroids. Gendron *et al.* (2008) also showed that the brassinopride effects could be reversed by adding brassinolide to the growth medium. The effects of brassinopride on the hypocotyl length and the brassinosteroid-controlled GUS expression and the reversal of its effects by brassinolide indicate an influence of brassinopride on brassinosteroid biosynthesis. A comparison of the negative screen on auxin-induced gene expression, introduced by Hayashi *et al.* (2001), with the positive screen relying on the active expression of the CPD::GUS reporter (Gendron *et al.*, 2008) shows that the type of screen has an influence on the MoA strategy. A stringent filter for false positive hits blocking transcription or translation needs to be applied when using a negative screen.

Finally, several natural products that induced a plant phenotype were initially described, but only a limited number of studies describing the MoA of these compounds were published (Table 3). It can be hypothesised that the lack of pure compounds of these phytoactive substances hinders a detailed MoA identification.

Table 3: Compounds resulting from a chemical screen in plants, but a detailed mechanism of action is still lacking

Compound source: Forward screen (FS), Reverse screen (RS), Compound type: synthetic (S), natural product (NP), Strategy: Phenotyping (P), Genetic screen (G), Biochemical screen (B), Target based (T); [1] compound from a company proprietary library; [2] Publicly available compound library (for details see Toth and van der Hoorn, 2010).

		Source of compound				Mode of Action			
Structure	Compound	Source	Cpd. Type	Origin	Reference	Organism for plant MoA studies	Pathway Target	Strategy	Reference
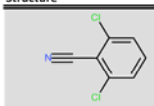	**Dichlobenil**	FS	S	Chemtura[1]	Koopman and Daams, 1960	Gossypium hirsutum	cell wall biosynthesis target in cellulose biosynthesis not known	P	Montezinos and Delmer 1980
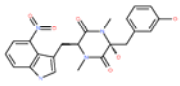	**Thaxtomin A**	Extract	NP	*Streptomyces scabies*	King *et al.* , 1989	*Arabidopsis thaliana*	cell wall biosynthesis target in cellulose biosynthesis not known	P	Fry and Loria, 2002 Scheible *et al.* , 2003 Bischoff *et al.* , 2009
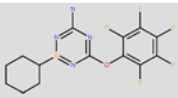	**CGA325615**, AE F150944, Indaziflam, Triaziflam	FS	S	Ciba-Geigy[1]	Peng *et al.* , 2001	*Glycine max (cell culture)*	cell wall biosynthesis target in cellulose biosynthesis not known	P	Peng *et al.* , 2001
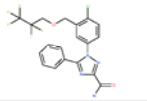	**Flupoxam**, Triazofenamide	FS	S	Kureha Chemical[1]	O'Keefe and Klevorn, 1991	*Arabidopsis thalian, Agrostis*	cell wall biosynthesis target in cellulose biosynthesis not known	P	Heim *et al.* , 1998
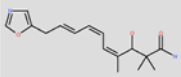	**Phthoxazolin**	FS	NP	*Streptomyces sp* . OM-5714	Omura *et al.* , 1990	*Phytophthora parasitica vs. Candida albicans, Acetobacter xylinum*	cell wall biosynthesis target in cellulose biosynthesis not known	P	Omura *et al.* , 1990
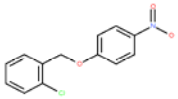	**Cobtorin**	FS	S	Microsouce Spectrum & LATCA[2]	Yoneda *et al.* , 2007	*Nicotiana tabacum (BY-2)*	cytoskeleton orientation and cell wall con no target described	P	Yoneda *et al.* , 2010
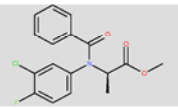	**Flamprop-M-Methyl**	FS	S	Shell Research Limited[1]	Jeffcoat and Harries, 1975	*various plant models sytstems, Zea mays*	cytoskeleton (regulation) no target described	P	Tresch *et al.* , 2008
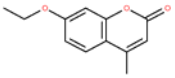	**Morlin**	FS	S	DiverSet plates 10,126–10,250 and 10,626–10,750[2]	DeBold *et al.* , 2007	*Arabidopsis thaliana*	cytoskeleton orientation and cell wall con no target described	P	DeBolt *et al.* , 2007
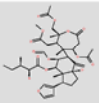	**Endosidin**, alternative name: Prieurianin	FS	S	Microsource Spectrum[2]	Robert and Chary, 2008	*Nicotiana tabacum (pollen)*	endocytosis involving an early SYP61/VHA-a1 endosomal compartment, no defined target described	P	Robert and Chary, 2008
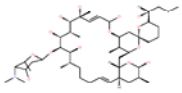	**Yokonolide B**	FS, reporter system	NP	*Streptomyces diastatochromogenes B59*	Hayashi *et al.* , 2001	*Arabidopsis thaliana*	hormone (auxin signal perception) auxin signaling	P	Hayashi *et al.* , 2003
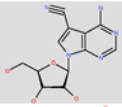	**Toyocamycin**	FS, reporter system	NP	*Streptomyces toyocansis*	Nishimura *et al.* , 1956	*Arabidopsis thaliana*	hormone (auxin signal perception) / RNA translation auxin signaling RNA synthesis / processing	P	Hayashi *et al.* , 2009 Sverak *et al.* , 1970
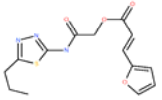	**Compound A**, B, C, D	FS, reporter system	S	DiverSet library[2]	Armstrong *et al.* , 2004	*Arabidopsis thaliana*	hormone (auxin signal perception) auxin signaling, anti-auxins	P	Armstrong *et al.* , 2004
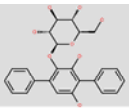	**Terfestatin A**	FS, reporter system	NP	*Streptomyces sp.*	Yamazoe *et al.* , 2004	*Arabidopsis thaliana*	hormone (auxin signal perception) modulator of aux/IAA stability	P	Yamazoe *et al.* , 2005
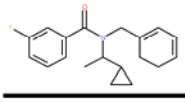	**Brassinopride**	FS, reporter system	S	DiverSet library[2]	Gendron *et al.* , 2008	*Arabidopsis thaliana*	hormone (brassinosteroid signaling) unknown	P	Gendron *et al.* , 2008

Table 3: continued

Structure	Compound	Source of compound				Mode of Action				
		Source	Cpd. Type	Origin	Reference	Organism for plant MoA studies	Pathway	Target	Strategy	Reference
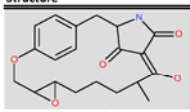	**Macrocidin A**	Extract	NP	*Phoma macrostoma*	Graupner *et al.* , 2003	-	unknown	induce bleaching symtpoms	P	-
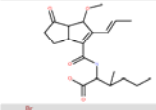	**Cinnacidin**	Extract	NP	*Nectria sp.* DA060097	Irvine *et al.* , 2008	-	unknown	structurally similar to coronatin	P	Irvine *et al.* , 2008
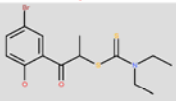	**Hypostatin**	FS	S	DiverSet NT488, LOPAC, Spectrum[2]	Zhao *et al.* , 2007	*Arabidopsis thaliana* (Ler)	unknown	UDP glycosyltransferase activates compound Hyp	G	Zhao *et al.* , 2007
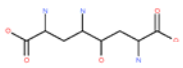	**Ascaulitoxin**	Extract	NP	*Ascochyta caulina*	Evidente *et al.* , 1998	*Lemna paucicostata* , various model systems	unknown	unknown	P	Duke *et al.* , 2011
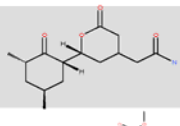	**A-75943**	Extract	NP	*Streptomyces griseolus*	Xu *et al.* , 2009	-	unknown	unknown	-	-
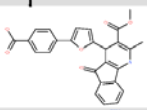	**Sortin**	FS	S	DiverSetE[2]	Zouhar *et al.* , 2004	*Saccharomyces cerevisiae, BY-2 cells, Arabidopsis thaliana*	vacuolar transport	unknown	G & P	Zouhar *et al.* , 2004 Rosado *et al.* , 2011
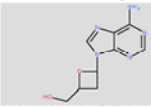	**Albucidin**	Extract	NP	*Streptomyces albus subsp. Chlorinus*	Hahn *et al.* , 2009	-	unknown	bleaching and chlorosis, no detail description of MoA	-	Hahn *et al.* , 2009
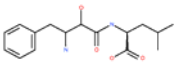	**Bestatin**	Extract	NP	*Streptomyces olivoreticuli*	Suda *et al.* , 1976	*Arabidopsis thaliana*	hormone perception (jasmonic acid)	described inhibitor of aminopeptidase, but detail target in plants is not	-	Zheng *et al.* , 2006
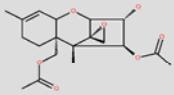	**4,15-Diacetoxyscirpenol**	FS	NP	Analyticon Discovery[2]	Serrano *et al.* , 2010	*Arabidopsis thaliana avrRpm1-RPM1*	unknown	most probably blocks protein translation	-	Serrano *et al.* , 2010
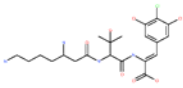	**Resormycin**	FS	NP	*Streptomyces platensis*	Igarashi *et al.* , 1997	*Selenastrum capricornutum*	protein synthesis	unknown	P	Igarashi *et al.* , 2001

4.4. A three-tier approach to optimise MoA identification

The classification of the compounds listed in Tables 1-3 with respect to the approach of detecting their target site, suggests some implications for straightforward MoA identification. Most of the target sites of compounds active in plant cells were identified by classical observations of the induced phenotype, followed by a detailed investigation of the associated selected pathways. This approach led to the identification of several compound targets in primary and secondary metabolism (Tables 1 and 2). Compounds that interact with processes in cell wall biosynthesis, the cytoskeleton or hormone signalling were either not finally described with a target protein or the target protein were identified by a genetic approach (Table 1-3). There is no clear preference of a specific model system, except within genetic studies. Because of the broad knowledge on the genetics of *Arabidopsis thaliana* and the availability of genetic tools, *Arabidopsis thaliana* is the preferred model in genetic studies to identify the MoA. With the phenotyping approach, whole plants from various species,

heterotrophic cells and single cell algae were successfully used. It was shown that the early focus on only one model system could mislead the primary MoA hypothesis; this was the case for chloroacetamides and the use of algae as a model (Couderchet *et al.* 1996; Matthes *et al.*, 1998). Rapid metabolism of phytoactive compounds is a well-known phenomenon in plants and strongly influences MoA identification efforts. Oxidative and hydrolytic reactions or conjugations with glucose or glutathione are the most common modifications (Hatzios, 2005). This was the case for sirtinol (Dai *et al.*, 2005) and compound A (Armstrong *et al.*, 2004) which were cleaved by an aldehyde oxidase or an esterase, respectively. The resulting compounds acted as well-known auxin mimics. Not only cleavage of the parent molecule, also activation by conjugation or e.g. phosphorylation can be necessary. In the case of hydantocidin, which is active in *in vivo* studies, only the phosphorylated form is recognised as a substrate-mimic and blocks the enzyme activity *in vitro* (Cseke *et al.*, 1996). For hypostatin, it was shown that glycosylation is needed to achieve its activity *in vivo* (Zhao *et al.*, 2007).
These implications confirm the level scheme presented in Figure 2 and allow some suggestions of how the different MoA approaches (Figure 3) should be applied. In the 1st level, a general phenotypical characterisation of the compound-induced effects should be done. One approach could be a detailed physiological profiling, which covers the most important aspects of plant physiology and indicates if the compound is active as an uncoupler or inducer or mediator of reactive oxygen species (Grossmann, 2005).
The following questions can guide this process:

- Is the compound in general cytotoxic?
- Does the compound act as an uncoupler or mediator of reactive oxygen species *in vivo*?
- Is the observed effect transferrable to other plant species? What is the most sensitive species?
- Does the compound act on primary metabolism, structural targets or the hormone system?
- Is the induced phenotype most likely based on an interaction with one primary target site?
- How is the stability and uptake of the compound in plant cells?
- Is there a SAR observable by using different derivatives of the initial hit?

Based on the initial characterisation in the 1st level, a decision can be made about what MoA approach (Figure 3) is applicable in the 2nd level. If the findings in the initial phenotypic characterisation indicate a MoA in primary metabolism, in most cases the phenotyping approach will lead to a straightforward target hypothesis. This approach is focussed on the physiological response in the *in vivo* system and integrates different results to generate the

target hypothesis. The available physiological, analytical and cytological methods cover a broad range of plant processes and describe the compound activity within a systems biology perspective. At the 2nd level, -omics technologies are also suitable to describe the plant response in a physiological context (Eckes *et al.*, 2004; Trenkamp *et al.*, 2009; Aliferis and Jabaji, 2011; Grossmann *et al.*, 2012a). So far, transcriptomic and metabolomic techniques were mostly used to describe the similarities of new compounds with well-characterised ones, but a substantial contribution to the description of a new target site has rarely been reported.

Genetic screens are a powerful tool to identify target sites in signalling cascades (Xie *et al.*, 1998; Walsh *et al.*, 2006; Park *et al.*, 2009) and targets that regulate cell structure (Scheible *et al.*, 2001). A genetic screen is, therefore, recommended if 1st-level studies indicate a target site in signalling pathways or targets that regulate cell structure. Because of the well-established genetic toolbox for *Arabidopsis thaliana*, this is the preferred model system. Single-cell systems, like heterotrophic cell cultures or algae cells, are in most cases easier to handle in an *in vivo* screen, but limitations due to the presence of several signalling cascades, like hormone perception cascades, or a different composition of the cell wall limit the use of these systems. Genetic screens for resistance to hypostatin or sirtinol identified resistant mutants with altered metabolic activation of the mentioned compounds (Zhao *et al.*, 2007). Therefore, the selection strategy and characterisation of the mutants had to take into account that resistance mechanisms based on altered compound metabolism is a common phenomenon (Hatzios, 2005).

The identification of the D1 protein as a target of atrazin is the only example in which a biochemical screen was successfully used for MoA identification (Pfister *et al.*, 1981; Michel *et al.*, 1986). This is not because of the weakness of the method, but rather due to the strict limitations for the use of the method, like accessibility of the lead compound for a photoaffinity label. Extensive SAR studies were necessary to recommend the synthesis of a photoaffinity-labelled compound (e.g., as shown for terfestatin A in Hayashi *et al.*, 2008). An in depth knowledge of the proteome of the model species could facilitate the identification of the labelled protein, but is not necessarily needed.

After generating a target hypothesis with any MoA identification approach, biochemical validation is needed. In this 3rd level, the choice of methods is both driven and limited by the accessibility of the hypothetical target to biochemical assays. Enyzme activity assays or affinity assays for receptor proteins were successfully established for all enzyme targets and the auxin hormone receptor, but not for the isoxaben target cellulose synthase. The validation of structural targets has to focus on the generation of transgenic plants or cell lines harbouring a wildtype gene as an overexpression construct or a mutated form of the hypothesised target.

4.5. Compounds as probes for plant research

Using compounds that modulate the activity of a specific cellular target protein is a well-accepted approach in plant research to study plant function (reviewed in Dayan *et al.*, 2010). In contrast to mutants or gene knock-out lines, which have been intensively used in plant functional genomics, small molecule compounds have some unique properties that make them complementary tools to study plant function. The advantages of chemical probes, which overcome the two major limitations of a genetic approach, were pointed out in several reviews (Blackwell and Zhao, 2003; Walsh, 2007; Toth and van der Hoorn, 2010). The first advantage is to overcome genetic redundancy that often results in single knock-out lines lacking an obvious phenotype (Cutler and McCourt, 2005). The second advantage of chemical probes over mutations and gene knock-out lines is that the latter often are not conditional; lethality is observed if essential gene functions are affected.

A single chemical probe can inhibit a set of homologous proteins. This is the case for inhibitors of very-long-chain fatty acid syntheses, which block a broad range of KCS proteins and induce a more dramatic phenotype than single knock-out lines of selected KCS proteins (Trenkamp *et al.*, 2004; Tresch *et al.*, 2012). In contrast to genetic mutations, the concentration of the chemical probe modulating the strength of the effect, the time and duration of treatment to investigate the effects on specific developmental stages or the combination with other probes or mutants is freely adjustable. A screen using a transgenic plant line with a trichome-defective phenotype and applying a set of various inhibitors led to the result that phospholipase A2 is involved in fatty acid-induced cell death (Reina-Pinto and Yephremov, 2009). In another case, the application of auxin-like compounds at different concentrations during various developmental stages allowed the detailed description of the auxin herbicide MoA in a time-dependent manner. With these studies, the auxin-triggered effects on metabolism and physiology were described as a three-phasic process, which includes stimulation, inhibition and decay (Grossmann, 2010). A further difference between chemical probes and genetic mutants is that a chemical probe can be used in various species and is not limited to model systems. This allows the investigation of the phenotype of interest in a broader perspective. In the case of ACCase inhibitors, this fact has contributed significantly to the understanding of the organization of fatty acid biosynthesis in monocot and dicot plants (Rendina and Felts, 1988; Alban *et al.*, 1994).

The compounds used in plant research can be grouped into two classes. One class contains compounds with a very well described target site and detailed descriptions of the primary MoA *in vitro* as well as *in vivo*. Such a compound can be used as a specific probe to explore the role of a defined protein in a broader biological context, as defined in a commentary by Frye (2010). The principles of a quality chemical probe as defined by Frye (2010) and listed in Table 4 are well transferrable to probes in plant science.

Table 4

Principles of a good quality probe as defined by Frye (2010)
Mechanism of action Activity in a cell-based or cell-free assay influences a physiologic function of the target in a dose-dependent manner.
Molecular profiling Sufficient *in vitro* potency and selectivity data to confidently associate its *in vitro* profile to its cellular or *in vivo* profile.
Identity of the active species Has sufficient chemical and physiological property data to interpret results as due to its intact structure or a well-characterised derivative.
Proven utility as probe Cellular activity data available to confidently address at least one hypothesis about the role of the molecular target in a cell's response to its environment.
Availability Is readily available to the academic community with no restrictions on use.

There is no need for additional requirements to probes in plant science, except two specifications of the molecular profiling criteria:

- Data about selectivity in various plant species should be provided to estimate the application range in different species.
- Uptake and translocation properties should be described to recommend the application of the probe for cell, tissue or whole-plant assays.

All compounds mentioned in Tables 1 and 2 mainly fulfill these criteria and, therefore, belong to the group of chemical probes. Several of these compounds were already used as probes, for example CPTA to study the effects of carotenoid biosynthesis inhibition (La Rocca *et al.*, 2007), fosmidomycin to investigate the two unrelated isoprenoid pathways in plants (Laule *et al.*, 2003) or 2,4-D to study the mechanism of auxin perception (Tan *et al.*, 2007).

The second class consists of compounds that are active on whole plants, cells or tissues, but detailed descriptions of the MoA are not available (Table 3). These compounds are in the process of MoA identification and are good candidates for future MoA identification projects. It is most likely that these compounds unravel uncharacterised protein functions in plants. Based on the three-tier approach discussed in section 4.1, some suggestions can be made as to what methodology is best suited to identify the compound's target site. It can be assumed that a genetic approach is appropriate for the compounds listed in Table 3, which influence cell wall biosynthesis or the cytoskeleton. Some of the compounds, such as dichlobenil (Montezinos and Delmer, 1980) or flamprop-m-methyl (Tresch *et al.*, 2008), are well characterised in terms of metabolisation and induction of specific cellular effects and are

well suited to start a genetic screen. Other compounds, such as sortin (Rosado *et al.*, 2011) or terfestatin A (Hayashi *et al.*, 2008), are actually in the 1st level of characterisation in terms of the three-tier model presented in section 4.1. For example, some SAR data exist for terfestatin A and the authors proposed to start a biochemical screen (Hayashi *et al.*, 2008).

4.6. New techniques for future MoA discovery

As described previously (see section 2.2), MoA identification is driven by technological progress. The availability of biochemical methods and the use of molecular biology techniques allowed the straightforward description of the MoA and the precise nomination of target sites for 34 compound (Table 1). Several omics-technologies (Wheelock and Miyagawa, 2006), like transcriptomics (Eckes *et al.*, 2004) and metabolomics (Trenkamp *et al.*, 2009; Aliferis and Jabaji, 2011; Grossmann *et al.*, 2012a), have been used for MoA identification. These methods produced large-scale datasets on transcript regulation and changes in metabolite levels. The value of the generation of a target hypothesis strongly depends on the functional annotation of the transcripts and integration of metabolites in biochemical pathways. Most of the published examples used the omics-technologies to apply multivariate or cluster analyses algorithms to compare the observed effects with effects induced by treatment with a well-described compound (Eckes *et al.*, 2004; Aliferis and Jabaji, 2011; Grossmann *et al.*, 2012a). Further progress in the functional annotation of gene transcription networks and the modelling of metabolic pathways will improve the future value of these techniques (Saever et al., 2012).

In addition, several new methods have been described in the literature that could be of benefit for MoA characterisation and hypothesis generation for target sites of phytoactive compounds. According to the principal methodologies for MoA identification (Figure 3), the new techniques can be assigned to the phenotyping, genetic or biochemical approach. The pattern of methods in the phenotyping approach is not well defined and adapted to the type of phenotype that is induced by the compound of interest. But, three technologies, RNA-seq (Wang *et al.*, 2009), super-resolution microscopy (Huang *et al.*, 2009; Gutierrez *et al.*, 2010) and mass spectrometry imaging (Horn *et al.*, 2012), are of broader interest for the investigation of new compounds and could be part of an phenotyping approach. Sequencing techniques with high-throughput capabilities allowing expression profiling by sequencing (RNA-seq) became available recently (reviewed by Metzker, 2010). With the use of RNA-seq, transcript profiling is no longer limited to model species with known transcript sequences; it is also applicable to non-model organisms. In addition, the main advantages are that the technique provides a very high dynamic range to analyse transcript level expression, and it allows the identification of transcripts that were originally not annotated (Wang *et al.*, 2009; Trapnell *et al.*, 2010). Recent progress in technologies providing high-resolution spatial imaging of proteins, cell metabolites or cell structures has the potential to

support the phenotyping approach, especially for inhibitor studies related to cell structures like the cell wall, cytoskeleton or membrane systems. New non-destructive microscopy technologies with a resolution not restricted by the diffraction limit, like stimulated emission depletion (STED) microscopy or stochastic optical reconstruction microscopy (STORM), can reveal insights in ultrastructural processes, which was not possible previously (Huang et al., 2009). The combination of these super-resolution microscopy technologies with fluorescence markers for protein-protein interactions or indicators for metabolite levels in cells (Wang *et al.*, 2008; Choi *et al.*, 2012) has the potential to valuably broaden the method portfolio for MoA identification in the future. In addition to the classical microscopy technologies, mass spectrometry imaging technologies emerged that allow the spatial detection of small molecules without prior labelling (reviewed by Lee *et al.*, 2012). This technique was recently used to visualise different lipid species in cotton seed tissue and unravel the non-uniform distribution of various species in the axis and cotyledons of the embryo (Hoorn *et al.*, 2012). This work showed the power of the technique even when some drawbacks in sample preparations, detection sensitivity of various molecule species or lower spatial resolution (20–50 µm) compared to light microscopy limit the current routine use (Lee *et al.*, 2012).

The exciting progress in DNA sequencing technologies mentioned before (reviewed by Metzker, 2010), will clearly affect the application of the genetic approach in MoA identification. The throughput of the next-generation-sequencing methods allows the fast re-sequencing of model organisms and crop plants from which a genome sequence is available. This will have an influence on the genetic mapping of resistant mutants of model organisms like *Arabidopsis thaliana*, which could now be mapped by sequencing (Schneeberger and Weigel, 2011; Austin *et al.*, 2011; Hamilton and Buell, 2012). The time-consuming generation of mapping populations is either not needed for heterozygous dominant mutations or only one cross is needed for homozygous mutations. Sequencing of pooled DNA of phenotypically uniform populations will allow a straightforward nomination of causative mutations (Hamilton and Buell, 2012). Further progress in sequencing techniques allowing much longer read lengths will also allow for sequencing projects with weed species or uncommon model systems. With such resources, mapping by sequencing approaches will be reachable for natural mutants like herbicide-resistant populations or resistant screens in non-model species.

In addition to the classical biochemical screen with concomitant compound labelling with a photoaffinity-group and a radioactive marker, the groups of Cravatt and van der Hoorn have established several biochemical screening protocols with new labelling procedures called activity-based-protein-profiling (ABPP) (Cravatt *et al.*, 2008; Kaschani *et al.*, 2009). They used azide or alkyle groups as ‘click chemistry’ tags for labelling with a fluorochrome or biotin

after inhibitor binding. These techniques were established for inhibitors binding covalently to the target. Therefore, only one label is needed for the detection of the coupled target protein. The need of an inhibitor that binds covalently to the target is a strict limitation of the technique, but for example it was described for chloroacetamides that they most probably bind covalently to the target protein KCS (Böger *et al.*, 2000; Eckermann *et al.*, 2003). An ABPP probe is, therefore, a possibility to detect the relevant KCS enzymes *in vivo*. ABPP is an additional biochemical screening opportunity if a covalent binding or very high affinity to the target protein is proposed. Development of additional 'minitags' for small molecules or protocols for inhibitors that bind non-covalently to the target could make this method much more valuable for MoA identification.

Another screening method, which is based on the well-established yeast two-hybrid system, has the potential to support MoA identification in the future. The system is called yeast three-hybrid (Y3H) and is based on the design of a bait that consists of a known probe with high affinity to a defined protein and is conjugated with a linker sequence to the molecule of interest. Details of the method were reviewed recently by Cottier *et al.* (2011) and Chidley *et al.* (2011). In contrast to ABPP, Y3H also allows for the detection of inhibitors that do not bind covalently to the target; however, a large linker group has to be coupled with the compound of interest. Detailed knowledge of the SAR is needed to design a biologically active bait, which interacts with the same target as the initial hit compound.

In additional to the three main methodologies for MoA identification, phenotyping, genetic screens and biochemical screens, *in silico* methods for target predictions could become valuable for plant research. This field was established to study the MoA of drugs, but could also be applied to plant biology (Keiser *et al.*, 2009; Koutsoukas *et al.*, 2011). The method used algorithms to compare the structure of a compound of interest with structures of compounds with described activities on proteins *in vitro* (Keiser *et al.*, 2009; Koutsoukas *et al.*, 2011). Several databases containing the bioactivity data of investigated compounds are publicly available (reviewed in Koutsoukas *et al.*, 2011); structural similarities of the compound of interest with high active compounds in an enzyme assay published elsewhere accelerate target hypothesis generation for the compound of interest.

4.7. Conclusion

The strategy to identify the MoA of phytoactive compounds has evolved from a phenotyping approach to a data-driven systems biology approach, pushed by the technological progress. The new genetic techniques and omics-technologies have not dispelled the old ones; rather they have supported the classical approach with additional possibilities to address the MoA. One of the general deductions that can be derived from the publicly available examples of

how to nominate the target of a new compound and from my own experience in this research area is the following simple statement: apply the right technique at the right time.

This is the consequence of the presented three-tier approach to studying the MoAs. Several of the misleadings in the nomination of target proteins were based on the application of a method that was not suited at that stage of characterisation. This does not mean that the method itself was improperly chosen, but the knowledge about some key characteristics of the compound was not sufficient at that time. To propose sound target hypotheses for new compounds in more advanced 2nd-level studies, it is recommended to address compound stability, uniformity of effects in different species, general cytotoxicity and the effect on common pathways like transcription and translation in 1st-level studies. This is especially important, if the lead compound originated from an *in vivo* screen, in which compounds interacting with these basic processes are often detected as hits.

After the initial characterisation, a clear decision can be made about which 2nd-level approach is applicable for the compound of interest. In particular, resistance screens in model systems with compounds targeting signalling pathways or targets influencing cell structures have an excellent potential to support the functional annotation of plant genes. In order to associate the possible *in vitro* data generated in the 3rd level with the *in vivo* data from 1st and 2nd levels, data integration and interpretation is one of the key processes for nomination of the primary target *in vivo*. This is especially true, if techniques are applied that generate large-scale datasets like metabolomics or any next-generation sequencing approach.

The presented three-tier approach is a reasoned path-forward strategy to investigate the MoA of phytoactive compounds. If a compound is successfully described with the *in vivo* target, according to the three-tier approach, the requirements for a high quality probe in basic research as defined by Frye (2010) are fulfilled. In terms of basic plant science, the application of this three-tier approach for compound characterisation is a complementary approach to genetic studies to support the functional annotation of plant genes or proteins.

5. References

Alban C, Baldet P, Douce R (1994) Localization and characterization of two structurally different forms of acetyl-CoA carboxylase in young pea leaves, of which one is sensitive to aryloxyphenoxypropionate herbicides. Biochemical Journal 300: 557–565

Aliferis K A, Jabaji S (2011) Metabolomics – A robust bioanalytical approach for the discovery of the modes-of-action of pesticides: A review. Pesticide Biochemistry and Physiology 100: 105–117

Anderson C, Gray J C (1991) Effect of gabaculin on the synthesis of heme and cytochrome f in etiolated wheat seedlings. Plant Physiology 96: 584–587

Anthony R G, Waldin T R, Ray J A (1998) Herbicide resistance caused by spontaneous mutation of the cytoskeletal protein tubulin. Nature 393: 260–263

Armstrong J I, Yuan S, Dale J M, Tanner V N, Theologis A (2004) Identification of inhibitors of auxin transcriptional activation by means of chemical genetics in *Arabidopsis*. Proceedings of the National Academy of Sciences 101: 14978–14983

Arntzen C J (1972) Inhibition of photophosporylation by tentoxin, a cyclic tetrapeptide. Biochimica et Biophysica Acta 283: 539–542

Asami T, Mizutani M, Fujioka S, Goda H, Min Y K, Shimada Y, Nakano T, Takatsuto S, Matsuyama T, Nagata N, Sakata K, Yoshida S (2001) Selective interaction of triazole derivatives with DWF4, a cytochrome P450 monooxygenase of the brassinosteroid biosynthetic pathway, correlates with brassinosteroid deficiency *in planta*. Journal of Biological Chemistry 276: 25687–25691

Ashkenazi T, Widberg A, Nudelman A, Wittenbach V, Flint D (2005) Inhibitors of biotin biosynthesis as potential herbicides: Part 2. Pest Management Science 61: 1024–1033

Attwood M M (1969) An investigation into the mode of action of actinonin. Microbiology 55: 209–216

Austin R S, Vidaurre D, Stamatiou G, Breit R, Provant N J, Bonetta D, Zhang J, Fung P, Gong Y, Wang P W, McCourt P, Guttman D S (2011) Next-generation mapping of *Arabidopsis* genes. The Plant Journal 67: 715–725

Ayaydin F, Vissi E, Mesaros T, Miskolczi P, Kovacs I, Feher A, Dombradi V, Erdödi F, Gergely P, Dudits D (2000) Inhibition of serine/threonine-specific protein phosphatases causes premature activation of cdc2MsF kinase at G2/M transition and early mitotic microtubule organisation in alfalfa. The Plant Journal 23: 85-96

Baird D D, Upchurch R P, Homesley W B, Franz J E (1971) Introduction of a new broadspectrum postemergence herbicide class with utility for herbaceous perennial weed control. Proceedings of the Northcentral Weed Control Conference 26: 64–64

Bajsa J, Pan Z, Dayan F E, Owens D K, Duke S O (2012) Validation of serine / threonine protein phosphatase as the herbicide target site of endothall. Pesticide Biochemistry and Physiology 102: 38–44

Barta I C, Böger P (1999) Purification and characterization of 4-hydroxyphenylpyruvate dioxygenase from maize. Pesticide Science 48: 109–116

Bayer E, Gugel K H, Hägele K, Hagenmeier H, Jessipow S, König W A, Zähner H (1972) Metabolic products of microorganisms. 98. Phosphinothricin and phosphinothricyl-alanyl-analine. Helvetica Chimica Acta 55: 224–239

Beckie H J, Tardif F J (2012) Herbicide cross resistance in weeds. Crop Protection 35: 15–28

Berg D, Tietjen K, Wollweber D, Hein R (1999) From genes to targets: Impact of functional genomics in herbicide discovery. Proceedings of the British Crop Protection Conference, Weeds 2: 491–500

Bischoff V, Cookson S J, Wu S, Scheible W R (2009) Thaxtomin A affects CESA-complex density, expression of cell wall genes, cell wall composition, and causes ectopic lignification in *Arabidopsis thaliana* seedlings. Journal of Experimental Botany 60: 955–965

Blackwell H E, Zhao Y (2003) Chemical genetic approaches to plant biology. Plant Physiology 133: 448–455

Böger P, Matthes B, Schmalfuß J (2000) Towards the primary target of chloroacetamides – new findings pave the way. Pest Management Science 56: 497-508

Botte C Y, Deligny M (2011) Chemical inhibitors of monogalactosyldiacylglycerol synthases in *Arabidopsis thaliana*. Nature Chemical Biology 7: 834–842

Bouvier F, Harlingue A, Camara B (1997) Molecular analyses of carotenoid cyclase inhibition. Archives of Biochemistry and Biophysics 346: 53–64

Brkljacic J, Grotewold E, Scholl R, Mockler T, Garvin D F, Vain P, Brutnell T, Sibout R, Bevan M, Budak H, Caicedo A L, Gao C, Gu Y, Hazen S P, Holt B F, Hong S Y, Jordan M, Manzaneda A J, Mitchell-Olds T, Mochida K, Mur L A, Park C M, Sedbrook J, Watt M, Zheng S J, Vogel J P (2011) *Brachypodium* as a model for the grasses: Today and the future. Plant Physiology 157: 3–13

Burton J D, Gronwald J W, Somers J A, Connelly J A, Gengenbach B G, Wyse D L (1987) Inhibition of plant acetyl-coenzyme A carboxylase by the herbicides sethoxydim and haloxyfop. Biochemical and Biophysical Research Communication 148: 1039–1044

Chen D Z, Patel D V, Hackbarth C J, Wang W, Dreyer G, Young D C, Margolis P S, Wu C, Ni Z J, Trias J, White R J, Yuan Z (2000) Actinonin, a naturally occurring antibacterial agent, is a potent deformylase Inhibitor. Biochemistry 39: 1256–1262

Chen Y S, Fabbri B J, CaJacob C A, Anderson J C, Duff S M (2007) Suppression of CtpA in mouseearcress produces a phytotoxic effect: Validation of CtpA as a target for herbicide development. Weed Science 55: 283–287

Chidley C, Haruki H, Pedersen M G, Fellay C, Moser S, Johnsson K (2011) Searching for the protein targets of bioactive molecules. Chimia 65: 720–724

Choi W, Swanson S J, Gilroy S (2012) High-resolution imaging of Ca^{2+}, redox status, ROS and pH using GFP biosensors. The Plant Journal 70: 118–128

Congreve M, Murray C W, Blundell T L (2005) Keynote review: Structural biology and drug discovery. Drug Discovery Today 10: 895–907

Cottier S, Mönig T, Wang Z, Svoboda J, Boland W, Kaiser M, Kombrink E (2011) The yeast three-hybrid system as an experimental platform to identify proteins interacting with small signaling molecules in plant cells: Potential and limitations. Frontiers in Plant Science 2: 1–12

Couderchet M, Schmalfuß J, Böger P (1996) Incorporation of oleic acid into sporopollenin and its inhibition by the chloroacetamide herbicide metazachlor. Pesticide Biochemistry and Physiology 55: 189–199

Cravatt B F, Wright A T, Kozarich J W (2008) Activity-based protein profiling: From enzyme chemistry to proteomic chemistry. Annual Reviews of Biochemistry 77: 383–414

Cseke C, Gerwick B C, Crouse G D, Murdoch M G, Green S B, Heim D R (1996) 2 α-phosphohydantocidin: The *in vivo* adenylosuccinate synthetase inhibitor responsible for hydantocidin phytotoxicity. Pesticide Biochemistry and Physiology 55: 210–217

Cutler S, McCourt P (2005) Dude, where's my phenotype? Dealing with redundancy in signaling networks. Plant Physiology 138: 558–559

Dai X, Hayashi K, Nozaki H, Cheng Y, Zhao Y (2005) Genetic and chemical analyses of the action mechanisms of sirtinol in *Arabidopsis*. Proceedings of the National Academy of Sciences 102: 3129–3134

Dayan F E, Duke S O, Grossmann K (2010) Herbicides as probes in plant biology. Weed Science 58: 340–350

Dayan F E, Ferreira D, Wang Y, Khan I A, McInroy J A, Pan Z (2008) A pathogenic fungi diphenyl ether phytotoxin targets plant enoyl (acyl carrier protein) reductase. Plant Physiology 147: 1062–1071

Dayan F E, Owens D K, Duke S O (2012) Rationale for a natural products approach to herbicide discovery. Pest Management Science 68: 519–528

Dayan F E, Rimando A M, Tellez M R, Scheffler B E, Roy T, Abbas H K, Duke S O (2002) Bioactivation of the fungal phytotoxin 2,5-anhydro-D-glucitol by glycolytic enzymes is an essential component of its mechanism of action. Zeitschrift für Naturforschung 57: 645–653

DeBolt S, Gutierrez R, Ehrhardt D W, Melo C V, Ross L, Cutler S R, Somerville C, Bonetta D (2007) Morlin, an inhibitor of cortical microtubule dynamics and cellulose synthase movement. Proceedings of the National Academy of Sciences 104: 5854–5859

Dharmasiri N, Dharmasiri S, Estelle M (2005) The F-box protein TIR1 is an auxin receptor. Nature 435: 441–445

Duff S M, Chen Y S, Fabbri B, Yalamanchili G, Hamper B C, Walker D M, Brookfield F, Boyd E, Ashton M R, Yarnold C J, CaJacob C A (2007) The carboxyterminal processing protease of D1 protein: Herbicidal activity of novel inhibitors of the recombinant and native spinach enzymes. Pesticide Biochemistry and Physiology 88: 1–13

Duke S O, Evidente A, Fiore M, Rimando A M, Dayan F E, Vurro M, Christiansen N, Looser R, Hutzler J, Grossmann K (2011) Effects of the aglycone of ascaulitoxin on amino acid metabolism in *Lemna paucicostata*. Pesticide Biochemistry and Physiology 100: 41–50

Duke S O (2012) Why have no new herbicide modes of action appeared in recent years?. Pest Management Science 68: 505–512

Eckermann C, Matthes B, Nimtz M, Reiser V, Lerderer B, Böger P, Schröder J (2003) Covalent binding of chloroacetamide herbicides to the active site cysteine of plant type III polyketide synthases. Phytochemistry 64: 1045–1054

Eckes P, van Almsick C, Weidler M (2004) Gene expression profiling, a revolutionary tool in Bayer CropScience herbicide discovery. Pflanzenschutz-Nachrichten Bayer 57: 62–77

Evidente A, Capasso R, Cutignano A, Taglialatela-Scafati O, Vurro M, Zonno M C, Motta A (1998) Ascaulitoxin, a phytotoxic bis-amino acid N-glucoside from *Ascochyta caulina*. Phytochemistry 48: 1131–1137

Ferguson A R, Johnston J S (1980) Phaseolotoxin: chlorosis, ornithine accumulation and inhibition of ornithine carbamoyltransferase in different plants. Physiological Plant Pathology 16: 269–275

Ferhatoglu Y, Barrett M (2006) Studies of clomazone mode of action. Pesticide Biochemistry and Physiology 85: 7–14

Feys B J F, Benedetti C E, Penfold C N, Turner J G (1994) *Arabidopsis* mutants selected for resistance to the phytotoxin coronatine are male sterile, insensitive to methyl jasmonate, and resistant to a bacterial pathogen. The Plant Cell 6: 751–759

Finn J, Langevine C, Birk I, Birk J, Nickerson K, Rodaway S (1999) Rational herbicide design by inhibition of tryptophan biosynthesis. Bioorganic & Medicinal Chemistry Letters 9: 2297–2302

Focke M, Lichenthaler H K (1987) Inhibition of the acetyl-CoA carboxylase of barley chloroplasts by cycloxydim and sethoxydim. Zeitschrift für Naturforschung 42: 1361–1363

Fonne-Pfister R, Chemla P, Ward E, Girardet M, Kreuz K E, Honzatko R B, Fromm H J, Cowman-Jacob S W (1996) The mode of action and the structure of a herbicide in complex with its target: Binding of activated hydantocidin to the feedback regulation site of adenylosuccinate synthetase. Proceedings of the National Academy of Sciences 93: 9431–9436

Friedinger T L (1978) The trifluoromethanesulfonanilide class of herbicides and plant growth regulators. In: Geissbuehler H, Brooks G T, Kearney P C, ed., Advances in pesticide science, Pergamon Press, Oxford, UK, pp. 261–270

Fry B A, Loria R (2002) Thaxtomin A: Evidence for a plant cell wall target. Physiological and Molecular Plant Pathology 60: 1–8

Frye S V (2010) The art of the chemical probe. Nature Chemical Biology 6: 159–161

Gardner G, Gorton H L (1985) Inhibition of phytochrome synthesis by gabaculine. Plant Physiology 77: 540–543

Gardner G (1981) Azidoatrazine: Photoaffinity label for the site of triazine herbicide action in chloroplasts. Science 211: 937–940

Gauvrit C (1984) Effects of the herbicides benzoylprop-ethyl and flamprop-isopropyl on rat liver mitochondria: An alteration in membrane fluidity. Pesticide Biochemistry and Physiology 21: 377–384

Gendron J M, Haque A, Gendron N, Chang T, Asami T, Wang Z Y (2008) Chemical genetic dissection of brassinosteroid-ethylene interaction. Molecular Plant 1: 368–379

Ghannoum M A, Rice L B (1999) Antifungal agents: Mode of action, mechanisms of resistance, and correlation of these mechanisms with bacterial resistance. Clinical Microbiology Reviews 12: 501–517

Giancaspro A, Rosellini D, Blanco A, Gadaleta A (2012) Gabaculine selection using bacterial and plant marker genes (GSA-AT) in durum wheat transformation. Plant Cell, Tissue and Organ Culture 109: 447–455

Giovanelli J, Owens L D, Mudd S H (1971) Mechanism of inhibition of spinach β-cystathionase by rhizobitoxine. Biochimica et Biophysica Acta 227: 671–684

Giovanelli J, Owens L D, Mudd S H (1972) β-Cystathionase *in vivo* inactivation by rhizobitoxine and role of the enzyme in methionine biosynthesis in corn seedlings. Plant Physiology 51: 492–503

Gordon J J, Kelly B K, Miller G A (1962) Actinonin: An antibiotic substance produced by an actinomycete. Nature 195: 701–701

Graupner P R, Carr A, Clancy E, Gilbert J, Bailey K L, Derby J A (2003) The macrocidins: Novel cyclic tetramic acids with herbicidal activity produced by *Phoma macrostoma*. Journal of Natural Products 66: 1558–1561

Grossmann K (2005) What it takes to get a herbicide's mode of action. Physionomics, a classical approach in a new complexion. Pest Management Science 61: 423–431

Grossmann K (2010) Auxin herbicides: Current status of mechanism and mode of action. Pest Management Science 66: 113–120

Grossmann K, Christiansen N, Looser R, Tresch S, Hutzler J, Pollmann S, Ehrhardt T (2012a) Physionomics and metabolomics - two key approaches in herbicidal mode of action discovery. Pest Management Science 68: 494–504

Grossmann K, Hutzler J, Tresch S, Christiansen N, Looser R, Ehrhardt T (2012b) On the mode of action of the herbicides cinmethylin and 5-benzyloxymethyl-1, 2-isoxazolines: Putative inhibitors of plant tyrosine aminotransferase. Pest Management Science 68: 482–492

Grossmann K, Tresch S, Plath P (2001) Triaziflam and diaminotriazine affect enantioselectively multiple herbicide target sites. Zeitschrift für Naturforschung 56: 559–569

Groth G (2002) Structure of spinach chloroplast F1-ATPase complexed with the phytopathogenic inhibitor tentoxin. Proceedings of the National Academy of Sciences 99: 3464–3468

Grozinger C M, Chao E D, Blackwell H E, Moazed D, Schreiber S L (2001) Identification of a class of small molecule inhibitors of the sirtuin family of NAD-dependent deacetylases by phenotypic screening. Journal of Biological Chemistry 276: 38837–38843

Guerineau F, Brooks L, Meadows J, Lucy A, Robinson C, Mullineaux P (1990) Sulfonamide resistance gene for plant transformation. Plant Molecular Biology 15: 127–136

Gutierrez R, Grossmann G, Frommer W B, Ehrhardt D W (2010) Opportunities to explore plant membrane organization with super-resolution microscopy. Plant Physiology 154: 463–466

Hahn D R, Grauper P R, Chapin E, Gray J, Heim D, Gilbert J R, Gerwick B C (2009) Albucidin: A novel bleaching herbicide from *Streptomyces albus* subsp. chlorinus NRRL B-24108. The Journal of Antibiotics 62: 191–194

Hamilton J P, Buell C R (2012) Advances in plant genome sequencing. The Plant Journal 70: 177–190

Hao G, Zuo Y, Yang S, Yang G (2011) Protoporphyrinogen oxidase inhibitor: An ideal target for herbicide discovery. Chimia 65: 961–969

Hatzios K K (2005) Metabolism and elimination of toxicants. In: Hock B, Elstner E F, ed., Plant toxicology, Ed 4th. Marcel Dekker, New York, USA, pp. 469–518

Hayashi K, Jones A M, Ogino K, Yamazoe A, Oono Y, Inoguchi M, Kondo H, Nozaki H (2003) Yokonolide B, a novel inhibitor of auxin action, blocks degradation of AUX/IAA factors. Journal of Biological Chemistry 278: 23797–23806

Hayashi K, Kamio S, Oono Y, Townsend L B, Nozaki H (2009) Toyocamycin specifically inhibits auxin signaling mediated by SCFTIR1 pathway. Phytochemistry 70: 190–197

Hayashi K, Ogino K, Oono Y, Uchimiya H, Nozaki H (2001) Yokonolide A, a new inhibitor of auxin signal transduction, from *Streptomyces diastatochromogenes* B59. Journal of Antibiotics 54: 573–581

Hayashi K, Yamazoe A, Ishibashi Y, Kusaka N, Oono Y, Nozaki H (2008) Active core structure of terfestatin A, a new specific inhibitor of auxin signaling. Bioorganic & Medicinal Chemistry 16: 5331–5344

He W, Brumos J, Li H, Ji Y, Ke M, Gong X, Zeng Q, Li W, Zhang X, An F, Wen X, Li P, Chu J, Sun X, Yan C, Yan N, Xie D Y, Raikhel N, Yang Z, Stepanova A N, Alonso J M, Guo H (2011) A small-molecule screen identifies L-kynurenine as a competitive inhibitor of TAA1/TAR activity in ethylene-directed auxin biosynthesis and root growth in Arabidopsis. The Plant Cell 23: 3944–3960

Heath R J, Rubin J R, Holland D R, Zhang E, Snow M E, Rock C O (1999) Mechanism of triclosan inhibition of bacterial fatty acid synthesis. Journal of Biological Chemistry 274: 11110–11114

Hedden P, Graebe J E (1985) Inhibition of gibberellin biosynthesis by paclobutrazol in cell-free homogenates of *Cucurbita maxima* endosperm and *Malus pumila* embryos. Journal of Plant Growth Regulation 4: 111–122

Heim D R, Cseke C, Gerwick B C, Murdoch M G, Green S B (1995) Hydantocidin: A possible proherbicide inhibiting purine biosynthesis at the site of adenylosuccinate synthase. Pesticide Biochemistry and Physiology 53: 138–145

Heim D R, Larrinua I M, Murdoch M G, Roberts J L (1998) Triazofenamide is a cellulose biosynthesis inhibitor. Pesticide Biochemistry and Physiology 59: 163–168

Hicks G R, Raikhel N V (2012) Small molecules present large opportunities in plant biology. Annual Review of Plant Biology 63: 261–282

Hopkins A L, Groom C R (2002) The druggable genome. Nature Reviews - Cancer 1: 727–730

Horn P J, Korte A R, Neogi P B, Love E, Fuchs J, Strupat K, Borisjuk L, Shulaev V, Lee Y, Chapman K D (2012) Spatial mapping of lipids at cellular resolution in embryos of cotton. The Plant Cell 24: 622–636

Hou C, Dirk L M, Pattanaik S, Das N C, Maiti I B, Houtz R L, Williams M A (2007) Plant peptide deformylase: A novel selectable marker and herbicide target based on essential cotranslational chloroplast protein processing. Plant Biotechnology Journal 5: 275–281

Hsu W J, Yokoyama H (1972) Carotenoid biosynthesis in *Blakeslea trispora*. Phytochemistry 11: 2985–2990

Huang B, Bates M, Zhuang X (2009) Super-resolution fluorescence microscopy. Annual Reviews of Biochemistry 78: 993–1016

Huppatz J L, Phillips J N, Rattigan B M (1981) Cyanoacrylates. Herbicidal and photosynthetic inhibitory activity. Agricultural and Biological Chemistry 45: 2769–2773

Hwang I, Choi J, Song H, Cho S, Lim H, Park N, Lee D (2010) Validation of 7-keto-8-aminopelargonic acid synthase as a potential herbicide target with lead compound triphenyltin acetate. Pesticide Biochemistry and Physiology 97: 24–31

Ichihara A, Shiraishi K, Sato H, Sakamura S, Nishiyama K, Sakai R, Furusaki A, Matsumoto T (1977) The structure of coronatine. Journal of American Chemical Society 99: 636–637

Igarashi M, Kawada M, Hamada M, Iinuma H, Hayashi H, Tsuchiya K, Hori M (2001) Some biological and biochemical activities of resormycin, a novel herbicidal antibiotic. Journal of Antibiotics 54: 1072–1079

Igarashi M, Kiroshita N, Idada T, Kameda M, Hamada M, Takeuschi T (1997) Resormycin, a novel herbicidal and antifungal antibiotic produced by a strain of *Streptomyces platensis*. Journal of Antibiotics 50: 1020–1025

Irvine N M, Yerkes C N, Graupner P R, Roberts R, Hahn D R, Pearce C, Gerwick B C (2008) Synthesis and characterization of synthetic analogs of cinnacidin, a novel phytotoxin from *Nectria sp.*. Pest Management Science 64: 891–899

Jaworski E G (1972) Mode of action of N-phosponomethylglycine: Inhibition of aromatic amino acid biosynthesis. Journal of Agricultural and Food Chemistry 20: 1195–1198

Jeffcoat B, Harries W N (1975) Selectivity and mode of action of flamprop-isopropyl, isopropyl (+-)-2-[N-(3-chloro-4-fluorophenyl)benzamido]propionate, in the control of *Avena fatua* in barley. Pesticide Science 6: 283–296

Kahn A, Kannangara C G (1987) Gabaculine-resistant mutants of *Chlamydomonas reinhardtii* with elevated glutamate 1-semialdehyde aminotransferase activity. Carlsberg Research Communications 52: 73–81

Kannangara C G, Schouboe A (1985) Biosynthesis of Δ-aminolevulinate in greening barley leaves. VII. Glutamate 1-semialdehyde accumulation in gabaculine treated leaves. Carlsberg Research Communications 50: 179–191

Kaschani F, Verhelst S H, Swieten P F, Verdoes M, Wong C, Wang Z, Kaiser M, Overkleeft H S, Bogyo M, van der Hoorn R A L (2009) Minitags for small molecules: Detecting targets of reactive small molecules in living plant tissues using 'click chemistry'. Plant Journal 57: 373–385

Keiser M J, Setola V, Irwin J J, Laggner C, Abbas A I, Hufeisen S J, Jensen N H, Kuijer M B, Matos R C, Tran T B, Whaley R, Glennon R A, Hert J, Thomas K L, Edwards D D, Shoichet B K, Roth B L (2009) Predicting new molecular targets for known drugs. Nature 462: 175–182

Kepinski S, Leyser O (2005) The *Arabidopsis* F-box protein TIR1 is an auxin receptor. Nature 435: 446–451

King R R, Lawrence C H, Clark M C, Calhoun L A (1989) Isolation and characterization of phytotoxins associated with *Streptomyces scabies*. Journal of the Chemical Society, Chemical Communications 13: 849–850

Koopman H, Daams J (1960) 2,6-Dichlorobenzonitrile: A new herbicide. Nature 186: 89–90

Koutsoukas A, Simms B, Kirchmair J, Bond P J, Witmore A V, Zimmer S, Young M P, Jenkins J L, Glick M, Glen R C, Bender A (2011) From *in silico* target prediction to multi-target drug design: Current databases, methods and applications. Proteomics 74: 2554–2574

Kuzuyama T, Shimuzu T, Takahasi S, Seto H (1998) Fosmidomycin, a specific inhibitor of 1-deoxy-D-xylulose 5-phosphate reductoisomerase in the nonmevalonate pathway for terpenoid biosynthesis. Tetrahedron Letters 39: 7913–7916

La R N, Rascio N, Oster U, Rüdiger W (2007) Inhibition of lycopene cyclase results in accumulation of chlorophyll precursors. Planta 225: 1019–1029

LaRossa R A, Schloss J V (1984) The sulfonylurea herbicide sulfometuron methyl is an extremely potent and selective inhibitor of acetolactate synthase in *Salmonella typhimurium*. Journal of Biological Chemistry 259: 8753–8757

Laule O, Fürholz A, Chang H, Zhu T, Wang X, Heifetz P B, Gruissem W, Lange M (2003) Crosstalk between cytosolic and plastidial pathways of isoprenoid biosynthesis in Arabidopsis thaliana. Proceedings of the National Academy of Sciences 100: 6866–6871

Leason M, Cunlife D, Parkin D, Lea P J, Miflin B J (1982) Inhibition of pea leaf glutamate synthase by methionine sulfoximine, phosphinothricin and other glutamate analogues. Phytochemistry 21: 855–857

Lee Y J, Perdian D C, Song Z, Yeung E S, Nikolau J (2012) Use of mass spectrometry for imaging metabolites in plants. The Plant Journal 70: 81–95

Lein W, Börnke F, Reindl A, Ehrhardt T, Stitt M, Sonnewald U (2004) Target-based discovery of novel herbicides. Current Opinion in Plant Biology 7: 219–225

Lever G B, Shearing S J, Batch J J (1982) P333 - A new broad spectrum growth retardant. Proceedings of the British Crop Protection Conference, Weeds 3–10

Li Y, MacKintosh C, Casida J E (1993) Protein phosphatase 2A and its [^{3}H] cantharidin / [^{3}H]endothall thioanhydride binding site - Inhibitor specifity of cantharidin and ATP analogues. Biochemical Pharmacology 46: 1435-1443

Mann S, Colliandre L, Labesse G, Ploux O (2009) Inhibition of 7,8-diaminopelargonic acid aminotransferase from *Mycobacterium tuberculosis* by chiral and achiral anologs of its substrate: Biological implications. Biochimie 91: 826–834

Matringe M, Camadro J M, Labbe P, Scalla R (1989) Protoporphyrinogen oxidase as a molecular target for diphenyl-ether herbicides. Biochemical Journal 260: 231–235

Matthes B, Schmalfuß J, Böger P (1998) Chloracetamide mode of action, II: Inhibition of very long chain fatty acid synthesis in higher plants. Zeitschrift für Naturforschung 53: 1004–1011

Mayer M P, Bartlett D L, Beyer P, Kleinig H (1989) The *in vitro* mode of action of bleaching herbicides on the desaturation of 15-cis-phytoene and cis-ζ-carotene in isolated daffodil chromoplasts. Pesticide Biochemistry and Physiology 34: 111–117

McMurry L M, Oethinger M, Levy S B (1998) Triclosan targets lipid synthesis. Nature 394: 531–532

Metzker M L (2010) Sequencing technologies – the next generation. Nature Reviews Genetics 11: 31–46

Meyer W L, Templeton G E, Grable C I, Sigel C W, Jones R, Woodhead S H, Sauer C (1971) The structure of tentoxin. Tetrahedron Letters 12: 2357–2360

Michel H, Weyer K A, Gruenberg H, Dunger I, Oesterhelt D, Lottspeich F (1986) The 'light' and 'medium' subunits of the photosynthetic reaction centre from *Rhodopseudomonas viridis*: Isolation of the genes, nucleotide and amino acid sequence. EMBO 5: 1149–1158

Min Y K, Asami T, Fujioka S, Murofushi N, Yamaguchi I, Yoshida S (1999) New lead compounds for brassinosteroid biosynthesis inhibitors. Bioorganic & Medicinal Chemistry Letters 9: 425–430

Mishima H, Kurihara H, Kobayashi K, Miyazawa S (1976) Gabaculine: γ-aminobutyrate aminotransferase inhibitor of microbial origin. Tetrahedron Letters 17: 537–540

Mitchell R E (1976) Isolation and structure of a chlorosis-inducing toxin of *Pseudomonas phaseolicola*. Phytochemistry 15: 1941–1947

Montezinos D, Delmer D P (1980) Characterization of inhibitors of cellulose synthesis in cotton fibers. Planta 305: 305–311

Moore R E, Niemczura W P, Kwok O C, Patil S S (1984) Inhibitors of ornithine carbamoyltransferase from *Pseudomonas syringae pv. phaseolicola*. Tetrahedron Letters 25: 3931–3934

Morejohn L C, Bureau T E, Molebajer J, Bajer A S, Fosket D E (1987) Oryzalin, a dinitroaniline herbicide, binds to plant tubulin and inhibits microtubule polymerization *in vitro*. Planta 172: 252–264

Moreland D E (1981) Interaction of perfluidone with mitochondrial, thylakoid, and liposome membranes. Pesticide Biochemistry and Physiology 15: 21–31

Mori I, Fonne-Pfister R, Matsunaga Si, Tada S, Kimura Y, Iwasaki G, Mano Ji, Hatano M, Nakano T, Koizumi Si, Scheidegger A, Hayakawa K, Ohta D (1995) A novel class of herbicides – Specific inhibitors of imidazoleglycerol phosphate dehydratase. Plant Physiology 107: 719–723

Morrison I N, Hill B D, Dushnicky L G (1979) Histological studies on the effects of benzoylprop ethyl and flamprop methyl on growth and development of wild oats. Weed Research 19: 385-393

Mulwa R M, Mwanza L M (2006) Biotechnology approaches to developing herbicide tolerance / selectivity in crops. African Journal of Biotechnology 5: 396–404

Mur L A, Allainguillaume J, Catalán P, Hasterok R, Jenkins G, Lesniewska K, Thomas I, Vogel J (2011) Exploiting the *Brachypodium* tool box in cereal and grass research. New Phytologist 191: 334–347

Nakajima M, Itoi K, Takamatsu Y, Kinoshita T, Okazaki T, Kawakubo K, Shindo M, Honma T, Thojigamori M, Haneishi T (1991) Hydantocidin: A new compound with herbicidal activity from *Streptomyces hygroscopicus*. Journal of Antibiotics 44: 293–300

Nishimura H, Katagiri K, Sato K, Mayama M, Shimaoka N (1956) Toyocamycin, a new anti-candida antibiotic. Journal of Antibiotics 9: 60–62

Nudelman A, Marcovici-Mizrahi D, Nudelman A, Flint D, Wittenbach V (2004) Inhibitors of biotin biosynthesis as potential herbicides. Tetrahedron 60: 1731–1748

Occhipinti A, Berlicki Ł, Giberti S, Dziedziola G, Kafarski P, Forlania G (2010) Effectiveness and mode of action of phosphonate inhibitors of plant glutamine synthetase. Pest Management Science 66: 51–58

Okami Y, Kitahara T, Hamada M, Naganawa H, Kondo S, Maeda K, Takeuchi T, Umezawa H (1974) Studies on a new amino acid antibiotic, amiclenomycin. Journal of Antibiotics 27: 656–664

O'Keefe M G, Klevorn T B (1991) A new pre- and post emergence herbicide for broad-leaf weed control in winter cereals. Proceedings of the British Crop Protection Conference, Weeds 1: 63–68

Okuhara M, Kuroda Y, Goto T, Okamoto M, Terano H, Kohsaka M, Aoki H, Imanaka H (1980) Studies on new phosphonic acid antibiotics. III. Isolation and characterization of FR-31564, FR-32863 and FR-33289. Journal of Antibiotics 33: 24–28

Omura S, Tanaka Y, Kanaya I, Shinose M, Takahashi Y (1990) Phthoxazolin, a specific inhibitor of cellulose biosynthesis, produced by a strain of *Streptomyces*. The Journal of Antibiotics 43: 1034–1036

Oono Y, Chen Q C, Overvoorde P J, Köhler C, Theologis A (1998) *age* mutants of *Arabidopsis* exhibit altered auxin-regulated gene expression. The Plant Cell 10: 1649–1662

Owens L D, Wright D A (1965) Production of the soybean-chlorosis toxin by *Rhizobium japonicum* in pure culture. Plant Physiology 40: 931–933

Park S Y, Fung P, Nishimura N, Jensen D, Fujii H, Zhao Y, Lumba S, Santiago J, Rodrigues A, Chow T, Alfred S E, Bonetta D, Finkelstein R, Provart N J, Desveaux D, Rodriguez P L, McCourt P, Zhu J K, Schroeder J I, Volkman B F, Cutler S R (2009) Abscisic acid inhibits type 2C protein phosphatases via the PYR/PYL family of START proteins. Science 324: 1068–1071

Peng L, Xiang F, Roberts E, Kawagoe Y, Greve L C, Kreuz K, Delmer D P (2001) The experimental herbicide CGA 325'615 inhibits synthesis of crystalline cellulose and causes accumulation of non-crystalline β-1,4-blucan associated with CesA protein. Plant Physiology 126: 981–992

Perola E, Herman L, Weiss J (2012) Development of a rule-based method for the assessment of protein druggability. Journal of Chemical Information and Modeling 52: 1027–1038

Pfister K, Steinback K E, Gardner G, Arntzen C J (1981) Photoaffinity-labeling of an herbicide receptor protein in chloroplast membranes. Proceedings of the National Academy of Sciences 78: 981–985

Phillips McDougall (2011) AgriService - Product section 2010 market.

Ploux O, Breyne O, Carillon S, Marquet A (1999) Slow-binding and competitive inhibition of 8-amino-7-oxopelargonate synthase, a pyridoxal-5'-phosphate-dependent enzyme involved in biotin biosynthesis, by substrate and intermediate analogs. Kinetic and binding studies. European Journal of Biochemistry 259: 63–70

Porter J W, Lincoln R E (1950) I. *Lycopersicum* selections containing a high content of carotenes and colorless polyenes II. The mechanism of carotene biosynthesis. Archives of Biochemistry and Biophysics 27: 390–402

Rattermann D M, Balke E (1988) Herbicidal disruption of proton gradient development and maintenance by plasmalemma and tonoplast vesicles from oat root. Pesticide Biochemistry and Physiology 31: 221–236

Rendina A R, Craig-Kennard A C, Deaudoin J D, Breen M K (1990) Inhibition of acetyl-coenzyme A carboxylase by two classes of grass-selective herbicides. Journal of Agricultural and Food Chemistry 38: 1282–1287

Rendina A R, Felts J M (1988) Cyclohexanedione herbicides are selective and potent Inhibitors of acetyl-coA carboxylase from grasses. Plant Physiology 86: 983–986

Robert S, Chary N (2008) Endosidin1 defines a compartment involved in endocytosis of the brassinosteroid receptor BRI1 and the auxin transporters PIN2 and AUX1. Proceedings of the National Academy of Sciences 105: 8464–8469

Rojas-Pierce M, Titapiwatanakun B, Sohn E J, Fang F, Larive C K, Blakeslee J, Cheng Y, Cutler S, Peer W A, Murphy A S, Raikhel N V (2007) *Arabidopsis* P-glycoprotein19 participates in the inhibition of gravitropism by Gravacin. Chemistry & Biology 14: 1366–1376

Rosado A, Hicks G R, Norambuena L, Rogachev I, Meir S, Pourcel L, Zouhar J, Brown M Q, Boirsdore M P, Puckrin R S, Cutler S R, Rojo E, Aharoni A, Raikhel N V (2011) Sortin1-hypersensitive mutants link vacuolar-trafficking defects and flavonoid metabolism in Arabidopsis vegetative tissues. Chemistry & Biology 18: 187–197

Rosellini D (2011) Selectable marker genes from plants: Reliability and potential. *In vitro* Cellular & Developmental Biology Plant 47: 222–233

Rueegg W T, Quadranti M, Zoschke A (2007) Herbicide research and development: Challenges and opportunities. Weed Research 47: 271–275

Rybel B D, Audenaert D (2009) Chemical inhibition of a subset of *Arabidopsis thaliana* GSK3-like kinases activates brassinosteroid signaling. Chemistry & Biology 16: 594–604

Salmon F, Taton M, Benveniste P, Rahier A (1992) Plant sterol biosynthesis: novel potent and selective inhibitors of cytochrome P450-dependent obtusifoliol 14 alpha-methyl demethylase. Archives of Biochemistry and Biophysics 297: 123–131

Sandmann G, Bramely P M, Böger P (1985) New herbicidal inhibitors of carotene biosynthesis. Journal of Pesticide Science 10: 19–24

Sandmann G, Linden H, Böger P (1989) Enzyme-kinetic studies on the interaction of norflurazone with phytoene desaturase. Zeitschrift für Naturforschung 44: 787–790

Sandmark J, Mann S, Marquet A, Schneider G (2002) Structural basis for the inhibition of the biosynthesis of biotin by the antibiotic amiclenomycin. The Journal of Biological Chemistry 277: 43352–43358

Sasaki Y, Nagano Y (2004) Plant acetyl-coA carboxylase: Structure, biosynthesis, regulation, and gene manipulation for plant breeding. Bioscience Biotechnology and Biochemistry 68: 1175–1184

Scheible W, Eshed R, Richmond T, Delmer D, Somerville C (2001) Modifications of cellulose synthase confer resistance to isoxaben and thiazolidinone herbicides in *Arabidopsis* Ixr1 mutants. Proceedings of the National Academy of Sciences 98: 10079–10084

Scheible W, Fry B, Kochevenko A, Schindelasch D, Zimmerli L, Somerville S, Loria R, Somerville C R (2003) An *Arabidopsis* mutant resistant to thaxtomin A, a cellulose synthesis inhibitor from *Streptomyces species*. The Plant Cell 15: 1781–1794

Schmalfuß J, Matthes B, Mayer P, Böger P (1998) Chloracetamide mode of action, I: Inhibition of very long chain fatty acid synthesis in *Scenedesmus acutus*. Zeitschrift für Naturforschung 53: 995–1003

Schmitzer P R, Graupner P R, Chapin E L, Fields S C, Gilbert J R, Gray J A (2000) Ribofuranosyl triazolone: A natural product herbicide with activity on adenylosuccinate synthetase following phosphorylation. Journal of Natural Products 63: 777–781

Schneeberger K, Weigel D (2011) Fast-forward genetics enabled by new sequencing technologies. Trends in Plant Science 16: 282–288

Schulz A, Ort O, Beyer P, Kleinig H (1993) SC-0051, a 2-benzoyl-cyclohexane-1,3-dione bleaching herbicide, is a potent inhibitor of the enzyme p-hydroxyphenylpyruvate dioxygenase. FEBS Letters 318: 162–166

Schulz A, Spönemann P, Köcher H, Wengenmayer F (1988) The herbicidally active experimental compound Hoe 704 is a potent inhibitor of the enzyme acetolactate reductoisomerase. FEBS Letters 238: 375–378

Schweitzer B A, Loida P J, CaJacob C A, Chott R C, Collantes E M, Hedge S G, Mosier P D, Profeta S (2002) Discovery of imidazole glycerol phosphate dehydratase inhibitors through 3-D database searching. Bioorganic & Medicinal Chemistry 12: 1743–1746

Scott B A, Vangessel M J, White-Hansen S (2009) Herbicide-resistant weeds in the United States and their impact on extension. Weed Technology 23: 599–603

Seaver S M, Henry C S, Hanson A D (2012) Frontiers in metabolic reconstruction and modelling of plant genomes. Journal of Experimental Botany 63: 2247–2258

Secor J, Ceske C (1988) Inhibition of acetyl-coA carboxylase activity by haloxyfop and tralkoxydim. Plant Physiology 86: 10–12

Serrano M, Robatzek S, Torres M, Kombrink E, Somssich I E, Robinson M, Schulze-Lefert P (2007) Chemical interference of pathogen-associated molecular pattern-triggered immune responses in *Arabidopsis* reveals a potential role for fatty-acid synthase type II complex-derived lipid signals. Journal of Biological Chemistry 282: 6803–6811

Serrano M, Hubert D A, Dangl J L, Schulze-Lefert P, Kombrink E (2010) A chemical screen for suppressors of the avrRpm1-RPM1-dependent hypersensitive cell death response in *Arabidopsis thaliana*. Planta 231: 1013–1023

Shaner D L (2003) Herbicide safety relative to common targets in plants and mammals. Pest Management Science 60: 17–24

Shaner D L, Anderson P C, Stidham M A (1984) Imidazolinones - Potent inhibitors of acetohydroxyacid synthase. Plant Physiology 76: 545–546

Sheard L B, Tan X, Mao H, Withers J, Ben-Nissan G, Hinds T R, Kobayashi Y, Hsu F, Sharon M, Browse J, He S Y, Rizo J, Howe G A, Zheng N (2010) Jasmonate perception by inositol-phosphate-potentiated COI1-JAZ co-receptor. Nature 468: 400–405

Siehl D L, Subramanian M V, Walters E W, Lee S F, Anderson R J, Toschi A G (1996) Adenylosuccinate synthetase: Site of action of hydantocidin, a microbial phytotoxin. Plant Physiology 110: 753–758

Singh B, Shaner D L (1995) Biosynthesis of branched chain amino acids: From test tube to field. The Plant Cell 7: 935–944

Sobolev V, Niztaev A, Pick U, Avni A, Edelman M (2002) A case study in applying docking predictions: Modelling the tentoxin binding sites of chloroplast F1-ATPase. Current Science 83: 857–867

Steele J A, Uchytil T F, Durbin R D, Bhatnagar P, Rich D H (1976) Chloroplast coupling factor 1: A species-specific receptor for tentoxin. Proceedings of the National Academy of Sciences 73: 2245–2248

Steinbrücken H C, Amrhein N (1980) The herbicide glyphosate is a potent inhibitor of 5-enolpyruvylshikimic acid-3-phosphate synthase. Biochemical and Biophysical Research Communication 94: 1207–1212

Stierle A, Upadhyay R, Strobel G (1991) Cyperine, a phytotoxin produced by *Ascochyta cypericola*, a fungal pathogen of *Cyperus rotundus*. Phytochemistry 30: 2191–2192

Strachen S D, Hess D (1983) The biochemical mechanism of the dinitroaniline herbicide oryzalin. Pesticide Biochemistry and Physiology 20: 141–150

Streit L, Moreau M, Gaudin J, Ebert E, Vanden B H (1991) A novel imidazole carboxylic acid ester is a herbicide inhibiting 14α-methyl-demethylation in plant sterol biosynthesis. Pesticide Biochemistry and Physiology 40: 162–168

Suda H, Aoyagi T, Takeuchi T, Umezawa H (1976) Inhibition of aminopeptidase B and leucine aminopeptidase by bestatin and its stereoisomer. Archives of Biochemistry and Biophysics 177: 196–200

Surpin M, Rojas-Pierce M, Carter C, Hicks G R, Vasquez J, Raikhel N V (2005) The power of chemical genomics to study the link between endomembrane system components and the gravitropic response. Proceedings of the National Academy of Sciences 102: 4902–4907

Sverak L, Bonar R A, Langlois A J, Beard J W (1970) Inhibition by toyocamycin of RNA synthesis in mammalian cells and in normal and avian tumor virus-infected chick embryo cells. Biochimica et Biophysica Acta 224: 441–450

Tan X, Calderon-Villalobos L I, Sharon M, Zheng C, Robinson C V, Estelle M, Zheng N (2007) Mechanism of auxin perception by the TIR1 ubiquitin ligase. Nature 446: 640–645

Tanaka T, Hanato K, Watanabe M, Abbas H K (1996) Isolation, purification and identification of 2,5-anhydro-D-glucitol as a phytotoxin from *Fusarium solani*. Journal of Natural Toxins 5: 317–329

The Arabidopsis Genome Initiative (2000) Analyses of the genome sequence of the flowering plant *Arabidopsis thaliana*. Nature 408: 796–815

Tice C M (2001) Selecting the right compounds for screening: Does Lipinski's Rule of 5 for pharmaceuticals apply to agrochemicals? Pest Management Science 57: 3–16

Tischler N, Bates J C, Quimba G P (1951) A new group of defoliant-herbicidal chemicals. Proceedings of the Annual Meeting of the Northeastern Weed Control Conference 4: 51–83

Toth R, van der Hoorn R A L (2010) Emerging principles in plant chemical genetics. Trends in Plant Science 15: 81–88

Trapnell C, Williams B A, Pertea G, Mortazavi A, Kwan G, Baren M J, Salzberg S L, Wold B J, Pachter L (2010) Transcript assembly and quantification by RNA-Seq reveals unannotated transcripts and isoform switching during cell differentiation. Nature Biotechnology 28: 511–515

Trebst A (2007) Inhibitors in the functional dissection of the photosynthetic electron transport system. Photosynthesis Research 92: 217–224

Trenkamp S, Martin W, Tietjen K (2004) Specific and differential inhibition of very-long-chain fatty acid elongases from *Arabidopsis thaliana* by different herbicides. Proceedings of the National Academy of Sciences 101: 11903–11908

Trenkamp S, Eckes P B, Fernie A R (2009) Temporally resolved GC-MS-based metabolic profiling of herbicide treated plants treated reveals that changes in polar primary metabolites alone can distinguish herbicides of differing mode of action. Metabolomics 5: 277–291

Tresch S, Heilmann M, Christiansen N, Looser R, Grossmann K (2012) Inhibition of saturated very-long-chain fatty acid biosynthesis by mefluidide and perfluidone, selective inhibitors of 3-ketoacyl-CoA synthases. Phytochemistry 76: 162–171

Tresch S, Niggeweg R, Grossmann K (2008) The herbicide flamprop-M-methyl has a new antimicrotubule mechanism of action. Pest Management Science 64: 1195–1203

Tresch S, Plath P, Grossmann K (2005) Herbicidal cyanoacrylates with antimicrotubule mechanism of action. Pest Management Science 61: 1052–1059

Tresch S, Schmotz J, Grossmann K (2011) Probing mode of action in plant cell cycle by the herbicide endothall, a protein phosphatase inhibitor. Pesticide Biochemistry and Physiology 99: 86–95

Ulmanov T, Murfett J, Hagen G, Guilfoyle T J (1997) Aux/IAA proteins repress expression of reporter genes containing natural and highly active synthetic auxin response elements. The Plant Cell 9: 1963–1971

Valadon L R, Kates M (1984) Effect of perfluidone on metabolism of lipids in maize (*Zea mays* L.) and sunflower (*Helianthus annuus* L.). Journal of Plant Growth Regulation 3: 111–120

van Almsick A (2009) New HPPD-inhibitors - A proven mode of action as a new hope to solve current weed problems. Outlooks on Pest Management 20: 27–30

Veerasekarana P, Kirkwood R C, Parnell E W (1981) Studies of the mechanism of action of asulam in plants. Part II: Effect of asulam on the biosynthesis of folic acid. Pest Management Science 12: 330–338

Vial J, Borrod G (1984) Short note on dihydropyrones, a new herbicidal family with bleaching properties. Zeitschrift für Naturforschung 39: 459–459

Vyvyan J R (2002) Allelochemicals as leads for new herbicides and agrochemicals. Tetrahedron 58: 1631–1646

Walsh T A (2007) The emerging field of chemical genetics: Potential applications for pesticide discovery. Pest Management Science 63: 1165–1171

Walsh T A, Bauer T, Neal R, Merlo A O, Schmitzer P R, Hicks G R, Honma M, Matsumura W, Wolff K, Davies J P (2007) Chemical genetic identification of glutamine phosphoribosylpyrophosphate amidotransferase as the target for a novel bleaching herbicide in *Arabidopsis*. Plant Physiology 144: 1292–1304

Walsh T A, Neal R, Merlo A O, Honma M, Hicks G R, Wolff K, Matsumura W, Davies J P (2006) Mutations in an auxin receptor homolog AFB5 and in SGT1b confer resistance to synthetic picolinate auxin and not to 2,4-dichlorphenoxyacetic acid or indole-3-acetic acid in *Arabidopsis*. Plant Physiology 142: 542–552

Walters E W, Lee S F, Niderman T, Bernasconi P, Subramanian M V, Siehl D L (1997) Adenylosuccinate synthetase from maize – Purification, properties, and mechanism of inhibition by 5'-phosphohydantocidin. Plant Physiology 114: 549–555

Wang Y, Shyy J Y, Chien S (2008) Fluorescence proteins, live-cell imaging, and mechanobiology: Seeing is believing. Annual Review of Biomedical Engineering 10: 1–38

Wang Z, Gerstein M, Snyder M (2009) RNA-Seq: A revolutionary tool for transcriptomics. Nature Reviews - Genetics 10: 57–63

Waterhouse P M, Helliwell C A (2003) Exploring plant genomes by RNA-induced gene silencing. Nature Reviews Genetics 4: 29–38

Weber H A, Gloer J B (1988) Interference competition among natural fungal competitors: An antifungal metabolite from the coprophilous fungus *Preussia fleischhakii*. Journal of Natural Products 51: 879–883

Weigel D, Ahn J H, Blazquez M A, Borevitz J O, Lamb C J (2000) Activation tagging in *Arabidopsis*. Plant Physiology 122: 1003–1013

Wessels J S, Vanderveen R (1956) The action of some derivatives of phenylurethan and of 3-phenyl-1,1-dimethylurea on the Hill reaction. Biochimica et Biophysica Acta 19: 548–549

Wheelock C E, Miyagawa H (2006) The omicization of agrochemical research. Journal of Pesticide Science 31: 240–244

Wielopolska A, Townley H, Moore I, Waterhouse P, Helliwell C (2005) A high-throughput inducible RNAi vector for plants. Plant Biotechnology Journal 3: 583–590

Williams M (2007) Enabling technologies in drug discovery: The technical and cultural integration of the new with the old. In: Taylor J B, Triggle D J, ed., Comprehensive medicinal chemistry II, Elsevier Ltd., Oxford, UK, pp. 265–287

Witschel M, Hoeffken W, Seet M, Parra L, Mietzner T, Thater F, Niggeweg R, Röhl F, Illarionov B, Rohdich F, Kaiser J, Fischer M, Backer A, Diederich F (2011) Inhibitors of the herbicidal target IspD: Allosteric site binding. Angewandte Chemie 50: 7931–7935

Xie D X, Feys B F, James S, Nieto-Rostro M, Turner J G (1998) COI1: An *Arabidopsis* gene required for jasmonate-regulated defense and fertility. Science 280: 1091–1094

Xu W, Tao L, Gu X, Shen X, Yuan S (2009) Herbicidal activity of the metabolite SPRI-70014 from *Streptomyces griseolus*. Weed Science 57: 547–553

Yamamoto E, Zeng L, Baird W (1998) Alpha-tubulin missense mutations correlate with antimicrotubule drug resistance in *Eleusine indica*. The Plant Cell 10: 297–308

Yamazoe A, Hayashi K, Kepinski S, Leyser O, Nozaki H (2005) Characterization of terfestatin A, a new specific inhibitor for auxin signaling. Plant Physiology 139: 779–789

Yamazoe A, Hayashi K, Kuboki A, Ohira S, Nozaki H (2004) The isolation, structural determination, and total synthesis of terfestatin A, a novel auxin signalling inhibitor from *Streptomyces sp*.. Tetrahedron Letters 45: 8359–8362

Yoneda A, Higaki T, Kutsuna N, Kondo Y, Osada H, Hasezawa S, Matsui M (2007) Chemical genetic screening identifies a novel inhibitor of parallel alignment of cortical microtubules and cellulose microfibrils. Plant Cell Physiology 48: 1393–1403

Yoneda A, Ito T, Higaki T, Kutsuna N, Saito T, Ishimizu T, Osada H, Hasezawa S, Matsui M, Demura T (2010) Cobtorin target analyses reveals that pectin functions in the deposition of cellulose microfibrils in parallel with cortical microtubules. Plant Journal 64: 657–667

Zeidler J, Schwender J, Müller C, Wiesner J, Weidemeyer C, Beck E, Jomaa H, Lichtenthaler H K (1998) Inhibition of the non-mevalonate 1-deoxy-D-xylulose-5-phosphat pathway of plant isoprenoid biosynthesis by fosmidomycin. Zeitschrift für Naturforschung 53: 980–986

Zhao Y, Chow T F, Puckrin R S, Alfred S E, Korir A K, Larive C K, Cutler S R (2007) Chemical genetic interrogation of natural variation uncovers a molecule that is glycoactivated. Nature Chemical Biology 3: 716–721

Zhao Y, Dai X, Blackwell H E, Schreiber S L, Chory J (2003) SIR1, an upstream component in auxin signaling identified by chemical genetics. Science 301: 1107–1110

Zheng W, Zhai Q, Sun J, Li C B, Zhang L, Li H, Zhang X, Li S, Xu Y, Jiang H, Wu X, Li C (2006) Bestatin, an inhibitor of aminopeptidases, provides a chemical genetics approach to dissect jasmonate signaling in *Arabidopsis*. Plant Physiology 141: 1400–1413

Zinkernagel R, König M (1967) 2,4,4'-Trichloro-2'-hydroxydiphenyl ether, a new antimicrobial agent. Seifen, Oele, Fette, Wachse 93: 670–684

Zouhar J, Hicks G R, Raikhel N V (2004) Sorting inhibitors (Sortins): Chemical compounds to study vacuolar sorting in *Arabidopsis*. Proceedings of the National Academy of Sciences 101: 9497–9501

Danksagung

[Personenbezogene Daten in der Danksagung sind gelöscht.]

Curriculum vitae

[Personenbezogene Daten sind gelöscht.]

Scientific publications

Tresch S, Heilmann M, Christiansen N, Looser R, Grossmann K (2012) Inhibition of saturated very-long-chain fatty acid biosynthesis by mefluidide and perfluidone, selective inhibitors of 3-ketoacyl-CoA synthases. Phytochemistry 76: 162–171.

Grossmann K, Christiansen N, Looser R, **Tresch S**, Hutzler J, Pollmann S, Ehrhardt T (2012) Physionomics and metabolomics - two key approaches in herbicidal mode of action discovery. Pest Management Science 68: 494–504.

Grossmann K, Hutzler J, **Tresch S**, Christiansen N, Looser R, Ehrhardt T (2012) On the mode of action of the herbicides cinmethylin and 5-benzyloxymethyl-1, 2-isoxazolines: Putative inhibitors of plant tyrosine aminotransferase. Pest Management Science 68: 482–492.

Tresch S, Schmotz J, Grossmann K (2011) Probing mode of action in plant cell cycle by the herbicide endothall, a protein phosphatase inhibitor. Pesticide Biochemistry and Physiology 99: 86–95.

Tresch S, Niggeweg R, Grossmann K (2008) The herbicide flamprop-M-methyl has a new antimicrotubule mechanism of action. Pest Management Science 64: 1195–1203.

Opalski K S, **Tresch S**, Kogel K, Grossmann K, Köhle H, Hükelhoven R (2006) Metrafenone: Studies on the mode of action of a novel cereal powdery mildew fungicide. Pest Management Science 62: 393–401.

Tresch S, Plath P, Grossmann K (2005) Herbicidal cyanoacrylates with antimicrotubule mechanism of action. Pest Management Science 61: 1052–1059.

Tresch S, Grossmann K (2003) Quinclorac does not inhibit cellulose (cell wall) biosynthesis in sensitive barnyard grass and maize roots. Pesticide Biochemistry and Physiology 75: 73–78.

Grossmann K, Kwiatkowski J, **Tresch S** (2001) Auxin herbicides induce H_2O_2 overproduction and tissue damage in cleavers (*Galium aparine* L.). Journal of Experimental Botany 52: 1811–1816.

Grossmann K, **Tresch S**, Plath P (2001) Triaziflam and diaminotriazine affect enantioselectively multiple herbicide target sites. Zeitschrift für Naturforschung 56: 559–569.

Ich versichere, dass ich die vorliegende Dissertation selbstständig verfasst und dabei keine anderen als die angegebenen Quellen und Hilfsmittel benutzt habe.

Ort, Datum

Unterschrift